UNIVERSITÀ DEGLI STUDI DI VERONA

DIPARTIMENTO DI BIOTECNOLOGIE

SCUOLA DI DOTTORATO DI SCIENZE, INGEGNERIA, MEDICINA

DOTTORATO DI RICERCA IN BIOTECNOLOGIE APPLICATE

XXIV° CICLO

TESI DI DOTTORATO

"Inhibition of HopAI1 activity during hypersensitive disease resistance response by nitric oxide-mediated *S*-nitrosylation"

S.S.D. BIO/18

Coordinatore: Ch.mo Prof. Massimo Delledonne

Tutor: Ch.mo Prof. Massimo Delledonne
Co-tutor: Dr. Diana Bellin

Dottorando: Tengfang Ling

Acknowledgments

Firstly I would like to acknowledge and extend my heartfelt gratitude to my supervisor, Prof. Massimo Delledonne, whose encouragement, guidance and support from the initial to the final level enabled me to complete this project.

My project would not have been made possible without the help of Dr. Diana Bellin, who also guided me in the entire project, and Dr. Elodie Spiazzi-Vandelle, whose technical assistance was vital.

I would like to show my gratitude to the other colleagues in the lab, Karina Kleinfelder Fontanesi for help with the NO fumigation; Jian Chen and Jingjing Huang for cooking meals; Anne-Marie Digby for solving problems with my house and my teeth; former members Barbara Sottocornola, Raman Pachaiappan and Jan Vitececk for their technical advice and encouragement. And thanks also go to Dr. Alejandro Giorgetti for helping me with the bioinformatics analysis.

I would also like to thank all the other people who helped me during the three-year PhD study: Alberto Ferrarini, Dougba Noel Dago, Luca Venturini, Marianna Fasoli, Andrea Anesi, Alessandro Alboresi and Fabio Finotti.

I owe sincere and earnest thanks to my friends, Aiqi Hu, Yinhua Chen and Yinjia Lin, especially Aiqi Hu for all the help on the nickel and dime in my three year’s Italian life.

I would like to thank Prof. Maria Luisa Chiusano (University "Federico II" of Naples) and Prof. Luisa Lanfranco (Universit à di Torino and Istituto Protezione Piante-CNRI) for sparing the time to read my thesis and become a member of my thesis defense panel.

And finally with the greatest pleasure, I wish to take this opportunity to thank my family members, my parents who have given me the greatest support and selfless love; and also my little nephew who sings me the most interesting and funny songs.

Index

1. Introduction

1.1 General concepts on plant disease resistance

All living organism, including plants, need to struggle with their enemies and defend themselves. Organisms potentially pathogenic on plants include fungi, oomycetes, bacteria, viruses, phytoplasmas, protozoa, nematode or insects (Jones and Dangl, 2006; Gohre and Robatzek, 2008; Dodds and Rathjen, 2010).

According to their way to feed on and to grow in plants, phytopathogens can be divided into three groups: necrotrophs, biotrophs and hemi-biotrophs (Glazebrook, 2005). Usually necrotrophs get the nutrients required for their growth from dead tissues by killing plant cells through the secretion of phytotoxins or tissue-degrading enzymes. For example, *Erwiniacarotovora* can invade various plant species (carrot, potato, tomato, leafy greens, green peppers, etc.) and cause host cell death by releasing plant cell wall-degrading enzymes including cellulases, proteases and pectinases into the host cell (Toth et al., 2003). On the opposite, biotrophs, like the bacterial pathogen *Xanthomonas oryzae* that cause blight and leaf streak on rice (Nino-Liu et al., 2006), get the nutrients from living plant tissues. Whereas the hemi-biotrophs can get the nutrients from both living and dead tissues that is dependent on the stages of their life cycle. For instance, *Pseudomonas syringae* invade a wide range of host plant species including several plants of agronomic interest, such as like tomato, tobacco or kiwi, as well as the model plant *Arabidopsis thaliana*, and induce speck, spot, and blight disease development on these plants. During the early stages of their life cycle, they do not induce plant cell death while they trigger tissue chlorosis or necrosis in sensitive plants in the later stages of their life cycle (Glazebrook, 2005; Pieterse et al., 2009). Over the past decade, the study of *Pseudomonas syringae* interaction with plants has become a hot spot in the field of plant-pathogen interaction. Supporting this concept, the genomes of 55 strains in *Pseudomonas syringae* have been sequenced until now (http://www.ncbi.nlm.nih.gov/genome?term=txid317%5Borgn%5D).

However, unlike mammals, plants as sessile organisms have not the capacity to escape and do not possess any adaptive immune system for defense. To overcome

such situations, plants have developed sophisticated mechanisms of resistance, rendering the disease more an exception than a rule. During a compatible interaction, a pathogen, defined virulent, is able to establish disease in a so-called susceptible plant. On the opposite, the infection of a resistant plant by an avirulent pathogen that induces plant defense response corresponds to an incompatible interaction.

The first defense layer in plants, called passive resistance, is represented by physical and chemical barriers which can prevent the infection of the plant by a pathogen. They include for instance cell wall composed of pectin and hemicellulose, and toxic compounds released by the vacuoles. In some cases the pathogen is able to overcome such barriers, like *Pseudomonas syringae* pv. *tomato* DC3000, which is living in the apoplast and uses some natural pores like stomata, hydathodes or wounding sites to enter into plant cells (Gohre and Robatzek, 2008; Dodds and Rathjen, 2010). Plants have thus evolved a second layer of defense that corresponds to an active resistance, due to the induction of defense mechanisms within the cells (Abramovitch et al., 2006; Gohre and Robatzek, 2008).

1.2 Mechanisms governing plant-pathogen interaction

1.2.1 The "zig-zag model"

The working model of the innate immunity system, named the "Zig-Zag model" and introduced by Jones and Dangl (2006), gives an extraordinary explanation of the interactions between plants and bacterial pathogens (Figure 1) (Jones and Dangl, 2006).

According to this model, the interaction is divided into different stages which include pathogen-associated or microbe-associated or danger-associated molecular patterns (PAMPs/MAMPs/DAMPs)-triggered immunity (usually named PTI), effector-triggered susceptibility (ETS), and effector-triggered immunity (ETI). During the infection of a plant, some molecules derived from the pathogen or released by the

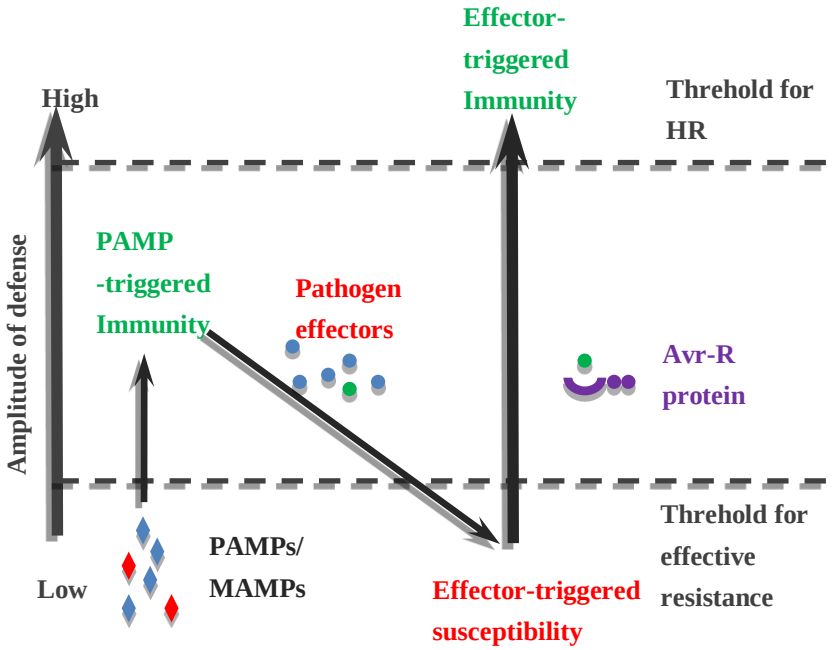

Figure 1 "Zig-zag model" during plant – pathogen interaction. Adapted from Jones and Dangl, 2006.

plant under the action of pathogen enzymes are recognized by pattern recognition receptors (PRRs) located on plant cell plasma membrane. Such recognition activates basal defense mechanisms that limit the growth of the pathogen, and that correspond to PAMP-triggered immunity. However virulent pathogens are able to release effectors, which are responsible for its pathogenicity, to suppress PTI induced by the plant. This stage of the interaction corresponds to the effector-triggered susceptibility in plants. In turn the plants have evolved resistance (R) proteins to recognize these effectors to trigger effector-triggered immunity (ETI), a stronger and more massive resistance response, termed hypersensitive response (HR), that limits the growth of the pathogen and is associated with a programmed cell death localized at the pathogen infection site (Coll et al., 2011), leading to the resistance of the plant.

1.2.1.1 PAMP-induced immunity (PTI): plant basal defense

As mentioned above PTI initiates with the recognition of general elicitors, PAMPs/MAMPs/DAMPs, by plant PRRs. PAMPs/MAMPs are conserved structures or molecules distributed in various microbes including pathogenic and non-adapted

microorganisms and absent in plant hosts, while DAMPs are molecules released from the plant by microorganisms secreted enzymes (Lotze et al., 2007; Gohre and Robatzek, 2008). A dozen of PAMPs have been found up to now, which include flagellin, chitin, elongation factor Tu (EF-Tu), peptidoglycan, cold-shock protein, peptidoglycan, harpin (HrpZ), lipopolysaccharides (LPS), rhamnolipids, etc. (Sanabria et al., 2010). These "danger signals" are often perceived by PRRs localized at the plasma membrane of plant cells. PRRs can be divided into two main groups: receptor-like kinases (RLKs) with an intracellular serine/threonine kinase domain and receptor-like proteins (RLPs) with a short cytoplasmic tail. Both of them display extracellular domains which contain either leucine-rich repeats (LRRs) or LysM-motifs (Gohre and Robatzek, 2008). RLKs family counts more than 610 members in the genome of Arabidopsis and 56 members have been found encoding for RLPs in this model plant (Shiu and Bleecker, 2001; Fritz-Laylin et al., 2005). Interestingly, only a dozen of PRRs have been identified in mammalians. This higher number of PRRs identified in plants could allow for their better adaptation to changing environment as compared with animals, to overcome the lack of mobility and of a classical adaptive immune system (Gimenez-Ibanez and Rathjen, 2010). Among them the most well-studied ones include the RLKs flagellin-sensing 2 (FLS2) and the associated BRI1-associated receptor kinase-1(BAK1), and elongation factor Tu receptor (EFR), and the RLPs chitin elicitor-binding protein (CEBiP), *Lycopersicon esculentum* ethylene-inducing xylanase responding locus protein (LeEIX1/2) (Postel and Kemmerling, 2009).

The interaction of the elicitor flg22 with FLS2 associated with BAK1 has been extensively characterized for the induction of defense responses in plants. Flg22 corresponds to the conserved 22-amino acid peptide localized at the N terminus of bacterial flagellin. It is recognized by the receptor FLS2 which is present in many higher plants species like for instance *Vitis vinifera*, *Arabidopsis thaliana*, *Oryza sativa* and *Populus trichocarpa* (Boller and Felix, 2009). The receptor BAK1 belongs to the protein kinase family LRR II which counts 14 members. In absence of flg22, FLS2 and BAK1 are located closely but do not interact each other (Figure 2 lower left

corner). With the binding of flg22 (step 1) to the LRR domain of FLS2 induces conformation change of the receptor (step 2) allowing its interaction with BAK1 and leading to the formation of a flg22/ FLS2/BAK1 complex. This mechanism brings the intracellular kinase domains of both receptors close together, resulting in the activation of the intracellular response, including rapid ion fluxes, the production of reactive oxygen species (ROS) and nitric oxide (NO), MAP kinase (MAPK) activation, the induction of defense gene expression and cell wall reinforcement (Delledonne, 2005; Zipfel, 2008; Boller and Felix, 2009; Gimenez-Ibanez and Rathjen, 2010).

In *Arabidopsis thaliana*, flg22 induces callose deposition, the induction of pathogenesis-related (*PR*) gene expression and a strong inhibition of plant growth. The efficiency of defense responses induced by flg22 has been further demonstrated by pre-treating wild-type *Arabidopsis thaliana* plants with flg22. Such plants appeared more resistance to the infection with the virulent *Pseudomonas syringae pv. tomato* (*Pst*) DC3000. On the opposite *fls2* mutant plants lacking the receptor to flg22 are more susceptible to *Pst* DC3000 (Zipfel et al., 2004). In the same way, the silencing of *NbFLS2* which is orthologous of *fls2* in tobacco led to an increased growth of compatible, non-host and non-pathogenic strains of *P. syringae*, confirming the role of flg22/FLS2 interaction in protecting plants against infection (Hann and Rathjen, 2007). However this first line of defense may be not sufficient in response to

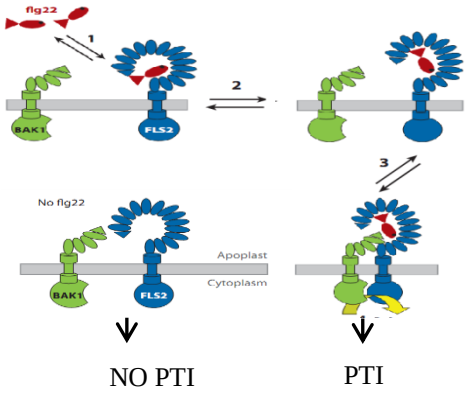

Figure 2 Model for flg22 induced interaction between FLS2 and BAK1. Adapted from Boller, T., and Felix, G. , 2009.

some pathogens able to regulate negatively these mechanisms.

Nowadays, DAMPs triggered immunity have been also reported (Boller and Felix, 2009), in which plant cell wall-derived oligogalacturonides (OGAs) can stimulate defense gene expression during pathogenesis (Doares et al., 1995), and HypSys and RALF can induce a MAPK cascade activation in tomato cells (Pearce et al., 2001b, a). However the DAMPs perception system remains poorly characterized. The best studied one is AtPep1/ PEPR1: the 23-aa peptide DAMP, AtPep1, which derives from a 92-aa precursor encoded within a small gene that is inducible by wounding, methyl jasmonate, and ethylene, has been found to be recognized by PERR (Arabidopsis RLKs), which leading to expression of the defensive gene (*PDF1.2*) and accumulation of H_2O_2 (Huffaker et al., 2006; Yamaguchi et al., 2006).

1.2.1.2 Effector-triggered susceptibility (ETS): suppression of plant defenses by the pathogen

Until now 57 families of effectors have been identified in *P. syringae* species (Baltrus et al., 2011; Lindeberg et al., 2012), among these strains *Pseudomonas syringae* pv. *tomato* DC3000 (*Pst* DC3000) represents an important model pathogen in molecular plant pathology (http://www.pseudomonas-syringae.org/pst_home.html). It uses the type III secretion system (TTSS) encoded by *hrp* (hypersensitive response and pathogenicity) / *hrc* (hrp conserved) genes to inject more than thirty distinct effectors into host cells during the infection, which suppress host cell defense responses at different levels and retrieve nutrients from the plant (Block et al., 2008; Gohre and Robatzek, 2008). The function of these effectors has been shown that plays a key role in pathogen virulence (Dodds and Rathjen, 2010; Gimenez-Ibanez and Rathjen, 2010; Block and Alfano, 2011; Lindeberg et al., 2012).

An overview of *Pseudomonas syringae* effectors and their effect on plant defense signaling has been shown in Figure 3. Some effectors can directly target PRRs to inhibit plant PTI. For instance, both AvrPtoB and AvrPto target FLS2 to block flg22-induced PTI through different mechanisms: AvrPtoB acts as an E3 ligase to

catalyze polyubiquitination of the kinase domain of FLS2 leading to receptor degradation, while AvrPto directly binds to the receptor kinase to block its activity (Gohre et al., 2008; Xiang et al., 2008). Some effectors target important regulators of plant defense mechanisms, such as AvrB, AvrRpm1 and AvrRpt2 that target and modify the protein RIN4 (RPM1-interacting protein 4) leading to the activation of this negative regulator of basal defense responses in *Arabidopsis thaliana* (Chisholm et al., 2006). Some effectors, like HopF2 (Wang et al., 2010) and HopAI1 (Zhang et al., 2007a), directly target and inhibit key components of defense signaling, such as MAPK cascades. HopAI1 mediates the dephosphorylation of AtMPK3, AtMPK4 and AtMPK6 (Zhang et al., 2007; Zhang et al., 2012) and is the only effector able to switch off MAPK cascade by directly targeting MAPKs by mimicking the function of the MAPK phosphatases (MKPs), while HopF2 inactivates the upstream MAPK activator MKK5 by ADP-ribosylation. Meanwhile some effectors do not directly target components of recognition or signaling but affect defense responses such as transcriptome reprogramming. One example is the effector HopU1, a

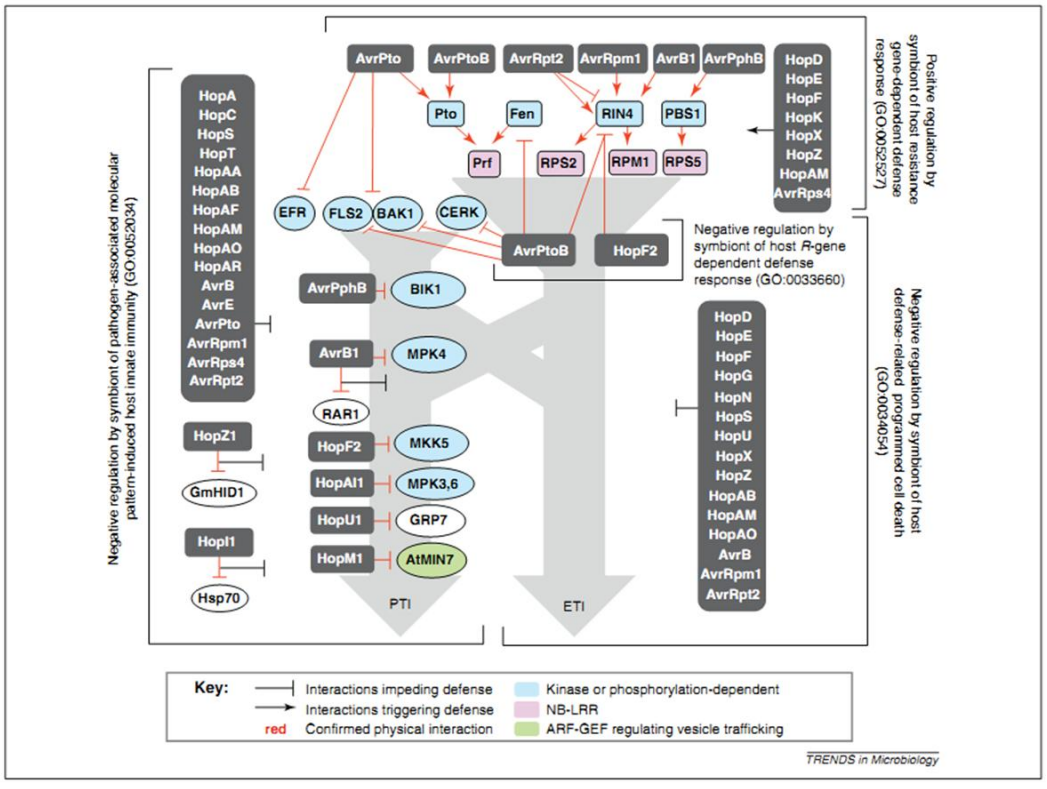

Figure 3 Overview of *Pseudomonas syringae* effector targets in PTI and ETI. Adopt from Lindeberg, M. et al 2012

mono-ADP-ribosyltransferase (ADP-RT) that ribosylates two glycine-rich RNA-binding proteins AtGrp8 and AtGrp7, which interfering with their ability to bind RNA and thus affecting RNA metabolism (Fu et al., 2007). Finally some effectors affect general cell processes such as vesicle trafficking, as demonstrated for HopM1. This virulence effector targets specifically AtMIN7, one of the eight members of the Arabidopsis adenosine diphosphate (ADP) ribosylation factor (ARF) guanine nucleotide exchange factor (GEF) protein family, triggering its degradation by the plant ubiquitination system (Nomura et al., 2006) and thus interfering with vesicle trafficking and extracellular secretion, which play important roles in plant immune response (Collins et al., 2003; Kwon et al., 2008).

To overcome PTI suppression by pathogen effectors, plants have evolved specific receptors able to recognize such virulence factors, synonymous of pathogen attack to induce strong defense mechanisms.

1.2.1.3 Effector-triggered immunity (ETI): the hypersensitive response

Pathogen type III effectors play like double-edged swords, because on one hand they promote pathogen virulence on susceptible plants, and on the other hand they expose the pathogen to a much stronger defense response in resistant plants. This effector-triggered immunity (ETI) is typically associated with a local cell death (HR) and the expression of defense-related genes leading to plant resistance. Over million years plants have evolved number of resistance (R) proteins to perceive these pathogenicity factors. R proteins are NB-LRR (nucleotide-binding site, leucine-rich repeat) proteins and as observed for PRR family, plants possess a higher number of these NB-LRR proteins as compared with vertebrates, with 125 different NB-LRR proteins identified in Arabidopsis and 460 in rice while only 20 in vertebrate (Meyers et al., 2003; Li et al., 2010; Lange et al., 2011). R proteins can be grouped into two main subclasses: coiled-coil (CC)-NB-LRR or Toll and human interleukin receptor (TIR) domain-NB-LRR (Lukasik and Takken, 2009; Eitas and Dangl, 2010).

Functional NB-LRR proteins can directly or indirectly recognize a specific bacterial type III effector during pathogen infection. For instance, type III effector PopP2 secreted by *R. solanacearum*, which belongs to the YopJ/AvrRxv protein family, is directly recognized by RRS1-R in Arabidopsis, which belongs to TIR-NBS-LRR subclass of R proteins and possesses a C-terminal WRKY motif characteristic of some plant transcriptional factors (Deslandes et al., 2003). In fact indirect recognition between effector and plant has been found more popular in the nature (Jones and Dangl, 2006; Maekawa et al., 2011). A well-established example of indirect recognition is the case of AvrRpt2 (Figure 4). AvrRpt2, a cysteine protease, is indirectly recognized by the R protein RPS2, via the modification of AvrRpt2 target RIN4, which normally forms a complex with RPS2. First AvrRpt2 is injected into plant cell by type III secretion system (step 1) and then is activated by the plant cyclophilin ROC1, which displays a peptidyl-prolyl*cis/trans*isomerase (PPIase) activity and leads to AvrRpt2 activation (step2). Activated AvrRpt2 processes itself and cleaves RIN4 (step3), resulting in the release of RPS2 from RIN4/RPS2 complex. Released RPS2 thus triggers the rapid activation of ETI (step 4), triggering HR and limiting pathogen growth in plant leaves (Figure 2) (Chisholm et al., 2006; Shindo and Van der Hoorn, 2008).In addition both AvrPtoB and AvrPto are also indirectly recognized by R protein in tomato resistance cultivars. Instead of directly binding with R protein Prf, AvrPtoB and AvrPto bind the tomato protein kinase Pto, which

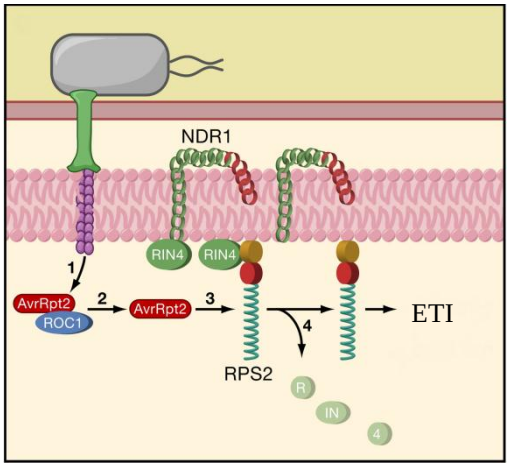

Figure 4 Model for AvrRpt2 induced ETI. Adapted from Chisholm, S.T. et al. 2006.

form a complex with Prf (Maekawa et al., 2011).

1.2.2 Signal transduction during plant defense

Although during PTI and ETI plant cells deploy different molecules to perceive PAMPs and effectors, they activate similar signaling pathways and signal events, which including ion fluxes, activation of mitogen-activated protein kinases (MAPKs), cGMP, alternation of hormone network, ROS burst and NO burst, and reprogramming of gene expression in plant (Dodds and Rathjen, 2010; Gimenez-Ibanez and Rathjen, 2010; Tsuda and Katagiri, 2010). Usually the outcome of disease response of PTI is considered to be more quicker, weaker and shorter than ETI, but now responses typically associated with ETI, which including HR and systemic acquired resistance (SAR), have been also observed in PTI (Tsuda and Katagiri, 2010; Thomma et al., 2011).

1.2.2.1 Second messengers: ion fluxes and cGMP

As one of the earliest plant cell cellular responses to pathogen, ion fluxes, including influx of H^+ / Ca^{2+} and efflux of K^+ / NO_3^-, occur within minutes after pathogen recognition and are responsible amongst others for an alkalization of the extracellular medium (Ma and Berkowitz, 2007; Boller and Felix, 2009). Among those ions, Ca^{2+} is one of the best characterized second messengers and it is involved in the activation of numerous downstream signaling events involved in the regulation of plant defense, such as production of ROS and NO, kinase (MAPKs and CDPKs) activation and the opening of other membrane ion channels (Ma and Berkowitz, 2007). The treatment of *Arabidopsis thaliana* seedling with the PAMPs flg22, elf18 or fungal N-acetylchitooctaose (ch8), or with the plant-derived DAMP Pep1, induce a strong $[Ca^{2+}]_{cyt}$ increases after less than 5 minutes. Pre-treatment of the seedlings with either $LaCl_3$ (a Ca^{2+} -channel blocker) or BAPTA (a membrane-impermeable Ca^{2+}chelator) completely inhibit the MAMP/DAMP-induced $[Ca^{2+}]_{cyt}$ elevations (Ranf et al., 2011).

A similar observation has been reported during ETI, where both Ca^{2+} -channel blockers $LaCl_3$ and $GdCl_3$ can block *Pst avrRpm1*-triggered HR in Arabidopsis. Ans the Ca^{2+} channel CYCLIC NUCLEOTIDE-GATED CHANNEL2 (CNGC2/DND1) seems responsible for the influx of Ca^{2+} into cells and provide a model linking Ca^{2+}current to downstream NO production during ETI- induced HR (Andersson et al., 2006; Ali et al., 2007).

These studies on cyclic nucleotide gated channels, which are known targets of cyclic nucleotides have suggested an involvement of cyclic nucleotides like cGMP and cAMP in plant response to biotic stresses (Meier and Gehring, 2006; Meier et al., 2009).

In animal systems cGMP is a well-known second messenger of NO and its level is controlled by guanylate cyclases (GCs), which soluble form of them can be activated by NO (Potter, 2011). Although in plants several of have been shown have guanylate cyclase activity, which including AtGC1(Ludidi and Gehring, 2003), AtBR1(Kwezi et al., 2007), CrCYG56 (de Montaigu et al., 2010), AtWakl10(Meier et al., 2010), AtPSK (Kwezi et al., 2011), AtpepR1 (Mulaudzi et al., 2011) and AtNOGC1 (Mulaudzi et al., 2011), the GC responsible for synthesizing cGMP during plant defence has not been clearly identified yet (Mulaudzi et al., 2011).

Nevertheless, as we already mentioned, an involvement for cyclic nucleotides both in PTI as well as in ETI is clearly emerging from current studies based on pharmacological approaches (Martinez-Atienza et al., 2007). NO accumulation in a guard cell system induced by the PAMP lipopolysaccarides (LPS) has been shown to be dependent on the presence of the calcium channel CNGC2 but also on cyclic nucleotides (Ali et al., 2007, Ma et al. 2009). Similarly, during ETI, the already reported Ca^{2+} cytosolic concentration increase linked to NO generation and HR is also dependent on cyclic nucleotides (Ma et al., 2009). Applying an inhibitor of cyclic nucleotide synthesis Ca^{2+} influx and HR development can be both strongly reduced. Furthermore by using GC inhibitors or cGMP analogs it has been shown the involvement of cGMP in defence gene induction during ETI (Durner et al., 1998), as well as in NO induced cell death (Clarke et al., 2000). Finally, recently a first direct

evidence about accumulation of cGMP upon pathogen infection has been also reported (Meier et al., 2009).

1.2.2.2 Mitogen-activated protein kinases (MAPKs)

Mitogen-activated protein kinases (MAPK or MPKs) represent a key component of signal transduction in eukaryotes. In plants, a large body of evidences supports a central role for MAPK during many physiological processes and in particular during plant defense responses (both PTI and ETI). Their involvement has been reported in Arabidopsis, parsley, tobacco, rice and tomato (Pitzschke et al., 2009; Rodriguez et al., 2010). Typically organized as phosphorylation cascades, they are responsible for the transduction of environmental and developmental signals from extracellular receptors into intracellular responses. A minimal MAPK module is composed of three components: a MAPK Kinase Kinase (MAPKKK), a MAPK Kinase (MAPKK) and MAPK. Upon stimulation, MAPKKK phosphorylates and actives MAPKK, which in turn can phosphorylate and active a downstream MAPK. The outcome of MAPK cascade is the phosphorylation of various substrates to regulate their function, such as transcription factors and other protein kinases (Pitzschke et al., 2009; Rodriguez et al., 2010; Tena et al., 2011). All the components of MAPK cascades are conserved in higher plants. For example, in the genome of *Arabidopsis thaliana* genes have been

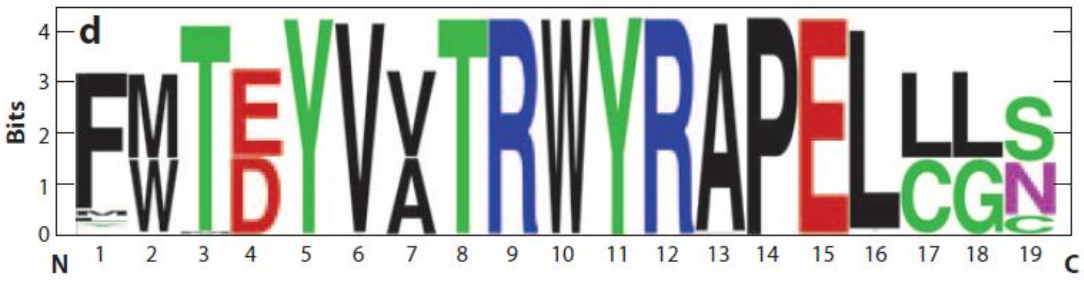

Figure 5 WebLogo of the most conserved consensus motifs in the catalytic domains of known MAPKs in plants. Adapted from Rodriguez, 2010

Stack heights represent conservation at aposition, and symbol heights within a stack represent the relative frequency of each residue.

identified encoding about 80 MAPKKKs, 10 MAPKKs, and 20 MAPKs (MAPK-Group, 2002). For instance TDY or TEY phosphorylation motifs are highly conserved in plant MAPK activation loops, which is similar to animal ERK kinases (Figure 5) (Rodriguez et al., 2010).

Some complete MAPK cascades have been reported during plant defense responses. In particular two of the best characterized cascades, MEKK1/MKKKx-MKK4/5/-MPK3/6 and MEKK1-MKK1/2-MPK4, have been shown in *Arabidopsis thaliana*. Both of them are rapidly activated during PTI, playing antagonistic roles during this process (Pitzschke et al., 2009; Dodds and Rathjen, 2010). Flg22 recognition by FLS2 in *Arabidopsis thaliana* activates MEKK1 and likely other still unknown MKKKs, leading to the activation of MKK4/MKK5, which in turn phosphorylate and activate MPK3 and MPK6 (Asai et al., 2002). Active MPK3/6 phosphorylate in turn a set of proteins, such as the protein PHOS32 (Merkouropoulos et al., 2008), an ethylene response factor (ERF104), the ACC synthase (ACS2/6) (Bethke et al., 2009). The phosphorylation of ACS2/6, involved in ethylene biosynthesis, increases their stability and activity leading to the production of the hormone (Liu and Zhang, 2004). Moreover AtMPK3/6 induce the expression of several transcription factors, including WRKY29 and WRKY22 that are positive regulators of plant disease resistance, regulating the expression of numerous defense-related genes (Asai et al., 2002). Furthermore *Arabidopsis thaliana* plants transiently expressing the active forms of MEKK1, MKK4 or WRKY29 exhibit enhanced resistance to both bacterial (*P. syringae*) and fungal pathogens (*B. cinerea*), demonstrating the role of this MAPK cascade in plant resistance (Asai et al., 2002). However, some contradictory results have been further obtained from genetic studies showing that MEKK1 is not required for flagellin-triggered activation of MPK3 and MPK6 but is involved in the activation of MPK4 via MKK1 and MKK2 (Ichimura et al., 2006; Suarez-Rodriguez et al., 2007; Gao et al., 2008). A mutant knock-out for *mekk1* exhibits dwarfism and lethality phenotype, although it shows a normal activation of MPK3 and MPK6 after treatment with flg22 (Ichimura et al., 2006). In the same way, *mkk1/mkk2* double mutant and *mpk4* mutant also show severe dwarfed

and lethal phenotype. All three mutants show an higher accumulation of H_2O_2, a constitutive pathogenesis-related gene expression and enhanced resistance to pathogens, which are likely caused by high levels of salicylic acid (Brodersen et al., 2006; Gao et al., 2008). According to such a phenotype, this MAPK cascade is considered to regulate negatively defense responses. Furthermore MPK4 seems to exert its function by suppressing the activity of its substrates, which include WRKY33, WRKY25 and MKS1 (Andreasson et al., 2005).

MAPK cascades are also involved in ETI and regulate Avr-triggered HR and SAR. The activation of MAPKs during ETI has been observed in several plants. For instance, fungal Avr9 effector activates the MAPKs SIPK and WIPK when applied on tobacco cells expressing the *Cf-9* resistance gene (Romeis et al., 1999). In the same way, the infection of *Arabidopsis thaliana* plants with *Pst* DC3000 carrying *avrRpt2* or *avrB* genes induce the activation of AtMPK3 and AtMPK6 (Underwood et al., 2007). In tobacco plants, a complete cascade has been reported to be involved during the HR. Indeed, the cascade involving MAPKKK-MEK1/MEK2-SIPK/NTF6 is required for Pto-mediated HR response and resistance against *Pseudomonas syringae* pv. tomato (Ekengren et al., 2003). Overexpression of an active MAPKKKα in leaves activates MAPKs and causes pathogen-independent hypersensitive-like cell death (Ekengren et al., 2003; del Pozo et al., 2004). Similarly the transient expression of the active form of NtMEK2, AtMEK4 and AtMEK5 in *Arabidopsis thaliana* or tobacco leaves trigger HR-like cell death via MAPK activation (Ren et al., 2002). In addition, MAPK cascades can regulate SAR triggered by effectors. Beckers, et al (2009) reported that *Arabidopsis thaliana mpk3* or *mpk6* mutants display a loss or reduction of defense gene expression priming and SAR establishment upon infection with *Pst* DC3000 carrying the avirulence gene *avrRpt2* (Beckers et al., 2009), while plants overexpressing AtMKK7 and or silenced for *mpk4* exhibit constitutive SAR, including increased SA levels, constitutive *PR* gene expression, and resistance to pathogens (Petersen et al., 2000; Zhang et al., 2007b).

1.2.2.3 Reactive oxygen species and reactive nitrogen species

As highly reactive radicals, reactive oxygen species (ROS), which consists of superoxide radical ($O_2^{\cdot -}$), hydrogen peroxide (H_2O_2), hydroxyl radical ($OH^{\cdot}$) and singlet oxygen ($^1O_2$), etc., and also reactive nitrogen species (RNS) including NO and the NO-derived molecules such as nitrogen dioxide ($^{\cdot}NO_2$), dinitrogen tridoxide (N_2O_3), peroxynitrite ($ONOO^-$), *S*-nitrosoglutathione (GSNO), etc. have been shown to play import roles in plant immunity (Torres et al., 2006; Hong et al., 2008; Leitner et al., 2009; Vellosillo et al., 2010).

Both production of ROS (primarily H_2O_2, and $O_2^{\cdot -}$) and RNS (primarily NO) are the ones of earliest cellular responses during PTI and ETI. PAMPs such as flg22, lipopolysaccharide (LPS) and cryptogein have been shown that can all induce a transient production of ROS (Felix et al., 1999; Meyer et al., 2001; Ashtamker et al., 2007) and NO (Zeidler et al., 2004; Melotto et al., 2006; Besson-Bard et al., 2008b). Similarly ETI also can trigger both ROS and NO production. Delledonne et al. (1998) reported that inoculation of soybean cell suspensions with the avirulent pathogen, *P. syringae pv. glycine*, induces a dramatical accumulation of NO and H_2O_2 in few hours (Delledonne et al., 1998). In line with this observation the challenge of wild-type *Arabidopsis thaliana* leaves with *P. syringae* DC3000 carrying *AvrB* and *AvrRpt2* can induce H_2O_2 accumulation after 5-7 h and NO accumulation after 3-6 h (Shapiro and Zhang, 2001; Zhang et al., 2003).

A. Production of reactive oxygen species and reactive nitrogen species

To date, both non-enzymatic and enzymatic sources of ROS and RNS, which also involve some organelles such as chloroplasts, mitochondria and peroxisome, have been found in plant under stress or normal conditions (Apel and Hirt, 2004; Mittler et al., 2004; Leitner et al., 2009; Torres, 2010; Frohlich and Durner, 2011).

The NADPH oxidase, also known as respiratory burst oxidase homologues (RBOH), has been proposed as a major source for ROS burst in most PTI and ETI. This enzyme catalyzes the production of superoxide that can be quickly dismutated to

O_2 and the H_2O_2 by superoxide dismutase (SOD) nearby (Torres et al., 2006; Suzuki et al., 2011). Additionally some other enzymes were also reported to be involved in the production of ROS during PTI and ETI, such as diamine oxidases and cell wall peroxidases (Torres, 2010). Recently by using both of genetic and pharmacologic tools Bolwell's group showed that two cell wall peroxidases, PRX33 and PRX34, contribute about half amount of the H_2O_2 which accumulates in response to MAMP including *F. oxysporum* cell wall elicitor, flg22, Elf26, and oligogalacturonide, and that NADPH oxidases and other sources, such as mitochondria, account for the remainder of the ROS (Daudi et al., 2012; O'Brien et al., 2012). Finally enzymes belonging to the scavenging/antioxidant systems may also contribute to ROS burst in PTI and ETI, such as SOD, catalases (CAT) which directly dismutate H_2O_2 into H_2O and O_2, and ascorbate peroxidases (APX) that function as scavengers of H_2O_2 (Mittler et al., 2004).

Very recently Frohlich and Durner summarized all the NO sources that have been reported or proposed so far in plants (Frohlich and Durner, 2011). Several of them are believed to produce NO during plant disease defense, including NOS-like enzyme, nitrate reductase (NR), and mitochondrial-dependent NR activity (Hong et al., 2008; Leitner et al., 2009; Frohlich and Durner, 2011). However which one is the main source of NO production during PTI and ETI is still under continuous debate. In animal, nitric oxide synthase (NOS) generates NO by conversion of L-arginine to L-citrulline, and represents the main enzymatic source of NO in this system (Palmer et al., 1993). However *in silico* searches failed to identify orthologous of mammalian NOS in plants, and NOS-like enzymes are still unidentified in green flowering plant. Nitrate reductase (NR) can catalyze the synthesis of NO and N_2O from nitrite, but under aerobic conditions it displays only 1% of its nitrate reduction capacity to produce NO even at saturating NADH and nitrite concentrations, meanwhile it can be inhibited by physiological nitrate concentrations (K_i 50μM). It thus appeared that NR is the main enzyme responsible for NO production from nitrite under aerobic conditions (Rockel et al., 2002). Similarly mitochondrial-dependent NR activity that can produce NO is also strongly favored by anaerobic conditions (Gupta et al., 2011).

B. Kinetics of mechanisms for ROS and RNS production

Although ROS and RNS bursts have been observed both during PTI and ETI, their kinetics are different depending on the level of defense response. ETI typically elicits a biphasic ROS and NO bursts, which include a fast and weaker first peek (within the first minutes) followed by a stronger and long-lasting peek (after few hours of infection) as compared with PTI-triggered ROS and RNS bursts (Lamb and Dixon, 1997; Delledonne et al., 1998).An experiment with soybean cell suspensions performed by Delledonne et al. (1998), a rapid, relatively weak NO production stimulation by both avirulent and virulent strains, which starts within 1h was shown , which then is followed by a several-fold greater second NO production (at 6 h), concomitantly with the Avr-dependent oxidative burst (Delledonne et al., 1998).

C. Direct and indirect effects of ROS and RNS

Due to the high reactive property of these radicals, ROS and RNS can act directly as antibiotic agents or work as secondary stress signals to induce various defense responses (Delledonne, 2005; Torres et al., 2006; Hong et al., 2008; Vellosillo et al., 2010). They signal in plant innate immunity either independently or coordinately. ROS alone have been proved to have several special functions, including to kill the pathogen, promote hydroxyl, cross linking of cell wall glycoprotein to help plant establishment of physical barriers, media defense gene activation by modification of transcription factors, and associate with SA signaling (Torres et al., 2006; Torres, 2010). Similarly RNS alone induce the expression of the defence-related genes including phenylalanine ammonia lyase (*pal*) and pathogenesis-related protein 1 (*pr1*), induce cGMP accumulation and are involved in SA signaling inducing SAR (Delledonne, 2005; Hong et al., 2008).

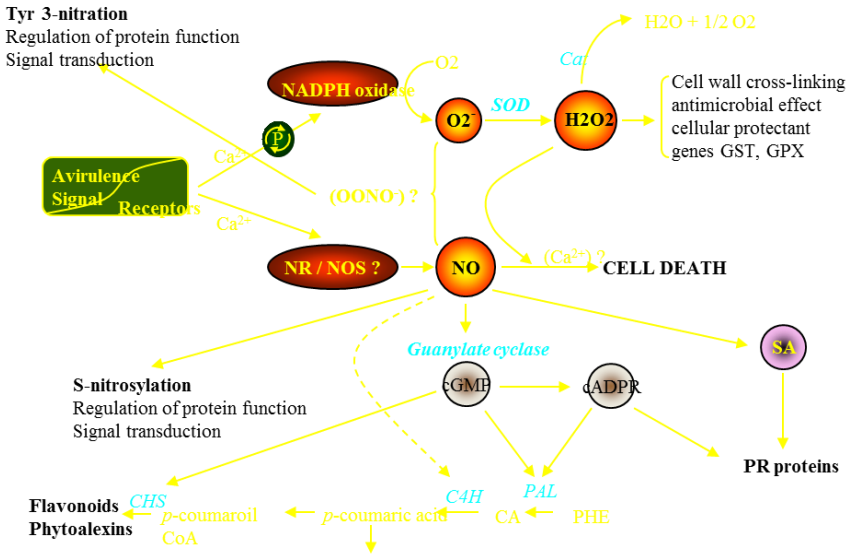

Figure 6 NO signaling in ETI. Adapted from Delledonne, M. 2005 and Leitner, M. et al., 2009
CA, cinnamic acid; Ca2+, calcium influx; cADPR, cyclic ADP ribose; Cat, catalase; C4H, cinnamic acid-4-hydroxylase; CHS, chalcone synthase; cGMP, cyclic GMP; GPX, glutathione peroxidase; GSNO, S-nitroso-l-glutathione; GST, glutathione S-transferase; NOS, nitric oxide synthase; $ONOO^-$, peroxynitrite; PAL, phenylalanine ammonia lyase; PHE, phenylalanine; PR, pathogenesis-related proteins; SA, salicylic acid; SOD, superoxide dismutase.

Moreover NO crosstalk with ROS also plays a central role in plant defense (Delledonne, 2005; Asai and Yoshioka, 2009). Especially in ETI it triggers HR cell death. The hypersensitive response has been shown to be dependent on simultaneous and balanced production of NO and ROS (Delledonne et al., 2001). Furthermore other aspects of NO signaling network which takes place during plant disease resistance (particular in ETI) have been described by Delledonne (Figure 6) (Delledonne, 2005). In animals NO cooperates with $O_2^{\cdot -}$ generated from NADPH oxidase to produce $ONOO^-$, which is responsible for killing the cells. In plants, instead, NO cooperates with H_2O_2, produced from $O_2^{\cdot -}$ dismutation catalyzed by superoxide dismutase (SOD), to regulate ETI triggered HR cell death.

ROS and RNS beside achieving their function by directly or indirectly reacting with a small molecules as described (like ROS, RNS and polyunsaturated fatty acids), they also react and modify macro biological molecules (like DNA and proteins) (Moller et al., 2007; Feelisch, 2008).

Nowadays post-translational modifications of proteins are emerging as a key mechanism used by ROS and RNS to exert their bioactivity (Moller et al., 2007; Besson-Bard et al., 2008a; Leitner et al., 2009). ROS and RNOS are generally responsible for protein oxidation, and RNS mediate metal-nitrosylation, tyrosine nitration and *S*-nitrosyatlion (Figure 7) (Besson-Bard et al., 2008a; Feelisch, 2008) .

Protein oxidation: ROS and RNOS usually cause protein oxidation by directly modifying some amino acids of target proteins, including Cys, Met, Trp, His, Arg. Only the oxidation of sulfur-containing amino acids (Cys and Met) appears to be reversible. Irreversible protein oxidation often leads to the degradation of the oxidized target by proteases or the autophagy process (Apel and Hirt, 2004; Moller et al., 2007). Although no proteins specifically oxidized during ETI or PTI have yet been identified, some evidences indicate that protein oxidation could play a role during these processes. For instance, the aconitase, which catalyzes the inter conversion of citrate and isocitrate in the Krebs cycle, has been shown to be oxidized on Trp residues even in absence of stress (Moller and Kristensen, 2006). Interestingly this enzyme has been also shown that regulates resistance to oxidative stress and cell death in *Arabidopsis thaliana* and *N. benthamiana* (Moeder et al., 2007). The infection of

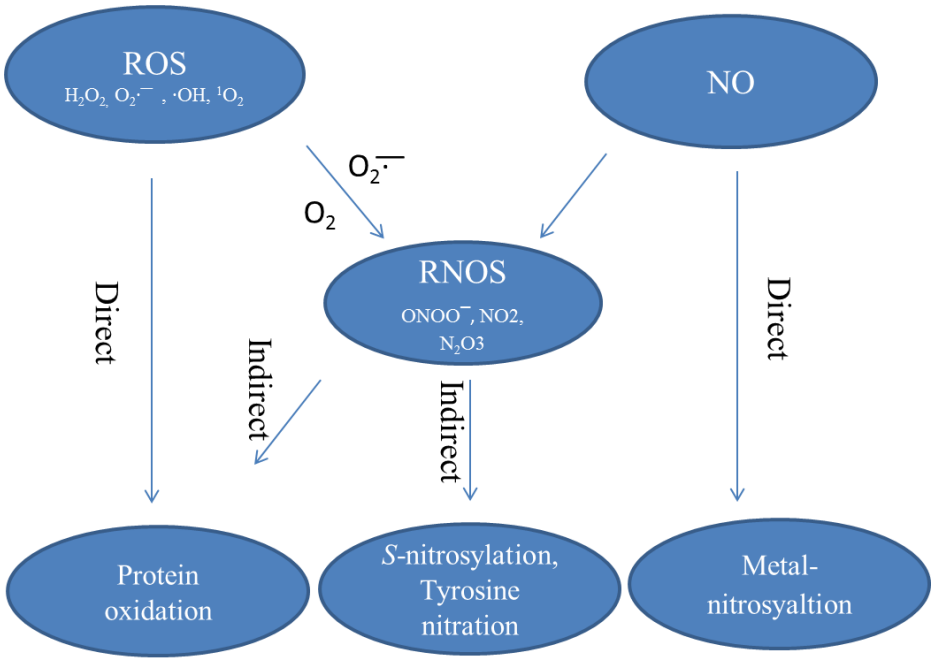

Figure 7 ROS and RNS mediated protein modification

aconitase-silenced *N. benthamiana* plants expressing the Pto transgene with *Pseudomonas syringae* pv. *tabaci* carrying *avrPto* displayed a delayed hypersensitive response (HR) and an increased susceptibility. Moreover several oxidized proteins have been found in mitochondria, including several other enzymes involved in the Krebs cycle, the superoxide dismutase, the glycine decarboxylase and some heat shock proteins (Moller and Kristensen, 2004).

Metal-nitrosyltaion: NO can reversibly bind transition metals in the centers of iron sulfur clusters, heme, and zinc-finger proteins by donating electrons (Besson-Bard et al., 2008a). Meltal-nitrosyaltion of proteins can induce conformational changes finally affecting their function. Several examples of plant proteins which can be subjected to metal-nitrosylation have been reported, including soybean lipoxygenase, avocado 1-aminocyclopropane-1-carboxylic acid (ACC) oxidase (ACCO), tobacco catalase and ascorbate peroxidase, leghemoglobin (Lb) (Nelson, 1987; Rocklin et al., 1999; Clark et al., 2000; Herold and Puppo, 2005).

Tyrosine nitration: NO_2^+, derived from NO_2, or $ONOO^-$ can attack one of the two equivalent carbons (carbon 3) in the aromatic ring of Tyr residues, leading to formation of 3-nitrotyrosine (Besson-Bard et al., 2008a; Vandelle and Delledonne, 2011). During the HR development induced by avirulent pathogens NO burst and ROS burst lead to an accumulation of both NO and $O_2^{\cdot -}$, which can easily form the $ONOO^-$. Indeed an accumulation of $ONOO^-$ during the HR, has been recently shown by using the specific peroxynitrite-sensitive fluorescent dye HKGreen-2 (Saito et al., 2006; Gaupels et al., 2011). According to these results a physiological role for tyrosine nitration in NO-mediated signaling in plant disease resistance has been hypothesized (Alamillo and Garcia-Olmedo, 2001; Saito et al., 2006; Vandelle and Delledonne, 2011). Furthermore, by applying a proteomic approach a first list of proteins undergoing Tyr-nitration during the HR in plant has recently been produced (Cecconi et al., 2009). A further characterization of nitrated proteins during defense will allow better clarifying the role of Tyr-nitration in defense signaling.

Table 1. List of well-studied *S* -nitrosylated proteins in plant. Adapted from Astier et al., 2011

Protein identified		Organism	Effect of S-nitrosylation
Non-symbiotic hemoglobin	AtHb1	*A. thaliana*	NO detoxification
Prometacaspase 9	AtMC9	*A. thaliana*	Inhibition of autoprocessing and activity
S-adenosylmethionine synthetase 1	SAMS1	*A. thaliana*	Inhibition of activity
Peroxiredoxine II E	PrxIIE	*A. thaliana*	Inhibition of activity
MYB domain protein 2	AtMYB2	*A. thaliana*	Inhibition of DNA Binding
Non expressor of pathogenesis related gene 1	NPR1	*A. thaliana*	Conformational changes
Salicylic acid-binding protein 3	AtSABP3	*A. thaliana*	Inhibition of activity and SA binding
TGAGG motif binding factor 1	TGA1	*A. thaliana*	Conformational and DNA/NPR1 binding behaviour changes
Phytochelatins	PC	*A. thaliana*	ND
Glyceraldehyde-3-phosphate dehydrogenase	GAPDH	*A. thaliana*	Inhibition of activity
Glyceraldehyde-3-phosphate dehydrogenase	GAPDH	*N. tabacum*	Inhibition of activity
Glycine decarboxylase	GDC	*A. thaliana*	Inhibition of activity
Ribulose 1,5 bisphophate carboxylase/oxygenase	Rubisco	*K. pinnata*	Inhibition of activity
Ribulose 1,5 bisphophate carboxylase/oxygenase	Rubisco	*B. juncea*	Inhibition of activity
NAPH oxidase	AtRBOHD	*A. thaliana*	Inhibition of activity

***S*-nitrosylation:** NO^+ attacks on thiol groups of Cys resisudes. In addition to direct NO^+ attack, *S*-nitrosylation can be mediated by small molecules (*S*-nitrosoglutathione, GSNO, for example) or nitrosylated proteins working as *S*-nitrosylation agents by a mechanism named transnitrosylation in which NO is exchanged between these molecules and proteins with the reactive thiolate (Astier et al., 2011).

Among NO-mediated posttranslational modifications of protein, *S*-nitrosylation, is the best characterized (Leitner et al., 2009; Astier et al., 2011). At proteomic level investigations on *S*-nitrosylated proteins in different physiological contexts have been done by several groups and dozens of target proteins have been identified (Lindermayr et al., 2005; Abat et al., 2008; Romero-Puertas et al., 2008; Abat and Deswal, 2009; Tanou et al., 2009; Palmieri et al., 2010). In more detail, *S*-nitrosylated proteins in *Arabidopsis thaliana* undergoing hypersensitive response (HR) have been identified which are mostly enzymes serving as intermediary metabolism or involved in signaling and antioxidant defense (Romero-Puertas et al., 2008).

To date, the structural, functional and physiological effects of *S*-nitrosylation have been further investigated on a number of plant *S*-nitrosylation target proteins. A complete list is shown in table 1 (Astier et al., 2011). According to these studies *S*-nitrosylation has been shown to affect protein activity, or localization, or ligand binding properties and these effects are often mediated by conformational changes induced by *S*-nitrosylation. Interestingly many proteins involved in plant defence are included in this list, like NPR1, PrxIIE, AtSABP3, GDC, GAPDH, AtMC9 and NADPH oxidase.

1.2.2.4 Hormone mediated pathways in plant defense signaling

The plant hormone SA (Salicylic acid), JA (Jasmonic acid), and ET (Ethylene) mediated signaling pathway can be also activated during both PTI and ETI and mediate the defense responses (Bari and Jones, 2009; Pieterse et al., 2009). SA- JA - ET are considered as backbone of the plant induced defense signaling network. Usually SA mediates plant resistance response only to biotrophs or hemibiotrophs by the induction of pathogenesis related (PR) genes. JA and ET instead work synergistically mediating plant resistance response to biotrophs, necrotrophs and herbivorous insects (Pieterse et al., 2009; Verhage et al., 2010). A strong crosstalk between these different pathways has been reported. SA suppress JA responsive gene expression (including *PDF2.*1 and *VSP2*) via activation of NPR1-WRKY/GRX480 singling pathway. Muntant plants deficient for these gene show strong decrease in SA mediated suppression of JA responsive gene expression (Pieterse et al., 2009). In turn, the JA-responsive JIN1/AtMYC2 transcription factor negatively regulates SA signaling. The *jin1* mutant plants showed reduced susceptibility to *PST* DC3000 and increased SA signaling marker genes *PR-1* (*pathogenesis-related-1*) expression which dependent on SA accumulation (Laurie-Berry et al., 2006). Furthermore ET bypasses the NPR1 dependency of the SA-mediated antagonistic effect on JA signaling and renders the JA response insensitive to subsequent suppression by SA (Leon-Reyes et al., 2009; Leon-Reyes et al., 2010). Finally recent studies have shown that also abscisic acid (ABA), auxins, gibberellins, and brassinosteroids are also involved in plant defense signaling pathways against *P.syringaes* (Bari and Jones, 2009; Pieterse et al., 2009; Gimenez-Ibanez and Rathjen, 2010).

1.2.2.5 Reprogramming of gene expression

During both PTI and ETI a dramatic reprogramming of the transcriptome in the host plant also takes place. Flg22 plant treatments lead to an alteration in expression for a large number of genes already after 30 minutes from the treatment. which include 966 of upregulated genes and 202 of downregulated genes. Some of fast upregulated genes have been reported to be involved in Flg22 induced PTI, including *fls2, mekk1, mkk4, mpk3* and *wrky22* (Zipfel et al., 2004). Furthermore during PTI a list of genes commonly up-regulated by different PAMPs (chitin, flg22 and elf26) has been identified, indicating an unknown downstream step leading to induction of common downstream genes (Wan et al., 2008).

Similarly different effectors have also been shown to induce common downstream genes probably triggering some unknown common signal transduction mechanisms. Inoculation of wild-type Arabidopsis plants with *Pst* carrying either *avrRpt2* or *avrB*, induced similar expression profiles both at early and late time points upon infection (Tao et al., 2003). After 3 h correlation between mRNA profiles is 0.96 between *Pst* carrying either *avrRpt2* or *avrB* , and even after 6 and 9 h the correlations between the mRNA expression profiles was still very high (0.92 at 6 h and 0.93 at 9 h). Futhermore an overlap between genes induced by PAMPs and effectors has also been reported at early time points upon infection (Navarro et al., 2004). Navarro et al found that approximately 45% of the flg22-rapidly elicited (FLARE) genes were induced 3 hpi with Pst carrying either *avrB* or *avrRpt2* while at 6 hpi a decrease in the overlap between FLAR E genes and genes up-regulated by AvrB and AvrRpt2 race-specific elicitors has been oberserved. At this time only approximately 25% of overlap was found between the flg22-induced genes and genes induced by either *avrB* or *avrRpt2*. These data are in agreement with data produced by genetic approaches which suggest PTI and ETI may share common signaling pathways.

2. Scope of the thesis

Among the strains of *Pseudomonas syringae*, the *Pseudomonas syringae* pv. tomato DC3000 (*Pst* DC3000), which induces bacterial speck both on tomato and *Arabidopsis thaliana*, represents an important model in molecular plant pathology (http://www.pseudomonas-syringae.org/pst_home.html) and has been the first completely sequenced *Pseudomonas syringae* strain. During the process of plant infection, we already mentioned that an important step for bacterial pathogenicity is the secretion of effectors into the apoplast or cytoplasm of plant cells, in order to suppress plant disease resistance and to promote bacterial virulence (Abramovitch et al., 2006; Cunnac et al., 2009). Like many animal and plant Gram-negative bacterial pathogens, *Pst* DC3000 uses the type III secretion system (TTSS), which is encoded by *hrp* (hypersensitive response and pathogenicity) / *hrc* (hrp conserved) genes to promote virulence by injecting 36 distinct effectors into host cells during the infection (Lindeberg et al., 2005; Lindeberg et al., 2006). Such effectors can suppress host cell defense responses at different levels and retrieve nutrients from the plant (Block et al., 2008; Gohre and Robatzek, 2008).

One mechanism employed by bacterial pathogen effectors to impair plant defense is the suppression of MAPK cascade activity, which plays a key role in the establishment of plant resistance to pathogens. Among the several effectors that target MAPK cascade. The function of HopAI1 was first reported by Li et al. (2005), who demonstrated its role in promoting nonpathogenic bacterial growth and in suppressing the expression of the flg22-induced *NHO1* gene, required for non-host resistance against *Pseudomonas*(Li et al., 2005). Later the same group described the enzymatic activity of HopAI1 that belongs to a new family of enzymes, the phosphothreonine lyases widely conserved in both plant and animal bacterial pathogens (Li et al., 2007). Unlike the dephosphorylation catalyzed by protein phosphatases that cleave the phosphate group at the CO-P bond from the phosphorylated amino acid, phosphothreonine lyases specifically cleave the C-OP bond from a phosphothreonine in the pThr-X-pTyr motif present in MAPKs (Li et al., 2007; Zhang et al., 2007a; Chen et al., 2008; Brennan and Barford, 2009). This mechanism of dephosphorylation, unlike the one catalyzed by phosphatases, is irreversible. Surprisingly, the first report

on HopAI1 capacity to suppress flg22-induced plant defense responses showed that HopAI1 does not inhibit flg22-induced MAPK activation in mesophyll cells (He et al., 2006). However, Zhang et al. (2007) reported later a strong inhibitory effect of HopAI1 that directly targets and irreversibly dephosphorylates AtMPK3 and AtMPK6 *in vivo*, resulting in the suppression of PTI induced by flg22 in *Arabidopsis thaliana*, including the inhibition of MAPK-mediated gene expression, ROS production and callose depostion, promoting pathogen virulence (Zhang et al., 2007a). Thus, it has been proposed that in overexpression experiments the ratio of HopAI1 to MAPK protein level may be critical for HopAI1 suppressor activity (Shan et al., 2007).

Curiously, despite the demonstrated capacity of HopAI1 to suppress basal defense mechanisms that could be beneficial for *Pseudomonas* virulence, it has been reported that in *Pst* DC3000 strain the gene encoding this effector belongs to a disrupted operon in which a transposon insertion into one of the genes (Greenberg and Vinatzer, 2003; Schechter et al., 2004) is predicted to abolish the expression of HopAI1. It has thus been hypothesized that the presence such cryptic or disrupted *hop* genes like *hopAI1* in *Pst* DC3000 could be the result of a selection based on evolution and that if these genes were functional, they would cause *Pst* DC3000 to become avirulent in susceptible hosts like tomato and *Arabidopsis thaliana* (Schechter et al., 2006). However, the expression of HopAI1 in *Pst* DC3000 did not lead to HR induction in none of the host plants analyzed, demonstrating that it is not recognized by R protein(s) and thus suggesting that another mechanism could be responsible for its elimination from *Pst* DC3000 effector repertoire (Schechter et al., 2006). An alternative would be that these effectors could be useless for pathogen fitness during host infection due to the existence of undiscovered host mechanisms to defend against these effectors. In accordance with this hypothesis, it has been reported that interestingly, contrary to the majority of the *Pseudomonas* effectors, HopAI1 expressed in an avirulent strain of *Pseudomonas fluorescens* was unable to suppress the HR induced by the avirulent HopA1 in tobacco plants (Guo et al., 2009). Indeed, it is well-known that the hypersensitive cell death induced by avirulent pathogens in tobacco is mediated by MAPK cascade (Romeis et al., 1999; del Pozo et al., 2004;

Menke et al., 2004). Thus if HR symptoms appear normal in plants infected with an avirulent bacterial strain able to deliver HopAI1, this suggests that MAPK activation occurs normally in these plants and thus that during the HR the activity of HopAI1 could be inhibited by host cells to allow defense establishment. In the same way, the T1 strain of *Pseudomonas syringae* pv. *tomato* that contrary to *Pst* DC3000 expresses and secretes HopAI1, induces an HR-like cell death in the non-host plant *Arabidopsis thaliana* (Almeida et al., 2009). Since like ETI, non-host resistance process requires MAPK activation (Takahashi et al., 2007), it can be assumed that generally HopAI1 is not functional during HR-inducing plant-pathogen interaction, confirming that HopAI1 does not participate in pathogen fitness, likely because of an inhibition of its phosphothreonine lyase activity by host cells. Consistent with this hypothesis, several works report host enzymatic inactivation of a pathogen virulence effector to confer immunity. For instance, in plants, the phosphorylation of the effector AvrPtoB caused by the host kinase Pto restores the normal function of effector recognition triggered HR, which leading to plant resistance (Ntoukakis et al., 2009). In the same way several reports in animal field showed the inhibition of virulence factors function by *S*-nitrosylation (Saura et al., 1999; Badorff et al., 2000; Cao et al., 2003; Padalko et al., 2004; Kemball et al., 2009; Ntoukakis et al., 2009; Savidge et al., 2011). For instance, NO-mediated *S*-nitrosylation of various viral proteinases, required for viral replication, inhibit the function of these enzymes and lead to a dramatic decrease of viral infectivity (Mannick, 2006). Very recently Savidge et al. (2011) also showed that host-mediated *S*-nitrosylation of two large exotoxins TcdA and TcdB can directly inhibit microbial exotoxin activity of *Clostridium difficile* (Savidge et al., 2011).

Since one feature of the HR induced in resistant plants is the massive production of NO and according to a possible inhibition of HopAI1 by host cells that would have led to its abolition from virulence machinery during the evolution, it could be assumed that NO-mediated *S*-nitrosylation could inhibit HopAI1 activity.

In this scenario, the aim of this thesis was to investigate the possible role of NO produced by challenged plants as an inhibitor of HR-suppressing effectors, in

particular HopAI1 from the model bacterial pathogen *Pst* DC3000.

For this purpose the work focused first on the *in vitro* study of HopAI1, including the analysis of its *S*-nitrosylation and the effect of NO treatment on its activity. Then, we tried to decipher the physiological relevance of this post-translational regulation mediated by NO *in vivo* using a transient expression system in tobacco and stable transformation of *Arabidopsis thaliana* plants.

3. Materials and methods

3.1 Materials

3.1.1 Plants

Wild Type *Arabidopsis thaliana* (Col-0) as well as transgenic lines obtained in the project were grown in growth chamber under short day conditions (10 h light /14 h dark). Relative humidity (RH) was around 60% and temperature was set to 22℃ day/24℃ night. The transgenic lines pER8-HopAI1 was obtained from Dr.Jianmin Zhou, National Institute of Biological Sciences, China

Nicotiana tabacum genotype (SR-1) was grown in green house under long day conditions (18 h day/ 6 h night).

3.1.2 Bacterial strains

Escherichia coli DH5α or DB3.1 and BL21 (Invitrogen) strains were used respectively for cloning procedures and for protein expression.

Agrobacterium tumefaciens GV3101 was used for transient plant transformation by agroinfiltration and plant stable transformation .

Pseudomonas syringae pv. tomato DC3000 (*Pst* DC3000) was used for *hopAI1* cloning. *Pseudomonas syringae pv. tomato* DC3000 carrying *avrB* and *Pseudomonas*

Table 1 Growth condition for bacterial strains.

Bacterial strains	Culture medium	Antibiotics
Escherichia coli DH5α /DB3.1/ BL21	LB	—
Agrobacterium tumefaciens GV3101	LB	Rif 50 + Gen 50
Pseudomonas syringae pv. tomato DC3000	KB	Rif50
Pseudomonas syringae pv. tomato DC3000 carrying *avrB* or *avrRPT2*	KB	Rif50 + Kan50

Rif50, Rifampicin 50 μg/ml; Kan50, Kanamycin 50 μg/ml; Gen 50, Gentamycin 50 μg/ml

syringae pv. tomato DC3000 carrying *avrRPT2* were used for plant infection.

The growth condition for bacterial strains was shown in Table 1.

3.1.3 Vectors

The cloning vector pENTR^{TM}/SD/D-TOPO (Invitrogen) was used for cloning purposes.

The expression vector pDEST17 (Invitrogen) was used for heterologous proteins expression in *E.coli* of proteins including an His-tag for purification.

The broad host range expression vector pRK415 (Keen et al., 1988) was used for expression of the effectors HopAI1 and HopAI1^{CS} *in Pseudomonas syringae pv. tomato* DC3000 carrying *avrB*.

The inducible construct pER8-HopAI1 used for plant transient transformation was received from Dr.Jianmin Zhou, National Institute of Biological Sciences, China.

The gateway compatible inducible vector pMDC7 used for transient and stable transformation of *hopAI1^{CS}* in plants was obtained from Mark Curtis & Ueli

Table 2 Vectors and their selection antibiotics

Vectors	Bacterial selectable antibiotics	T-DNA selectable antibiotics
pENTR™/SD/D-TOPO	Kanamycin	–
pENTR™/D-TOPO	Kanamycin	–
pDEST17	Carbenicillin	–
pRK415	Tetracycline	–
pER8	Spectinomycin	Hygromycin B
pMDC7	Spectinomycin	Hygromycin B

The concentration of selection antibiotics in the expreriment were used as follow: of kanamycin or carbenicillin or spectinomycin, 50 μg/ml ; Tetracycline, 20 μg/ml; Hygromycin B, 30 μg/ml.

Grossniklaus, Institute of Plant Biology, University of Zurich.

The antibiotics used for selection of various vectors were shown in Table 2.

3.1.4 Mediums

Lysogeny broth medium (LB):10 g/l tryptone, 5 g/l yeast extract, 10 g/l NaCl, adjust pH to 7.0 and autoclave at 121 ℃ for 15 min before use.

King's B medium (KB):10 g/l peptone, 1.5 g/l anhydrous K2HPO4, 1.5 g/l MgSO47H2O 1% glycerol, adjust pH to 7.2 and autoclave at 121 ℃ for 15 min before use.

Murashige & Skoog medium including B5 vitamins (MS) was bought from Duchefa.

3.1.5 Primers

The primers used in our experiment were designed by Pimer3 (http://primer3.wi.mit.edu/) and shown in Table 3.

3.2 Methods

3.2.1 Extraction of bacterial plasmid or genomic DNAA homemade mini prep protocol established by Prof. Massimo Delledonne was used for extraction of genomic and plasmid bacterial DNA with some modifications, which is based on columns (Promega) packed with a diatomaceus earth (Sigma D5384). For extraction of genomic bacterial DNA an incubation step of 10 min at 65 ℃ after cell lyses.

Table 3 Primers

Name of Primers	Sequence
HopAI1$^{7-245}$-For	CACCCATATGCTCGCTTTGAAGCTG
HopAI1$^{7-245}$-Rev	TGCCTCGAGGTCGGGAAATGAAACCAATTGG
HopAI1^{CS}-For (FmP)	GGAAAGTCACCGACATGAGTAGCGCGAGTTCC
HopAI1^{CS}-Rev (RmP)	GGAACTCGCGCTACTCATGTCGGTGACTTTCC
HopAI1-T-For (FP)	CACCATGCCCATAAACAAGCCCAT
HopAI1-T-Rev (RP)	TCACTTATCGTCATCGTCCTTGTAATCGCGAGTCCAGGGCG GTGG
HopAI1/HopAI1^{CS}-RT-For	GTCTTATCGCAATGAACAC
HopAI1/ HopAI1^{CS} -RT-Rev	TCGGGAAATGAAACCAAT
HopAI1-B-For	CACCCTGCAG ATGCCCATAAACAAGCCCAT
HopAI1-B-Rev	GGATCCTCACTTATCGTCATCGTCCTTG

3.2.2 PCR, Restriction digestion and ligation

DNA amplification, restriction digestions and ligations for construct preparations were performed according to standard molecular biology protocols following the manufacturer instructions.

3.2.3 Purification of DNA fragments from agarose gel

GENECLEAN® Kit from MP Bio medicals was used for purifying DNA from agarose gel according to provided instructions.

3.2.4 TOPO® cloning

TOPO® cloning reaction (Invitrogen cloning kit) was set up according to manufacturer instructions. The molar ratio of PCR product: TOPO® Vector was set to

1:1.

3.2.5 LR reaction

LRreactions (LR clonase, Invitrogen) were performed according to manufacturer instructions.

3.2.6 *In vitro* site-directed mutagenesis

QuikChange® Primer Design Program was used to design primers for point mutation. Site-directed mutagenesis was performed by QuikChange® II XL Kit (Agilent technologies) according to the instructions.

3.2.7 Mutagenesis by overlap extension PCR

Over lapping extension PCR is performed as descripted by Higuchi et al (Higuchi et al., 1988) with some modification, and the schematic cloning strategy of *hopAI1*^{CS} is shown in Figure 1.

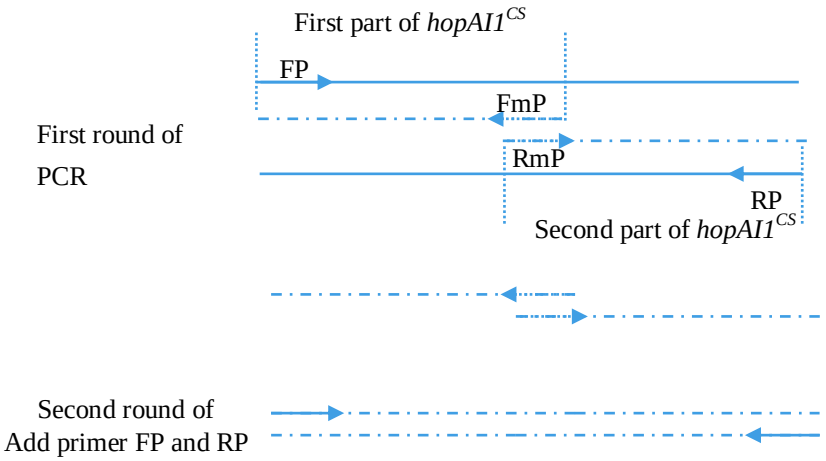

Figure 1 Schematic cloning strategy of hopAI1^{CS} by overlap extension PCR.
FP and RF flank the region to be amplified; FmP and RmP contain the mutagenized site. FP, HopAI1-T-For; RmP, HopAI1^{CS}-Rev; FmP, HopAI1^{CS}-For RP, HopAI1-T-Rever

10 ng of Pst DC3000 Genomic DNA was used as template for performing a standard PCR with two different primer pairs (FP/RmP or FmP/RP see Table 3) as shown in Figure 1.Each PCR products was then purified by agarose gel using the gene clean protocol (Methods 3.2.3).Finally a standard PCR was performed with primer FP/RP (see Table 3), using as template equal amount of amplified first part and second part of *hopAI1*^{CS}. The PCR product was then purified and sub-cloned in the vector pENTR^{TM}/D-Topo using the Topo cloning strategy described in Methods 3.2.4.

3.2.8 Protein expression

A pre-inoculum grown for 16h at 37 ℃ of bacteria *E.coli* BL21 strain carrying the expression constructs pDEST17- HopAI1 or pDEST17- HopAI1^{CS} was diluted 1:100 in a LB plus selective antibiotic carbenicillin at proper concentration of 50 µg/ml. The induction was started when the OD_{600} of culture reached 0.6. For optimize the expression of HopAI1 and HopAI1^{CS}, different concentration of IPTG (0.05 mM, 0.2 mM, 0.5mM), temperature (16 ℃ and 28 ℃) and collection time (0.5 h, 1h, 2h, 4h, 6h, 8h) were tested. Unfortunately in all the condition most of HopAI1 and HopAI1^{CS}

were expressed in the inclusion body confirmed both by SDS-PAGE and western blotting by using anti-His antibody. Finally the induction of HopAI1 and HopAI1^{CS} were performed at 28 ℃ for 6 h by using 0.2 mM IPTG. Then bacterial culture was centrifuged and pellet was stored -80 ℃.

3.2.8.1 Isolation of inclusion bodies

Inclusion bodies were isolated according to the following protocol:

1. The cell pellet from a 500 ml culture of *E. coli* was resupended in 15 ml lysis buffer (20 mM Tris-HCl, 0.5M NaCl, 1mM PMSF, 1 mM EDTA, Triton X-100 1%, 0.5 M NaCl, 10% Glycerol, pH 7.5).
2. Cells were disrupted with sonication on ice (6× 30 s, stop for 1 min after each 30 s sonication) and centrifuged at 12,000g for 30min at 4 ℃. .
3. The pellet, containing the inclusion bodies, was washed with 10 ml lysis buffer once and then stored -80 ℃ for later processing.

3.2.8.2 Protein purification and refolding

A. Solubilization and preparation of inclusion bodies

1. The inclusion bodies were resuspended in 15ml solubilization buffer **(**20 mM Tris-HCl, 0.5 M NaCl, 5 mM imidazole, 8M Urea, 1 mM 2-mercaptoethanol, pH 7.50).
2. After stirring for 30–60 min at room temperature and centrifugation at 12, 000 g for 15 min, at 4 ℃.
3. Remaining particles were removed by passing the sample through a 0.45 μm filter.

B. Protein purification

Purification of HopAI1 and HopAI1^{CS} was performed using prepacked His GraviTrap columns (GE healthcare) for chromatography affinity to purify proteins

carrying a His-tag. Purification was performed following manufacturer instruction for purification in denaturing conditions. 10 mM imidazole was used in equilibration buffer and washing buffer. And then different concentration of imidazole was used in elution buffer as shown in the Figure 4 and 8 in Results.

C. Protein refolding

1. Refolding was performed according protocol provided by Porf. J. R. Alfano (Center for Plant Science Innovation, University of Nebraska) with some modifications: Samples were diluted with elution buffer to a concentration of 0.2 mg/l protein.

2. Urea was replaced by dialysis against refolding buffer (20 mM Tris-HCl, 150 mM NaCl, pH 7.4) using multiple steps gradient of urea (6, 4, 2, 1, 0.8, 0.6, 0.4, 0.2, 0 M urea) with dialysis membrane (The cutoff is 12 KDa, Sigma). Each step was performed for at least 4 h at 4℃. In the last step 10% glycerol was added to the refolding buffer.

3. Sample were finally collected by centrifuging at 16, 000 g for 30 min and filtered with 0.2 μm filter.

3.2.9 SDS-PAGE

Stacking gel (4%) and resolving gel (10%) were prepared (as shown in Table 4 for one gel) in the Mini-PROTEAN® 3 Cell (Bio-Rad).

1. Protein samples were mixed with 6 x SDS loading buffer (0.375 M Tris, pH 6.8, 12% SDS, 60 % glycerol, 30 % 2-mercaptoethanol, 0.6 % bromophenol blue) boiled for 5 min and then centrifuged at 12,000 g for 3 min and the supernatant loaded into the wells.

2. Gels were stained with a staining solution (45 % methanol, 0.1 % Coomassie Brilliant Blue R250, 10 % acetic acid) for 2 h at room temperature. Destaining of gels was done in destaining solution (7.5% methanol, 10% acetic acid).

Table 4 Gel solutions		
Reagent	4% Stacking gel	10% Resolving gel
Acrylamide/Bis 40%	0.2 ml	1.25ml
4xTris-HCl (0.5 M), pH6.8	0.5 ml	—
4xTris-HCl (1.5 M), pH8.8	—	1.25ml
APS 10%	20µl	50µl
TEMED	2µl	5µl
H_2O	1.2 ml	2.5 ml

3.2.10 Western blotting

Proteins were transferred from the gel to Amersham Hybond ECL membranes in liquid system by Mini Trans-Blot Cell (Bio-Rad). Membranes were stained with a Ponceau S staining solution (0.1% Ponceau S and 0.05% acetic acid) for 3-5min at room temperature and then destained with Milli-Q water to confirm the transfer.

Western blotting was performed as described in instruction manual of Amersham ECL Prime Western Blotting Detection Reagent. The antibodies (Sigma) used in the experiment were diluted as follow: Anti-His antibody, 1:5, 000 dilution; Anti-Flag, 1:2, 000 dilution; Anti-Biotin antibody, 1:5, 000 dilution) and corresponding secondary antibody, 1:5, 000 dilution.

3.2.11 Determination of protein concentration

Protein concentration was measured using the Bradford protein assay (Bradford, 1976)

3.2.12 GSNO treatment of proteins *in vitro*

HopAI1 or HopAI1^{CS} (5 μg for Biotin Switch Test, 15μg for DAN assay) were incubated with 0.5 mM or 1 mM GSNO at room temperature in the dark for 30 min. Excess GSNO was removed either by cold acetone precipitation or by dialysis against refolding buffer performed in Slide-A-Lyzer MINI Dialysis Devices (The cutoff is 10 KDa, Pirece).

3.1.13 Acetone protein precipitation

1. Two to three volumes of ice cold acetone were added to the protein solution and keep at -20 ℃ for at least 20 min.
2. Proteins were collected by centrifugation at 4, 000g, 4 ℃, for 20min.
3. Discard the supernatant and wash the protein pellet with half volume of initially added acetone. Centrifuged at 10, 000 g, 4 ℃, for 5 min.
4. Finally the pellet was resuspended in appropriate buffer.

3.1.14 Biotin switch test

In the Biotin Switch Test, *S*-nitrosylated protein was selectively labeled by biotin and the biotin-labeled protein was detected by standard western blotting. The used protocol was as following:

A. Blocking of free SH-groups

1. Add 3 volumes of blocking buffer (HEN-buffer, 2 .5 % SDS, 20 mM Methyl methanethiosulfonate) to samples and vortex them.
2. Incubate samples at 50 ℃ for 20 min and vortex them frequently.
3. Remove Methyl methanethiosulfonate (MMTS) by cold acetone precipitation
4. Air-dry pellet and re-suspend protein in HENS-buffer.

B. Biotinylation

1. Add 1:10 volume of 10 mM Na-ascorbate and 1:10 volume of 10 mM biotin-HPDP to the samples and vortex.

2. Incubate at room temperature in the dark for 60 min.

C. Detection of biotin-labeled proteins

1. Add appropriate volume of 4 x SDS-PAGE non-reducing sample buffer and perform standard procedure SDS-PAGE without heating sample.

2. Perform a standard western blotting with anti-biotin mouse monoclonal antibody as primary antibody and anti-mouse IgG-peroxidase as secondary antibody.

3.2.15 Dan assay

In the DAN assay, NO is released from S-nitrosylated proteins by $HgCl_2$ treatment. The reagent 2, 3-diaminonapthalene (DAN) reacts with NO (in presence of O_2) to form a fluorescent product, 2, 3-naphthyltriazole, which can be detected by a fluorometer.

1. Adjust sample volume to 100 µl with dd H2O.

2. Add 0.1 mg/ml DAN dissolved in 0.62 M HCl and 5 µl 4 mM $HgCl_2$ into sample and incubate at room temperature in the dark for 10 min.

4. Add 5.5 µl 1 M K_2HPO_4 and 11 µl 0.5 M 5-sulfosalicylic acid and incubate on ice for 10 min (dark).

5. Centrifuge at 2, 500 g, at room temperature for 10 min and transfer 110 µl of the supernatant to a 96-well plate.

6. Add 10 µl 2.8 M NaOH into well and incubate at room temperature in the dark for 15 min.

7. Measure the amount of fluorescent produced by using a fluorometer, Wallac Victor3 (Perkin Elmer), with λ_{ex} 380 nm / λ_{em} 450 nm.

3.2.16 Phosphothreonine lyase activity assays

Phosphothreonine lyase activity was detected as described by Zhang (Zhang et al., 2007a).

1. Incubate 1μg of HopAI1 or HopAI1^{CS} with synthetic MAPK phosphopeptide (SESDFM-pTE-pYVVTR; Sangon, Shanghai) in a 40 μl reaction buffer (10 mM HEPES, 150 mM NaCl, and 1 mM EDTA, pH 7.4) at 30 ℃ for 1h.

2. Add Malachite Green Dye (Millipore) into the mixture above. Measure absorbance at 620 nm. Potassium phosphate monobasic, KH_2PO_4, at different concentration was used for preparation of standard curve.

3.2.17 Plant transient transformation by agroinfiltration in tobacco leaves

The followed procedure was adapted from Lee and Yang, 2006 with few modifications(Lee and Yang, 2006).

1. Streak *Agrobacterium tumefaciens* GV3101 carrying constructs (pMDC7-*AtMKK4*^{DE}, pMDC7-*AtMKK5*^{EE}, pMDC7-*EV*, pER8-*hopAI1* and pMDC7-*hopAI1*^{CS}) on LB agar plates with proper antibiotics. Incubate plates at 28 ℃ for 2 d.

2. Pick up single colony and inoculate agrobacteria into 3 mL LB broth with proper antibiotics and grow overnight at 28 ℃ on a shaker (200 rpm).

3. Collect 2 mL overnight cultures by centrifugation (4, 000 g for 5 min) and wash pellet twice with infiltration medium (10 mM MgSO4, 10 mM MES, pH 5.6).

4. Resuspend bacterial cells in the infiltration medium to 0.8 OD at 600 nm.

5. Infiltrate first and second leaf (count from top to down) of tobacco plant, *Nicotiana tabacum* genotype (SR-1), with *Agrobacterium* carrying various constructs, and then place the plant in growth chamber for 2 d.

6. Perform induction with 40 μM *β*-estradiol for 6 h and observe symptoms

development in 2 d.

3.2.18 Plant NO fumigation

A homemade NO fumigation system has been used to apply controlled amount of NO to plant.

1. Gas from Air and from an NO cylinder (600 ppm) were mixed by flow mass controller controlled by an electronic system to get 50 ppm NO.
2. A flow speed of 300 ml/min air or 50ppm NO were applied to a plexiglass fumigation chamber, in which tobacco plant infiltrated with *Agrobacterium* carrying constructs were placed , under continuous light continuous light (30-40 μmol/m^2/s) at room temperature.
3. Observe symptoms development and the photos were taken in 2 d.

3.2.19 Acquisition of chlorophyll fluorescence images of plant leaves

Images Chlorophyll fluorescence emitted by tobacco leaves were obtained at room temperature by using an imaging fluorometer FluorCam 700MF (Photon System Instruments) according to the instructions provided by the manufacturer. Plants were placed in the dark for 30 min prior acquisition of images. Then leaves were treated with a 1-s pulse of saturating light (2000 μmol/ m^2 /s) and Fm (maximum fluorescence yield) images were captured with the instrument. Image data acquired were normalized to color scale with extreme values of 0 (lowest) and 3800 (highest).

3.2.20 Stable transformation of plants by floral dip of Arabidopsis plants

Stable transformation of plants was performed according to Clough and Bent, Zhang (Clough and Bent, 1998; Zhang et al., 2006).

1. Streak *Agrobacterium tumefaciens* GV3101 carrying pMDC7-Empty Vector or pMDC7-HopAI1^{CS} on selection media with proper antibiotics from -80 ℃ and incubate 28 ℃ for 2 days.

2. Pick up a single colony and inoculate into 3 ml of LB liquid with 50 μg / ml Rif, 50 μg / ml Gent and 50 μg / ml Spec, then incubate with shaking at 28 ℃ for one day.

3. Collect Agrobacterium cells by centrifugation at 4, 000g for 10 min at room temperature.

4. Wash cells twice with 25mL of 5 % sucrose in water and resuspend the pellet with 50mL of 5 % sucrose in water.

6. Measure the OD_{600} of *Agrobacterium* solution and dilute the mixture with appropriate amount of 5% sucrose in water to the final OD_{600} of 0.8.

7. Add silwett L-77 to Agrobacterium solution at the final concentration of 0.02 % and mix well.

10. Dip above-ground parts of flowering Arabidopsis plant, still with closed flowers, in Agrobacterium solution for 5 min and absorb the residue liquid on the plant by clean tissue paper.

11. Cover dipped plants with a plastic cover and then wrap them with plastic film. Lay down the treated plants on their sides for 24 h to maintain high humidity.

12. Grow plants in green house and harvest dry seed.

3.2.21 Selection of transgenic Arabidopsis homozygous lines

Homozygous transgenic lines were selected as explained

1. Sterilize the seeds obtained from transformed plants with 75 % ethanol for 1 min.

2. Add commercial 50 % sodium hypochlorite solution and incubate at room temperature for 15 min.

3. Wash the seeds with 1 ml sterilized H_2O and resuspend in 1 ml of 0.1 % phyto agar.

4. Transfer seeds on MS media with proper antibiotics with sterilized glass Pasteur pipette.

5. Seal the petri dishes with parafilm and put the dish plates in the growth chamber under normal plant grown conditions.

After 10 days the seedlings presenting longer roots and bigger leaves than the WT seedlings growth on the same selection media were considered as positive transgenic plants. Performing a segregation analysis on selected T1 lines presenting high level of expression for the transgene, transgenic plants carrying one copy of the transgene integrated in the genome were selected. Then these lines were used for production of homozygous T3 plants.

3.2.22 Extraction of total RNA

Total RNA was extract from Arabidopsis leaves using the TRIZOL® reagent (Invitogen).

1. Homogenize about 0.1 g of liquid nitrogen frozen Arabidopsis leaves placed in 1.5 ml eppendorf tube with glass beads by a homogenizer.

2. Add 1ml of TRIZOL® reagent and vertex. Incubate for 5min at room temperature, and then centrifuge 12,000 g for 10 min at 4 ℃.

3. Transfer supernatant to a new tube and add 0.2 ml of chloroform. Vortex 15 s and incubate for 2 min at room temperature. Centrifuge at 12,000 g for 5 min at 4 ℃.

4. Transfer the aqueous phase to a fresh tube and add 0.5 ml of isopropyl alcohol. Vertex for 15 s and incubate for 10min at room temperature, centrifuge at

12,000 g for 10 min at 4 ℃.

5. Discard the supernatant and wash the RNA with 1ml of 75% ethanol twice. Centrifuge 12,000 g for 10 min at 4 ℃.

6. Dry the RNA under the hood and dissolve it in RNase free water. After checking the quality of RNA by measuring A_{260}/A_{280} ratio and by loading an agarose gel, RNA is stored at -80 ℃.

3.2.23 Synthesis of first-strand cDNA

First-strand cDNA synthesis was synthesized by SuperScript™ II reverse transcriptase. First total RNA was treated with TURBO DNA-free™ Kit to eliminate genomic DNA.

1. 1 μg of total RNA was used in 20-μL reaction volume, in which containing 1 μl of Oligo $(dT)^{12-18}$ (500 μg/mL), 1 μl of dNTP Mix (10 mM each), 1 μl of Sterile. Add the distilled water to make 12 μl of reaction mixture. Incubate mixture at 65 ℃ for 5 min and quick chill on ice.

2. Add the mixture with 4 μl of 5 x First-Strand Buffer, 2 μl of 0.1 M DTT. Incubate for 2 min at 42 ℃.

3. Add 1 μl of SuperScript™ II RT and incubate at 42 ℃ for 50 min.

4. Inactivate the reaction by heating at 70 ℃ for 15 min. Dilute the mixture 10 times with sterilized H_2O and store it at -20 ℃.

3.2.24 Real time PCR

Real time PCR was performed with Platinum® SYBR® Green qPCR SuperMix-UDG by using the *Atactin 2* (GenBank accession number: AF428330.1) as an internal standard.

1. 1 μ l of cDNA was used in 20-μL reaction volume, in which containing 10 μl

of Platinum® SYBR® Green qPCR SuperMix-UDG, 0.4μl of Forward primer and Reverse primer (10 μM) and 9.8μ l of sterilized H_2O

2. Seal the reaction PCR plate and gently mix. Centrifuge briefly if needed.

3. Place reactions in a preheated Mx3000P™ (Stratagene). Calculation was made according to $2^{-\Delta\Delta CT}$ method as described by Livak and Schmittgen (Livak and Schmittgen, 2001).

3.2.25 Phenotypic analysis of HR development

P. syringae pv. tomato DC3000 carrying avrRpt2 was prepared as descripted by Katagiri et al (Katagiri et al., 2002).

1. Streak *P. syringae pv. tomato* DC3000 carrying avrRpt2 on KB agar medium with proper antibiotics and Incubate plates at 28℃ for 2 d.

2. Pick up single colony and inoculate agrobacteria into 3 mL KB medium with proper antibiotics and grow overnight at 28℃ on a shaker (200 rpm).

3. Collect 2 mL overnight cultures by centrifugation (4, 000 g for 5 min). And wash pellet twice with infiltration medium (10 mM $MgCl_2$).

4. Resuspend and dilute bacterial cells in the infiltration medium to 0.1 or 0.02 (equal to $1x10^7$ /ml or $5x10^7$/ml) OD at 600 nm.

5. Prepared *P. syringae pv. tomato* DC3000 carrying *avrRpt2* were infiltrated in to leaves of 6-7 week-old Arabidopsis plants that were pre-sprayed with 40 μM estradiol for 24 h with 1 ml syringe, and then place them to normal growth condition.

6. Photos were taken by Nikon D3000 Digital SLR Camera at the indicated time points after infection.

3.2.26 Trypan blue staining

Trypan blue staining was used to reveal dead plant cells in plant tissues. The protocol we used was adopted from Choi et al (Choi et al., 2007)

Plant leaves induced and infiltrated with a bacterial inoculums as described in Methods 3.2.25 were harvested at the indicated time points after infiltration and boiled for 3 min in freshly prepared lactophenol-trypan blue solutions by diluting (1:1) a stock solution prepared mixing10 mL lactic acid, 10 mL glycerol, 10 g phenol, 10 mL distilled water and 10 mg trypan blue with ethanol. After 1 hour the lactophenol-trypan blue solution was discarded, and then samples were resupended in a destaining solution (2.5 g chloral hydrate dissolved in 1 mL distilled water). Destaining solution was changed for several times until the leaf sections without cell death became clear. Leaves were then placed in 60% glycerol and photos were taken.

3.2.27 Electrolyte leakage assay

Electrolyte leakage assay was used in order to quantify HR response (Mackey et al., 2003). The procedure we followed was according to Mackey.

Transgene expression was induced by spraying plants with 40 mM estradiol. After 24 h, leaf discs (8 mM diameter) were excised from Arabidopsis leaves with a cork borer and placed in Petri dish with Milli-Q water.

Leaf discs were vacuum infiltrated with $5x10^7$/ml *P. syringae pv. tomato* DC3000 carrying *avrRpt2* (prepared as shown in Methods 3.2.25) in a 10 ml syringe and then floated in 50 ml of water for 30 min.

Six leaf discs pooled from different plants for each replicate were transferred into petri dishes (5 mM diameter) with 6 ml Milli-Q water and placed under normal light on a shaker (80 rpm/min). Conductance was measured over time for 48 hours by

using the B-173 compact conductivity meter (HORIBA).

3.2.28 Bacterial growth assay

Bacterial growth kinetics in plants were assayed as reported in Katagiri et al with some modifications (Katagiri et al., 2002). Induce transgene expression by spraying plants with 40 mM estradiol. After 6 hr infiltrate Arabidopsis leaves with a bacterial inoculum diluted at $5x10^5$ /ml of *P. syringae pv. tomato* DC3000 carrying *avrRpt2* (prepared as shown in Methods 3.2.25).

1. Excise 6 leaf discs (6 mM diameter) from Arabidopsis leaves of different plants for each replicate and then transfer them into 1.5 ml sterilized eppendorf tube with 100 µl of sterilized water. Grind the discs by electric grinder and then add sterilized water to 1ml.

2. Samples are then serially diluted into sterilized water and then 15µl of samples are plated on KB agar plates with proper selection antibiotics.

3. Incubate plates at 28℃ for 2 days and count the number of colonies and calculate the total cfu/ml, according to volume and dilution used for plating.

This procedure was performed on samples harvested at the same day of pathogen infiltration and in the subsequent 2 days (T0, T1, T2).On day zero, only concentrated extract were plated, while in the following two days 1:10 and 1:100 serial dilution from plant extract were plated.

3.2.29 Computational models of HopAI1 and *S*-nitrosylated HopAI1

To model of three-dimensional (3D) structure of HopAI1 and *S*-nitrosylated HopAI1 binding with synthetic peptide, Protein sequence of *hopAI1* was submitted to The iterative threading assembly refinement (I-tasser) server, which is an integrated platform for automated protein structure and function prediction based on the

sequence-to-structure-to-function paradigm (Roy et al., 2010). The structure of OspF with its substrate (Protein bank ID: 2q8yA) was used as template p to model HopAI1 binding with synthetic peptide by I-tasser. *S*-nitrosylated HopAI1 was then predicted by Pymol (Schrödinger LLC)(Seeliger and de Groot, 2010). The electrostatic potential distribution of HopAI1and *S*-nitrosylated HopAI1 was calculated and imaged by Molsoft ICM-Pro (Molsoft LLC.)(Abagyan et al., 1994).

4. Results

4.1 Cloning and expression of the recombinant HopAI1 protein

To ensure optimum stability and purification of the protein, only the core fragment of the protein HopAI1 corresponding to the sequence from 7 to 245 ($HopAI1^{7-245}$) has been cloned Zhang et al (2007). This fragment lacks the N-terminal 6 amino acids that are not required for its function and the C-terminal 22 amino acids that are not conserved in the HopAI1 family (Zhang et al., 2007a). The primers were designed for the cloning of $hopAI1^{7-245}$ using the Gateway technology (Invitrogen). The amplification of the gene by PCR using genomic DNA from *Pst* DC3000 as a template produced a unique fragment at the expected size of 733 bp (Figure 1).

Then, the gene *HopAI1* has been cloned into the entry vector pENTR-SD/D-TOPO (Invitrogen) and the construct has been controlled by sequencing (Figure 1 in the Appendix).

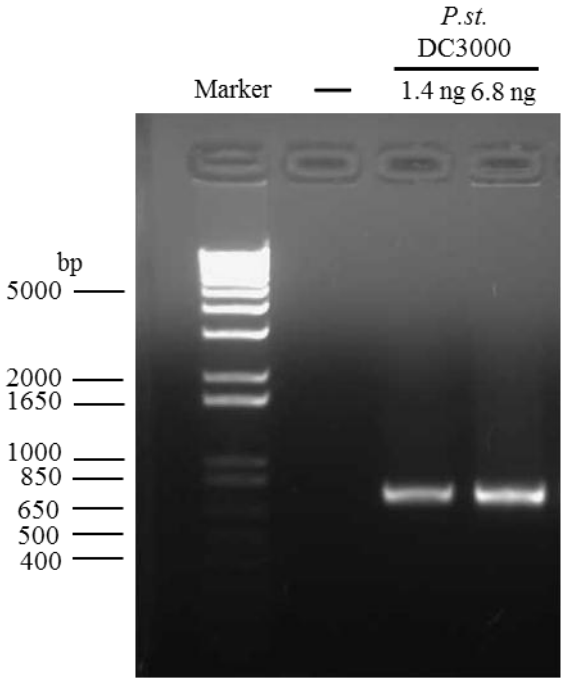

Figure 1 PCR amplification of HopAI1 from genomic DNA of *Pst* DC3000. The amplification has been performed from different amount of template genomic DNA as indicated. — negative control.

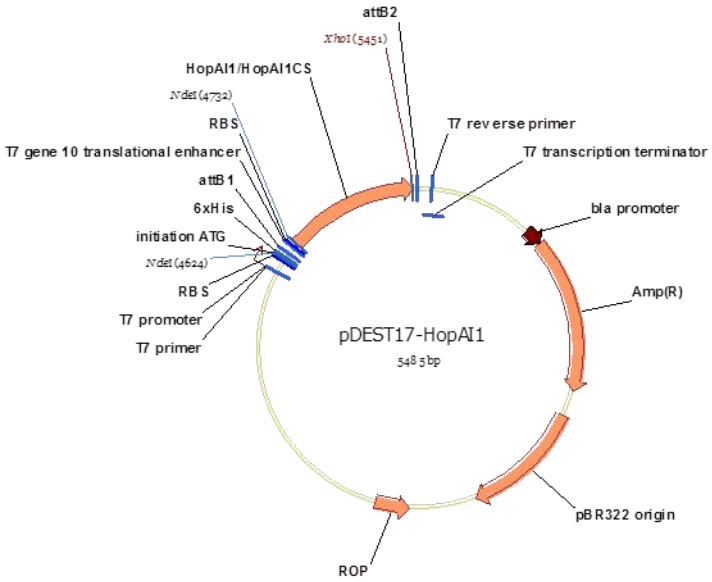

Figure 2 Map of the construct pDEST17 in which has been cloned *hopAI1*.
Restriction sites used in the cloning procedure are indicated in red or italics.

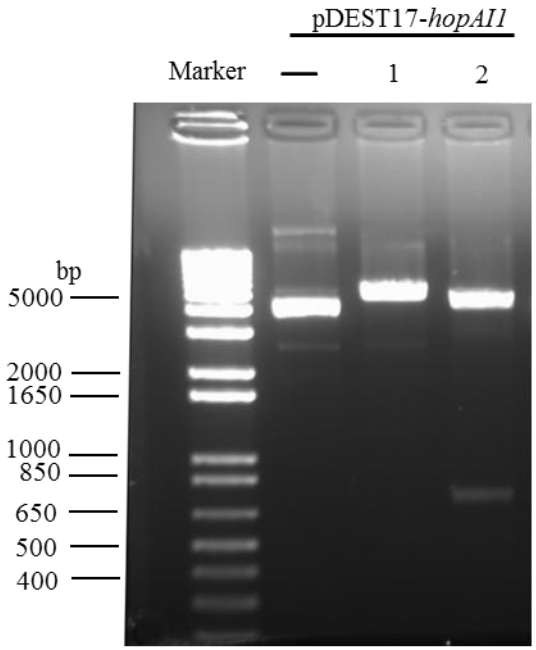

Figure 3 Restriction enzyme digestion to control pDEST17-HopAI1 construct
—, undigested pDEST17-HopAI1; 1, construct digested with XhoI; 2, construct digested with XhoI and NdeI exciding the insert.

The vector pDEST17 has been chosen as expression vector, since it allows the insertion of a poly-histidine (6×His) tag at the N-terminal of the protein and is useful for successive protein purification and detection. The gene *HopAI1* has been introduced in pDEST17 by LR recombination and the construct (pDEST17-HopAI1; Figure 2) has been controlled by double digestion with restriction enzymes, leading to the production of two fragments of 4752 bp and 733bp as shown in Figure 3.

E.coli BL21 cells have been transformed with the construct pDEST17–*HopAI1* for expression. Different temperatures (16 ℃ and 28 ℃) and different concentrations of IPTG (0.05mM, 0.2mM and 0.5 mM) for induction of the expression have been tested in order to optimize the recovery of the recombinant protein in the soluble fraction. Unfortunately in all the conditions tested most of the recombinant protein HopAI1 remained in the insoluble fraction. For this reason, it has been decided to purify the recombinant protein from the inclusion bodies, according to the refolding protocol provided by Prof. Alfano, J. R. The recombinant HopAI1 has been purified under denaturing condition (8M Urea) by affinity chromatography using His

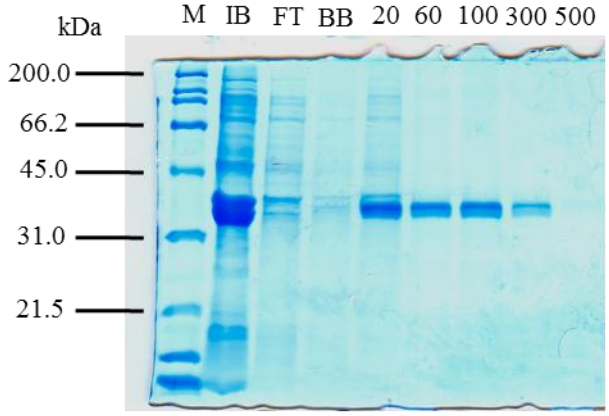

Figure 4 Control of the purification of the recombinant HopAI1 protein expressed in *E. coli* BL21.
The different fractions obtained during purification process were run on an SDS-PAGE 10% and the proteins were stained with Coomassie brilliant blue R-250. Predicted molecular weight of HopAI1 is 35.3 kDa; IB, Inclusion bodies; FT, Flow through; BB, Binding buffer; 40, 60, 100, 300 and 500 correspond to different concentrations of imidazole in mM used for protein elution in presence of 8M Urea

GraviTrap column with a nonlinear gradient of imidazole for its elution (Figure 4). Then the purified protein has been dialyzed against the refolding solution (see the Materials and methods) in order to get the active folded protein. The yield of pure recombinant HopAI1 obtained was 2 mg/L.

4.2 HopAI1 is *S*-nitrosylated by NO *in vitro*

The *S*-nitrosylation of the recombinant HopAI1 has been first analyzed using the biotin-switch assay, that allows the specific replacement of the S-NO bond by a S-biotin that can be detected by western blot with an antibody anti-biotin. For this assay the recombinant protein has been incubated with 1 mM GSNO as NO donor followed by the biotin switch assay. The Figure 5A shows the presence of a signal after treatment of the protein with both concentrations of GSNO and in presence of ascorbate for reducing HopAI1–SNO to HopAI1–SH, indicating that HopAI1 is *S*-nitrosylated *in vitro*. Moreover the specificity of the signal is ensured by the control with DTT treatment that is able, as a reductant, to reverse *S*-nitrosylation. To confirm this result, HopAI1 *S*-nitrosylation has been further analyzed using another technique,

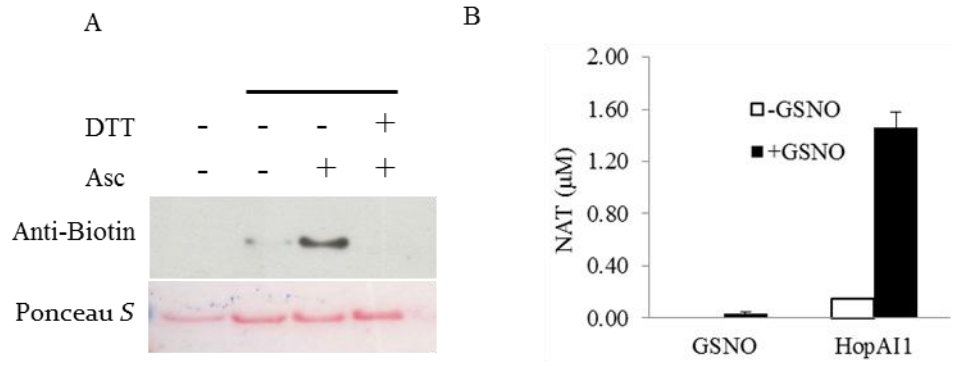

Figure 5 *In vitro S*-nitrosylation of recombinant HopAI1 by GSNO.
(A) Immunodetection of HopAI1 incubated with 1 mM GSNO for 1h at room temperature and then subjected to biotin-switch. Protein loading was controlled by Ponceau *S* staining of the membrane after protein transfer. DTT, 10mM; Asc, 1mM Ascobate;
(B) Recombinant HopAI1 protein was incubated with 0.5 mM GSNO for 1h at room temperature. SNO-HopAI1 thus generated was assessed by DAN assay.
Error bars indicate standard deviation.

i.e. the DAN assay, which detects the release of NO group from *S*-nitrosothiols by measuring the conversion of DAN to the fluorescent compound 2, 3-naphthyltriazole (NAT). According to the results obtained with the biotin switch, the treatment of HopAI1 with GSNO resulted in a significant increase of the fluorescent intensity as compared with the non-treated control, indicating the presence of *S*-nitrosothiols within the protein, and thus confirming that HopAI1 is *S*-nitrosylated by GSNO *in vitro* (Figure 5B).

4.3 HopAI1 activity is inhibited by NO *in vitro*

We investigated the functional effect of nitric oxide treatment on HopAI1 phosphothreonine lyase activity, by measuring the dephosphorylation of a synthetic phosphopeptide corresponding to a portion of the HopAI1 substrate AtMPK6 (SESDFM-pTE- pYVVTR) in presence of HopAI1 treated or not with GSNO. The Figure 6 shows that GSNO treatment reduces strongly phosphate release from the phosphopeptide, indicating an inhibition of HopAI1 activity, in a dose-dependent manner (Figure 6). This inhibition is quite efficient since more than 50% of inhibition is already observed with only 0.1 mM GSNO (Figure 6).

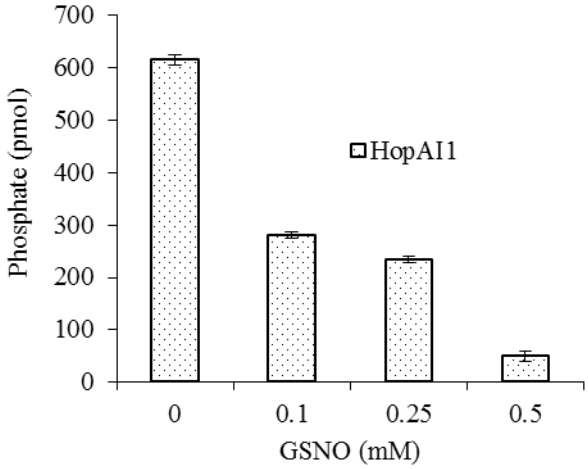

Figure 6 Inhibition of the phosphothreonine lyase activity of recombinant HopAI1 by GSNO *in vitro*.
1 µg of HopAI1 was pre-incubated with different concentrations of GSNO for 1h in the dark at room temperature and then subject to *in vitro* phopshothreonine lyase assay.

Taken together these results suggest that NO blocks HopAI1 activity and the *S*-nitrosylation of the protein could account for such inhibition.

4.4 Bioinformatics analysis of HopAI1 family

S-nitrosylation corresponds to NO^+ attack on thiolate from cysteine residues. The analysis of the sequence of HopAI1 from *Pst* DC3000 used in this study shows that

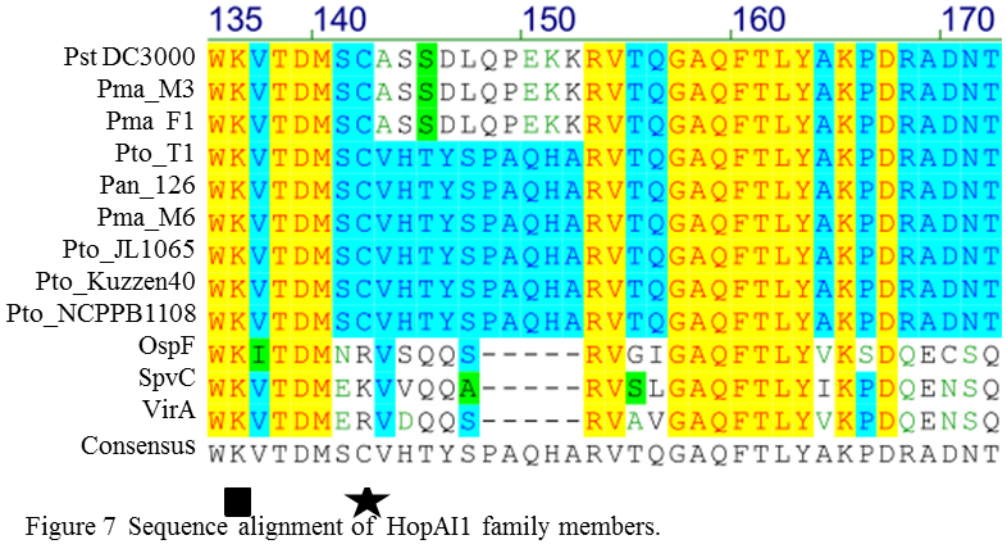

Figure 7 Sequence alignment of HopAI1 family members.
The Figure shows only the region surrounding the conserved Cys residue in proteins belonging to Pseudomonas. Catalytic residue is marked with a black square and conserved Cys is marked with a black star at the bottom. Alignment was performed using Align X (Vector NTI9.0, Invitrogen) and data available from *Pseudomonas syringae* Assemblies Project, http://pseudomonas-syringae.org

the protein contains only on Cys residue as potential target of *S*-nitrosylation. This Cys residue is located nearby the key catalytic residue (Lys), suggesting that its modification by NO could account for HopAI1 inhibition. Interestingly, the alignment of different members of HopAI1 family shows that such Cys is conserved among all the HopAI1 proteins of Pseudomonas species, whereas it is missing in the sequences of enzymes from animal pathogens, including OspF of *Shigella flexneri*, VirA of *Chromobacterium violaceum* and Spv C of *Salmonella enterica* (Li et al., 2007; Zhang et al., 2007a; Chen et al., 2008).

4.5 Mutations of HopAI1 and expression of the mutant HopAI1^{CS}

To confirm that *S*-nitrosylation is responsible for HopAI1 inhibition by NO, the unique Cys residue identified above has been then mutated into Ser to produce the HopAI1^{CS} mutant insensitive to *S*-nitrosylation. Site-directed mutagenesis has been performed using the QuikChange® II XL Kit (Stratagene) with the construct pDEST17-HopAI1 as template. The construct containing the mutated gene

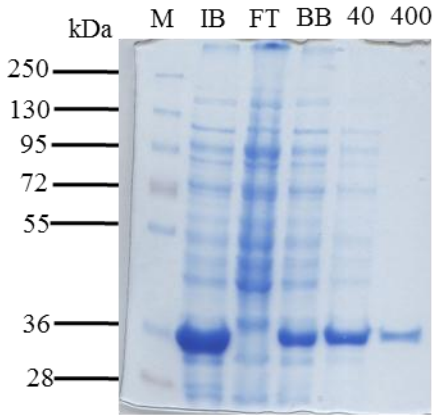

Figure 8 Control of the purification of the recombinant mutant HopAI1^{CS} protein expressed in *E. coli* BL21.
The different fractions obtained during purification process were run on an SDS-PAGE 10% and the proteins were stained with Coomassie brilliant blue R-250. Predicted molecular weight of HopAI1^{CS} is 35.3 kDa; IB, Inclusion bodies; FT, Flow through; BB, Binding buffer; 40 and 400 correspond to different concentrations of imidazole in mM used for protein elution in presence of 8M Urea

(pDEST17-HopAI1^{CS}) has been controlled by sequencing.

E.coli BL21 cells have been transformed with the construct pDEST17-*HopAI1*^{CS} and the expression of the recombinant mutated protein as well as its purification have been conducted in the same conditions as described above for HopAI1 (Figure 7). The yield of pure recombinant HopAI1^{CS} obtained was 2 mg/L.

4.6 HopAI1^{CS} lacking Cys^{138} is not *S*-nitrosylated by NO *in vitro*

As expected, the HopAI1^{CS} mutant lacking the unique Cys present in HopAI1 sequence does not give any signal of *S*-nitrosylation using both the biotin-switch assay (Figure 9A) and the DAN assay (Figure 9B), confirming that the mutate protein is insensitive to *S*-nitrosylation by GSNO.

Moreover these results confirm that the signals detected with the native form of the protein in both experiments are effectively due to the post-translational modification of HopAI1 by NO.

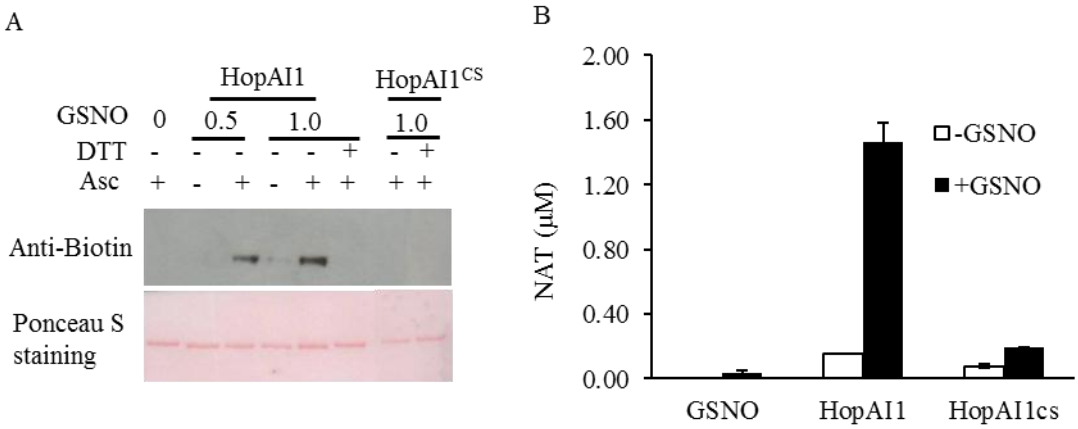

Figure 9 Comparison of recombinant HopAI and HopAI^{CS} sensitivity toward *in vitro S*-nitrosylation by GSNO.
(A) Immunodetection of HopAI1 and HopAI1^{CS} incubated with the indicated concentrations of GSNO for 1h at room temperature and then subjected to biotin-switch. Protein loading was controlled by Ponceau *S* staining of the membrane after protein transfer. DTT, 10mM; Asc, 1mM Ascobate;
(B) Recombinant HopAI1 and HopAI1^{CS} proteins were incubated with 0.5 mM GSNO for 1h at room temperature. Treated recombinant proteins were then assessed by DAN assay.
Error bars indicate standard deviation.

4.7 The activity of HopAI1^{CS} lacking Cys^{138} is not affected by NO treatment *in vitro*

In order to demonstrate that the inhibition of HopAI1 by NO is due to the *S*-nitrosylation, phospholyase activity of HopAI1CS has been analyzed after treatment with different concentrations of GNSO and compared to HopAI1 (Figure 10). Whereas, as previously shown, the activity of HopAI1 is strongly inhibited by GSNO, the activity of the mutated protein is not affected by such treatment, even at high NO donor concentration. This result confirms that NO inhibits HopAI1 activity by S-nitrosylating Cys138. It is also noteworthy that the total activity of the mutated protein is about 30% of the activity of the native HopAI1. This observation strongly supports the fact that Cys137 residue is crucial for HopAI1 activity and is in line with an inhibition of the activity of the protein by modification of such residue.

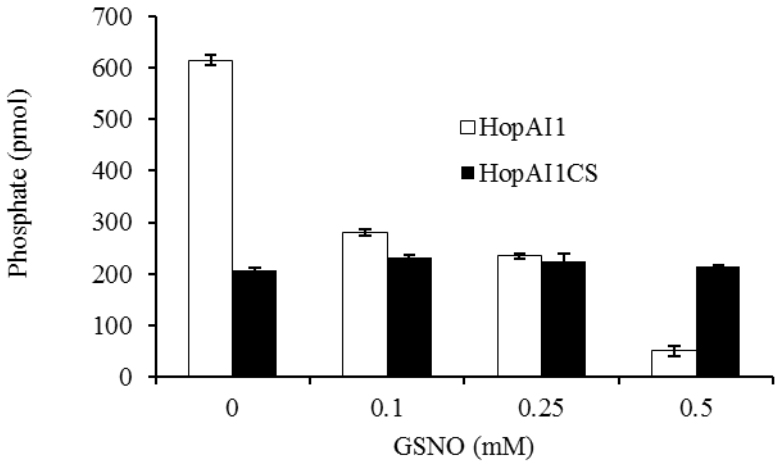

Figure 10 Comparison of the effect of GSNO treatment on HopAI1 and HopAI1CS phosphothreonine lyase activities *in vitro*.
1 µg of HopAI1 and HopAI1^{cs} were pre-incubated with different concentrations of GSNO for 1h in the dark at room temperature and then subject to *in vitro* phosphothreonine lyase assay.

4.8 Prediction of the structure and the mode of action of S-nitrosylation

To elucidate the mechanism of HopAI1 *S*-nitrosylation and to decipher the consequence of such modification on HopAI1 structure and thus activity, the 3D structure of the protein has been modeled using I-TASSER server. The model has been built for both *S*-nitrosylated and non-modified proteins in presence of the synthetic peptide Erk5 phosphopeptide (QYFM-pT-E-pY-VA), mimicking the substrate of HopAI1 AtMPK6 (Figure 11).

Several works have reported that amino acids surrounding Cys residues are determinant for their *S*-nitrosylation by NO (Hess et al., 2005; Marino and Gladyshev, 2010). Among the different models that have been proposed so far, the most popular is the so-called 'acid–base' motif in which basic and acidic amino acids surrounding a Cys residue can promote its *S*-nitrosylation by NO (Stamler et al., 1997). In this model basic amino acids (usually Arg, Lys, His) promote the release of H^+ from the -SH of the target Cys while acidic amino acids (usually Asp, Glu) promote the transfer of the NO group. These amino acids are usually located at a distance inferior

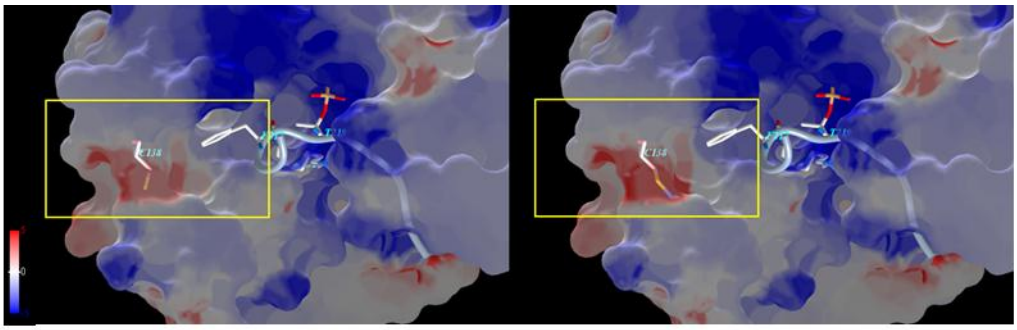

Figure 11 Computational modeling of *S*-nitrosylation effect on electrostatic potential distribution in HopAI1.
Left panel, untreated HopAI1 structure; Right panel, S-nitrosylated HopAI1 structure. In blue, positively charged areas; In red, negatively charged areas; In white, neutrally charged areas. The Cys and SNO-Cys are highlighted in the yellow square frame. Binding site of HopAI1 and HopAI1^{CS} have been predicted by I-TASSER server and electrostatic potential distribution has been analyzed by Molsoft ICM 3.5 (Molsoft,LLC)

to 6 Å from the target Cys. According to this model, the structure of HopAI1 shows the presence of basic amino acids, i.e. Lys^{73} and Lys^{75}, respectively at 11.6 and 13.9 Å from Cys^{138}, and acidic amino acid, i.e. Asp^{135} and $Asp^{142,}$ respectively at 3.7 Å and 6.4 Å from Cys^{138}. Despite the distance of basic amino acids from the target Cys that is a bit higher than 6 Å, it is very likely that these amino acids could thus account for Cys138 *S*-nitrosylation by NO.

Concerning the consequences of such post-translational modification on HopAI1 structure that could account for the inhibition of its activity, the 3D model shows that Cys^{138} is located at the bottom of the pocket that may be responsible for the binding of the Phe (F) residue of the synthetic phosphopeptide Erk5. The prediction shows *S*-nitrosylation of Cys^{138} significantly modifies the electrostatic potential distribution of HopAI1, which electrostatic potential of microenvironment around SNO-Cys become more negatively charged (Figure 11).

4.9 Production of HopAI1 and HopAI1^{CS} constructs for transient expression in plants

In order to study the effect of HopAI1 *S*-nitrosylation *in vivo* several constructs have been produced in order to express both native and mutated HopAI1 proteins in plants.

The construct pER8-HopAI1-3xFLAG for the inducible expression of the native form of the protein harboring a C-terminal 3xFLAG has been provided by Dr. Jianming Zhou (NIBS, China).

The mutated *HopAI1*^{CS} has been inserted into the pMDC7 vector, a gateway-compatible binary T-DNA destination vector derived from pER8 (Curtis and Grossniklaus, 2003). It was not possible to use the pDEST17-HopAI1^{CS} as a template for gene amplification and sub-cloning into a vector for plant expression because it contained the truncated form of the protein (core fragment 7-245). Thus, full length

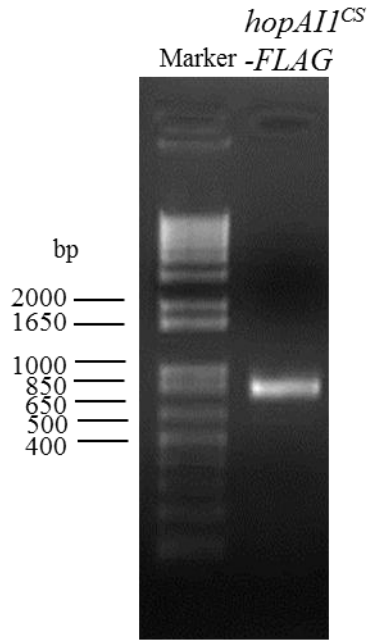

Figure 12 PCR amplification of *HopAI1*^{CS}*-FALG* from genomic DNA of *Pst* DC3000.
The length of full *HopAI1* ^{CS}*-FLAG* predicted by Vector NTI is 832 bp.

sequence of *HopAI1* was cloned from genome of *Pst* DC3000 and the mutation of Cys^{138} as well as a C-terminal FLAG sequence have been inserted by overlap extension PCR. This technique allowed the direct cloning of the mutated form HopAI1^{CS} fused to a C-terminal FLAG tag using two couples of primers producing two parts of the gene of interest. Then the two PCR products have been mixed for a second step of PCR in order to get the entire fragment (Figure 12).

The fragment was then sub-cloned into the pENTR/D-TOPO vector (Invitrogen) and the resulting construct pENTR/D-TOPO-HopAI1^{CS}-*FLAG* has been controlled by sequencing.

The construct pMDC7-HopAI1^{CS}-FLAG (Figure 13) for expression in plants has been then obtained by LR recombination reaction and further controlled by colony PCR (Figure 14).

To use as a control of transformation in further experiments, the empty pMDC7 (pMDC7-EV) has been produced by digestion of the vector pMDC7 with the restriction enzyme Sal I and successive ligation to remove the gateway reading frames region (Gateway Cassette attR (4216-4345)—CM resitance Marker (4454-5113) and ccd B (5455-5760)—attR2 (5801-5925) (Figure 2 in Appendix)

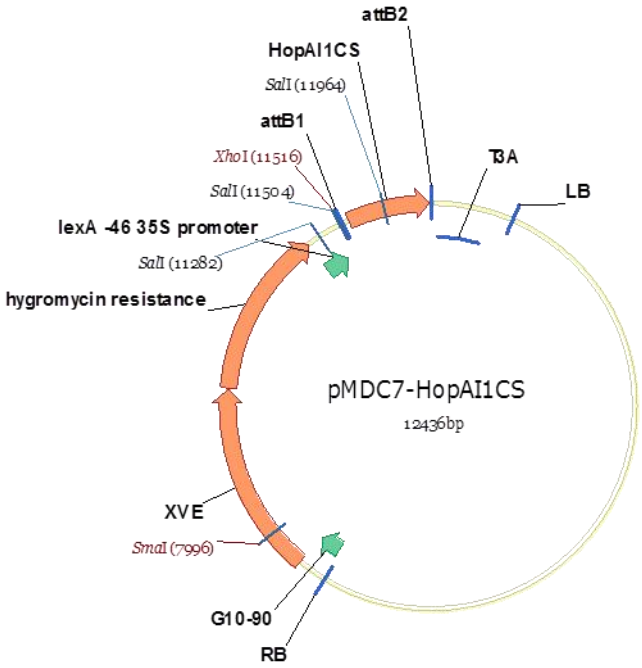

Figure 13 Map of the construct pMDC7-*HopAI1*^{CS} *-FLAG*
Restriction sites used in the cloning procedure are indicated in red or italics.

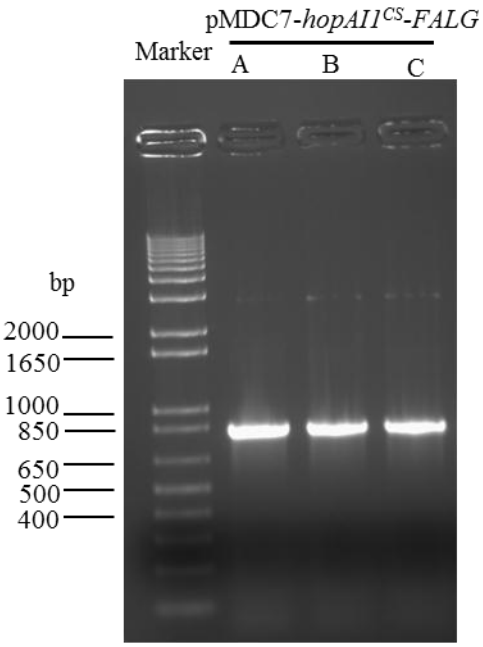

Figure 14 Control of colonies containing of pMDC7-*HopAI1*^{CS} *-FLAG* by colony PCR.
A, B, C indicate three different colonies that have been analyzed. The length of *HopAI1*^{CS} *-FLAG* predicted by Vector NTI is 832 bp.

For successive plant transformation by agro-infiltration, the strain GV3101 of *Agrobacterium tumefaciens* has been transformed with each of the constructs obtained, *i.e.* pER8-HopAI1-3xFLAG, pMDC7-HopAI1^{CS}-FLAG and pMDC7-EV.

4.10 Transient expression in tobacco of active AtMKKs and HopAI1/HopAI1^{CS}

A large body of evidence shows that mitogen-activated protein kinase (MAPK) cascades play a fundamental role during PAMP-triggered immunity (PTI) and effector-triggered immunity (ETI) (Chisholm et al., 2006). It has been shown that the transient expression of the constitutively active forms of the MAPKK, AtMEK4 and AtMEK5, in tobacco leaves lead to HR-like cell death via the activation of the MAPKs SIPK and WIPK which are the homologs of Arabidopsis AtMPK6 and AtMPK3 respectively (Ren et al., 2002). Since AtMPK3 and AtMPK6 are of dephosphorylation by HopAI1 (Zhang et al., 2007), it can be assumed that HopAI1 would be able to dephosphorylate their homologs in tobacco as well, blocking the cell death induced by active

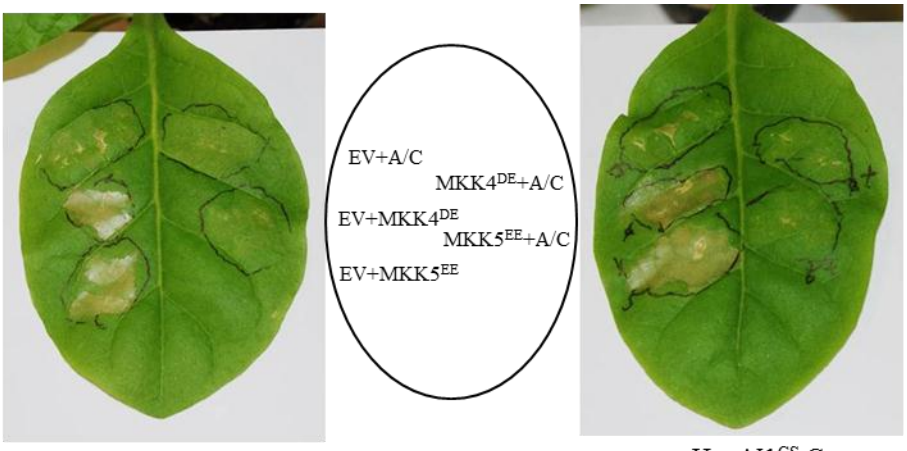

Figure 15 Co-expression of HopAI1 and HopAI1^{CS} with constitutively active forms of AtMKK4 and AtMKK5 in tobacco plants.
Nicotiana. tabacum cv. SR1 leaves were co-infiltrated with *A. tumefaciens* GV3101 carrying vectors as following and show in the middle panel. *A. tumefaciens* GV3101 carrying pER8-HopAI1 mixed with other *A. tumefaciens* GV3101 carrying vector are shown in left panel. *A. tumefaciens* GV3101 carrying pMDC7-HopAI1^{CS},C mixed with other *A. tumefaciens* GV3101 carrying other vectors are shown in the right panel.
EV+A/C, pMDC7-Empty Vector + pER8-HopAI1/pMDC7-HopAI1^{CS}; EV+MKK4^{DE}, pMDC7-Empty Vector + pMDC7-AtMKK4^{DE}; EV+MKK5^{EE}, pMDC7-Empty Vector + pMDC7-AtMKK5^{EE}; MKK4^{DE}+A/C, pMDC7-AtMKK4^{DE} + pER8-HopAI1/pMDC7-HopAI1^{CS}; MKK5^{EE} + A/C, pMDC7-AtMKK5^{EE} + pER8-HopAI1/pMDC7-HopAI1^{CS}; Photos have been taken 36 h after expression induction with 40 μM β-estradiol.

MAPKKs. Thus, this system has been chosen to study the effect of HopAI1 *S*-nitrosylation *in vivo*.

First we test if HopAI1 and HopAI1^{CS} can suppress the cell death induced by active AtMKK4 and AtMKK5 as shown in Ren's results (Ren et al., 2002). Two kinds of tobacco plants were used for the transient expression. *Nicotiana*. *tabacum* cv. SR1 leaves were co-infiltrated with *Agrobacterium. tumefaciens* GV3101 carrying various vector as show in Figure 15, and the transgene expression was induced by the application of 40 μM *β*-estradiol for 6 h.Thirty-six hour after induction both of tobacco leaf area expressing either active AtMKK4 (AtMKK4^{DE}) or AtMKK5 (AtMKK5^{EE}) showed a serious HR-Like cell death (EV+MKK4^{DE}/ MKK5^{EE} in Figure 15) in agreement with Ren's results, while no cell death was observed in tobacco leaf area expressing either *hopAI1* or *hopAI1*^{CS} (EV + A/C in Figure 15). The HR-like cell death induced by AtMKK4 or AtMKK5 was suppressed *in vivo* in tobacco leaf area co-expressing AtMKK4^{DE} or AtMKK5^{EE} with either HopAI1 or HopAI1^{CS} (MKK4^{DE}/ MKK5^{EE} + A/C in Figure 15). These results demonstrate that HopAI1 and HopAI1^{CS} work *in vivo* in a tobacco transient system suppressing the HR cell death induced by active AtMKK4 and AtMKK5.

4.11 Transient expression in tobacco of active AtMKK5 and HopAI1/HopAI1^{CS} in presence of NO

The transient system described in the previous paragraph was used then to test if

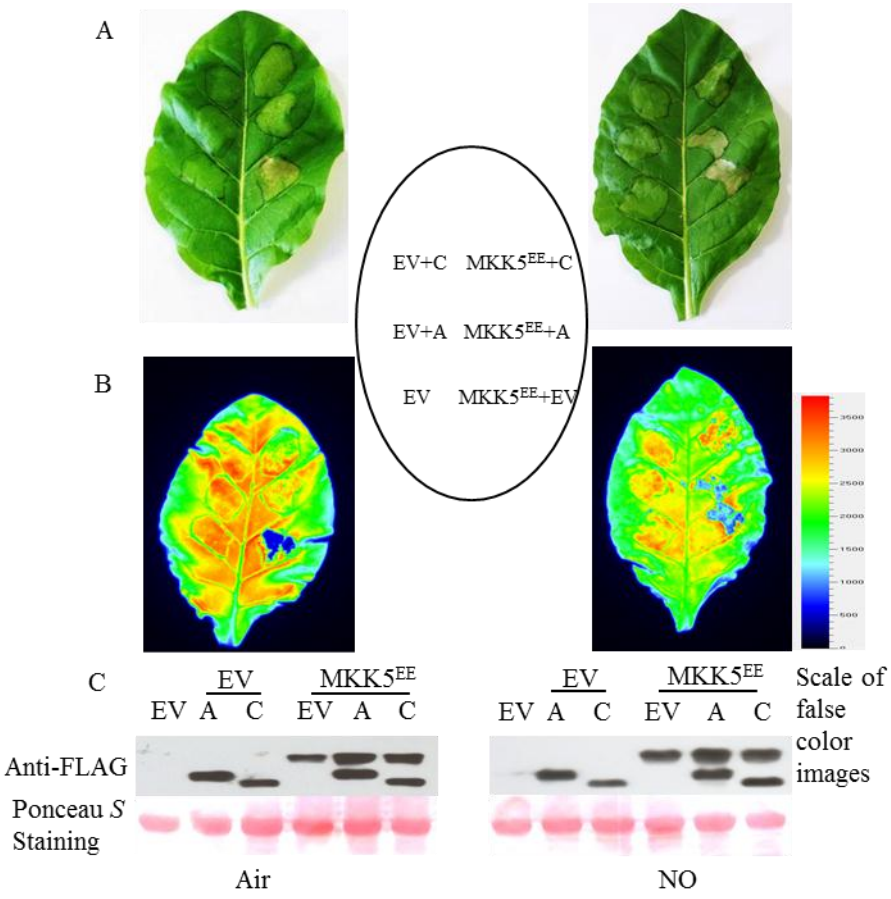

Figure 16 Effect of NO on active AtMKK5-mediated cell death inhibition by HopAI1 and HopAI1^{CS}.

Nicotiana. tabacum cv. SR1 leaves were co-infiltrated with *A. tumefaciens* GV3101 carrying different vectors. After expression induction with 40µM β-estradiol for 6 h, infiltrated tobacco plants were placed in the air or under fumigation with 50 ppm NO for 48h, both with continuous light (30-40 µmol/m2/s). Pictures of cell death phenotype (A) and false color images obtained with the FluorCam700MF (Photon Systems Instruments) (B) were taken after the 48h-treatment. (C) Expression of the transgenes were monitored by western blotting with polyclonal antibody anti-FLAG (Sigma) after induction for 18 h . Protein loading has been controlled by Ponceau *S* staining of the membrane. (D) The infiltration positions of each treatment .

EV, pMDC7-Empty Vector; EV+A, pMDC7-Empty Vector + pER8-HopAI1; EV+C, pMDC7-Empty Vector + pMDC7-HopAI1^{CS} ; EV+MKK5^{EE}, pMDC7-Empty Vector + pMDC7-AtMKK5^{EE}; MKK5^{EE}+A, pMDC7-AtMKK5^{EE} + pER8-HopAI1; MKK5^{EE}+C, pMDC7-AtMKK5^{EE} +p MDC7-HopAI1^{CS};

the presence of NO gas could inhibit HopAI1 activity *in vivo* by *S*-nitrosylation, as previously shown *in vitro*.

For this purpose an NO fumigation chamber facility previously established in our lab to supply NO gas in known concentration to plants was employed. *Nicotiana. tabacum* cv. SR1 plants were selected for this study. Plants were infiltrated with bacteria carrying the indicated constructs, and the transgene expression was induced by the application of 40 μM β-estradiol for 6 hours after agro-infiltration. Plants were then either put in the fumigation chamber using a flow speed of 300 ml/min, and a concentration of 50 ppm NO in air (Figure 16) or in a fumigation chamber under air. Two days after induction tobacco leaf area expressing AtMKK5^{EE} (MKK5^{EE}+EV in Figure 16), showed HR-like cell death symptoms both in plants under air or 50 ppm NO. No cell death was observed in leaf area expressing either EV or HopAI1 or HopAI1^{CS} alone (EV, EV+A and EV+C in Figure 16). In agreement with results presented in the previous paragraph, HR-like cell death was suppressed in leaf area co-expressing AtMKK5^{EE} with either HopAI1 or HopAI1^{CS} in the air. However, only in the presence of NO, leaf area co-expressing the AtMKK5^{EE} and HopAI1 still showed HR-like death (MKK5^{EE} + A in the Figure 16 NO), indicating that NO can reverse the inhibition of HR mediated by HopAI1. Nevertheless in leaf area co-expressing AtMKK5^{EE} and the mutated form HopAI1^{CS} the HR-like cell death was still suppressed like in air, (MKK5^{EE} + C in the Figure 16) indicating, that the mutated form HopAI1^{CS} is insensitive to NO (behaving the same as in the air). Chlorophyll fluorescence picture are also given to better highlight area undergoing HR (blue area in Figure 16B). In addition the expression level of AtMKK5^{EE}, HopAI1 and HopAI1^{CS} are similar in infiltrated leaf area as confirmed by western blotting (Figure 16 C). Taken together, these findings suggest that NO could block the HopAI1 inhibitory effect on active AtMKK5-mediated cell death, and that this NO effect was dependent on the presence of the only cysteine residue in HopAI1 protein.

4.12 Production of *Pst avrB* expressing HopAI1 and HopAI1^{CS}

To confirm the data we got from tobacco transient expression, we also tried to transfer *hopAI1/hopAI1*^{CS} into *Pst* DC3000 *avrB*, in which *hopAI1* is not expressed to check the function of them when delivered from *P.syringae*. The pRK415, which is broad-host-range plasmid vector (Keen et al., 1988), was used to express *hopAI1/hopAI1*^{CS} *in PST* DC3000 *avrB.*

First *HopAI1* and *HopAI1*^{CS} were separately cloned from pER8-HopAI1 and pENTR/D-Topo-HopAI1. And then both of them with right size were sub-cloned into the pENTR/D-TOPO vector (Invitrogen) and the resulting constructs pENTR/D-TOPO-*hopAI1/hopAI1*^{CS}*-FLAG* has been controlled by sequencing. Then the fragments of *hopAI1/hopAI1*^{C}*-FLAG* were got by double digestion from these two constructs.

The constructs of pRK415-*hopAI1/hopAI1*^{C}*-FLAG* (Figure 17) for expression have been then obtained by ligation double-digested pRK415 and *hopAI1/hopAI1*^{C}*-FLAG* further controlled by double digestion (Figure 18). pRK

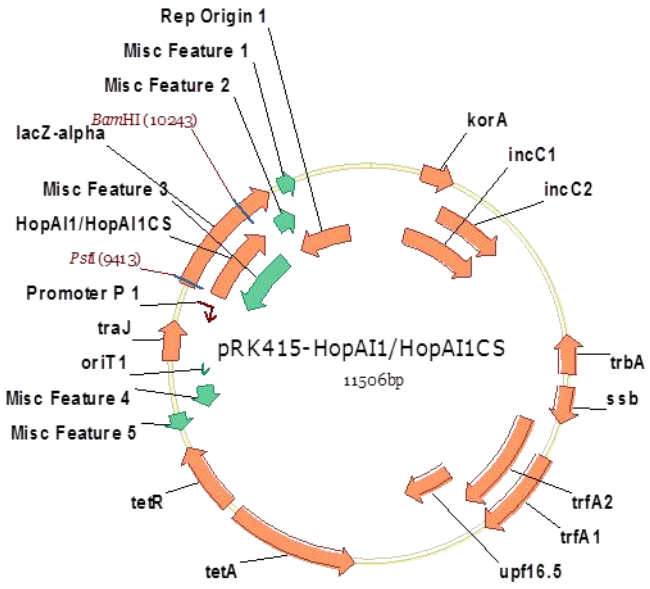

Figure 17 2 Map of the constructs pRK415-*HopAI1/HopAI1*^{CS}.
Restriction sites used in the cloning procedure are indicated in red or italics

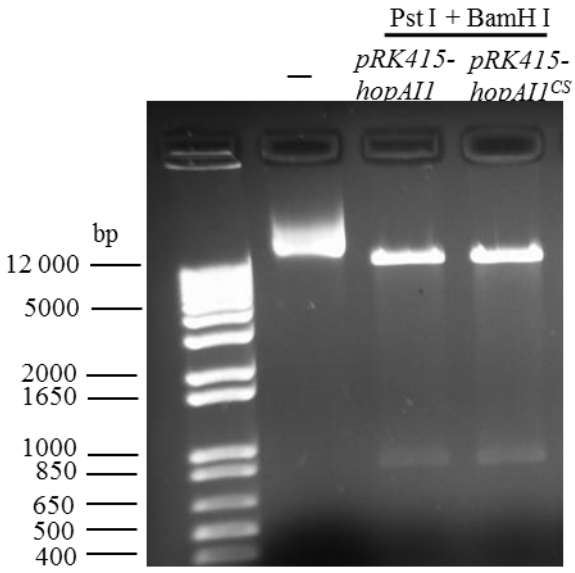

Figure 18 Control of the constructs pRK415-*HopAI1/HopAI1*^{CS} *by* double digestion of the plasmids with restriction enzymes
—, undigested pRK415-*HopAI1*

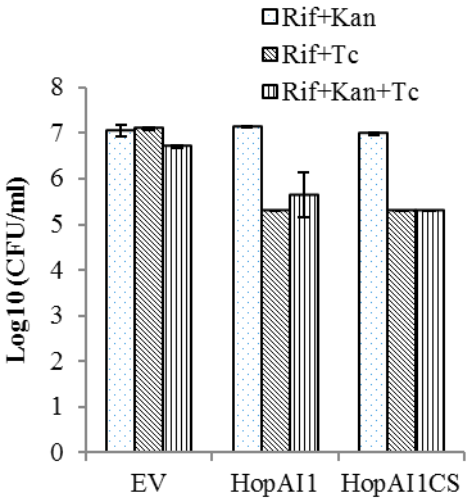

Figure 19 Bacterial growth of strains of *Pst* DC3000 carrying *avrB* and *EV* or *hopAI1* or *hopAI1*^{CS}.
The different strains have been grown in 3ml of KB medium without antibiotics at 28°C overnight. Then each inoculum has been diluted at OD_{600} 0.02 and plated on plates containing KB agar medium with different antibiotics as indicated.
Rif, rifampycin 50 µg /ml ; Kan, kanamycin 50 µg /ml; Tc, tetracyclin 20 µg /ml. The number of colonies have been counted after 2 d at 28°C. Error bars indicate the standard deviation.

415 was used as a control of transformation in further experiments (pRK415-*EV*).

Unfortunately we found it seems pRK415-*hopAI1/hopAI1*^{CS} isn't stable during the *PST* DC3000 *avrB* growth (data are not shown).We inoculated *Pst* DC3000 *avrB* carrying pRK415-EV/HopAI1/HopAI1^{CS}, which grew on KB agar medium with 50µg/ml Rif (selection towards *Pst* DC3000), 50µg/ml Kan (selection towards vector carrying *avrB*), and 20µg/ml Tc (selection towards pRK415-*EV*/*hopAI1/hopAI1*^{CS}), in KB liquid without antibiotics overnight. Then we counted number of the bacterium growing on the KB agar medium with 50µg/ml Rif, 50µg/ml Kan, 50µg/ml Rif, and 20µg/ml Tc, 50µg/ml Rif, 50µg/ml Kan, 50µg/ml Rif, and 20µg/ml Tc. The result showed pRK415-*hopAI1/hopAI1*^{CS} werenot stable during the *PST* DC3000 *avrB* growth, which both of the number of *Pst* DC3000 *avrB* carrying pRK415-HopAI1/HopAI1^{CS} growing on the selection medium with Rif+Tc and Rif+Kan+Tc was much less than the number of the ones growing on the selection medium with Rif+Kan (Figure 19). In contrary, the pRK415-EV in *Pst* DC3000 *avrB* carrying was stable and grew similarly among different selection medium with Rif+Tc and Rif+Kan+Tc. Thus we used another system, which expressing *hopAI1/hopAI1*^{CS}

in planta to validate our data from transient expression

4.13 Production of Arabidopsis HopAI1^{CS} stable transgenic lines and assessment of HopAI1 transgenic lines

To further confirm *in vivo* data from the previously described transient system, stable Arabidopsis transgenic lines carrying and expressing upon induction *hopAI1* and *hopAI1*^{CS} bacterial transgenes have been obtained.

Stable Arabidopsis transgenic lines carrying *hopAI1* were obtained from Dr. Jianming Zhou's lab. These lines were prepared as described in Li's paper (Li et al.,

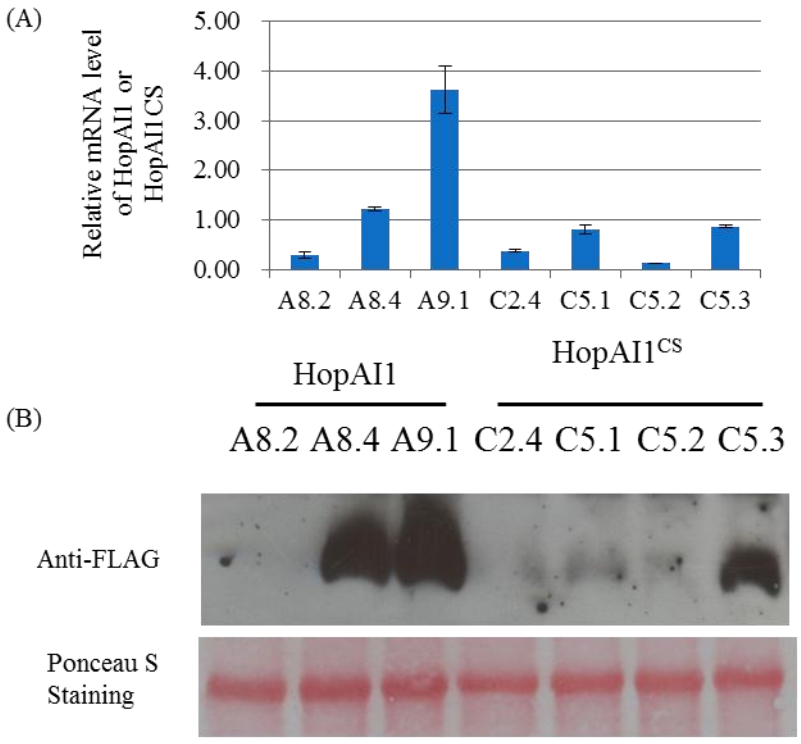

Figure 20 Analysis of the level of expression of HopAI1 and HopAI1CS in stable transgenic *Arabidopsis thaliana* lines.
(A) Real-time RT-PCR using specific primers for *hopAI1* and *hopAI1*^{CS}. The level of expression of both genes was normalized to the expression of the gene encoding for *actine 2*. Error bars indicate standard deviation.
(B) Western blot using an polyclonal antibody anti-FLAG (Sigma). Protein loading has been controlled by Ponceau staining of the membrane.
Total RNA and total proteins used for real-time RT-PCR and western blot respectively have been extracted from leaves of different *Arabidopsis thaliana* transgenic lines (A, pER8-*hopAI1*; C, pMDC7-*HopAI1*^{CS}) harvested 12h after expression induction with β-estradiol.

2005).

Furthermore stable Arabidopsis transgenic lines carrying the mutated form of the bacterial gene *hopAI1*^{CS} were prepared using the previously described pMDC7-HopAI1^{CS} inducible construct, as well as stable Arabidopsis transgenic lines carrying just the empty vector to be used as control. Homozygous T2 lines carrying a single copy gene were selected.

The expression of transgenes in Arabidopsis transgenic lines carrying *hopai1* and *hopai1*^{cs} has been checked by real time RT-PCR. Among Arabidopsis transgenic carrying *hopai1*, lines A8.4 and A9.1 showed the strongest expression after induction by 40 μM β-estradiol for12 h. Similarly lines C5.1 and C5.3 showed the highest expression for the transgene *hopAI1*^{CS} (Figure 20A). By western blotting an high protein content was confirmed for lines A8.4, A9.1 and C5.3 (Figure 20B). Therefore these lines have been selected for further studies.

4.14 Challenge of transgenic Arabidopsis lines with *Pst avrRpt2*

In Arabidopsis plants the effector AvrRpt2 triggers HR development upon recognition by the plant R-protein RPS2 (REF). It has been published as well that AvrRpt2 induce the activation of MPK3 and MPK6 (Underwood et al., 2007) which are therefore supposed to mediate the HR-cell death development. We used this system to test whether HopAI1 /HopAI1^{CS} can suppress MPK3 and MPK6 activation and consequently attenuate the AvrRpt2- induced HR development *in vivo*.

To this aim the transgenic Arabidopsis lines carrying *hopAI1* and *hopAI1*^{CS} genes previously described, 24 hours after gene induction by estradiol were infiltrated with inocula of the bacterial pathogen *Pseudomonas syringae* DC3000 carrying *avrRpt2* prepared at two different concentrations. Similarly, also transgenic lines carrying the empty PMDC7 vector were induced and infiltrated as control. The development of the

HR-cell death was visualized by the trypan blue staining. As shown in Figure 21 a normal HR development was visible 20 hours after infection in transgenic lines carrying the empty vector or the *hopAI1*. The development of HR was instead at least partially suppressed in Arabidopsis transgenic lines expressing the mutated form *hopAI1*^{CS} which was insensitive to NO.

The HR development in the same transgenic lines was also followed by measuring ion conductivity in water due to ion released by leaf discs upon pathogen infection. Ion released and conductivity are proportional to the amount of cell death. For this experiment plants were challenged, 24 hours after estradiol gene induction, with a *Pseudomonas syringeae avrRpt2* bacterial inoculum prepared at the concentration of 5x10^7 cfu/ml and conductivity was measured for 48 hours after infection. This experiment confirmed previous results showing a stronger reduction in HR development in transgenic lines carrying the mutated NO insensitive *hopAI1*^{CS} transgene. Nevertheless a partial reduction in HR was also consistently reported in *hopAI1* lines while no HR developed using a mock solution for infection (Figure 22). .

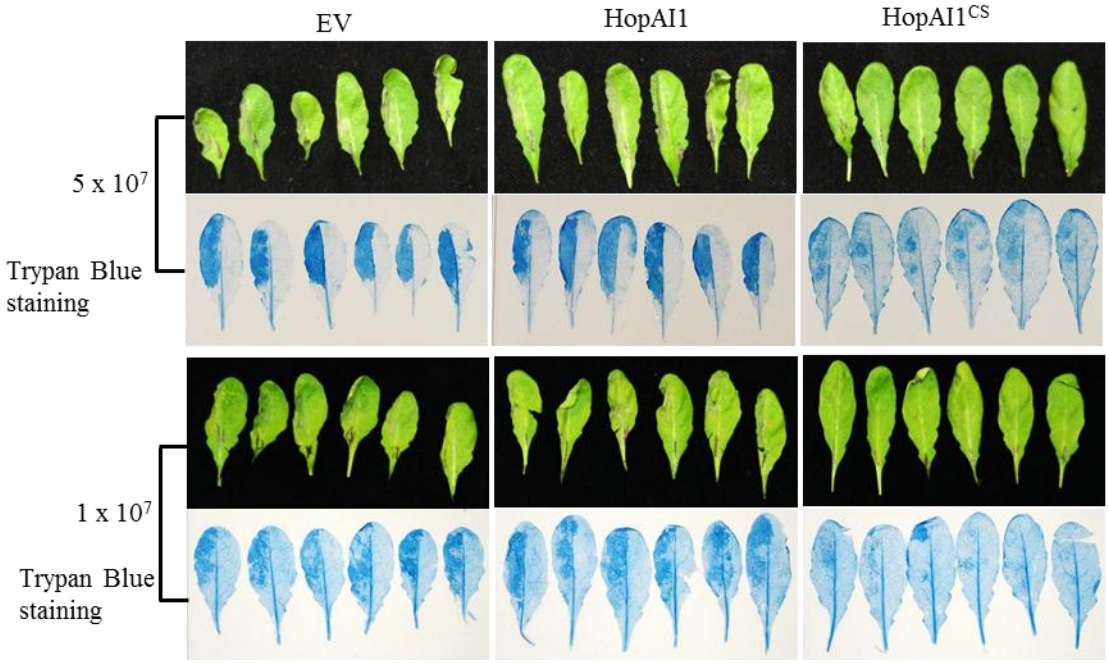

Figure 21 Analysis of the hypersensitive cell death induced by the avirulent strain of *Pst* DC3000 carrying *AvrRpt2* in transgenic lines expressing HopAI, HopAI^{CS} or the empty vector. HopAI1^{CS} not HopAI1suppresses the HR induced by *PST* DC3000 carrying *AvrRpt2*. Seven-week-old empty vector (EV), HopAI1 and HopAI1^{CS} transgenic plants were sprayed with 40 µM β-estradiol for 24 h. Half-leaves were infiltrated with 1×10^7 or 5×10^7 *Pst* DC3000 carrying *AvrRpt2*. The pictures were taken 20h post-infection. Typan blue staining was performed on the same leaves.

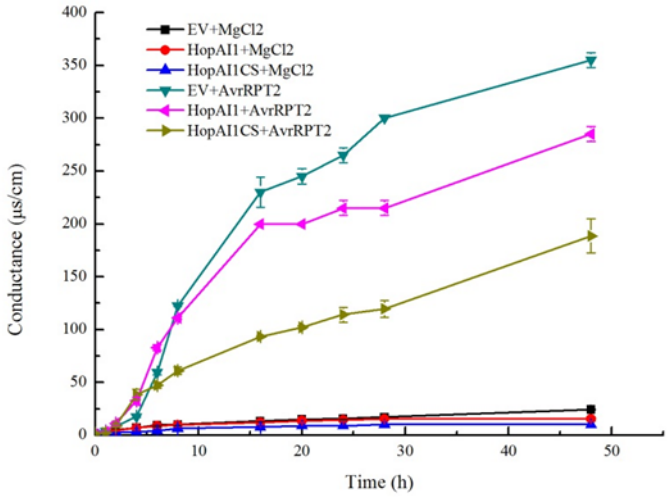

Figure 22 Measurement of the hypersensitive cell death induced by the avirulent strain of *Pst* DC3000 carrying *avrRpt2* in transgenic lines expressing HopAI1, HopAI1^{CS} or the empty vector. Ion leakage was performed with leaf disks from seven-week-old Empty vector (EV), HopAI1 and HopAI1^{CS} transgenic plants sprayed with 40 μM β-estradiol for 24 h before infection with 5×10^7/ml *Pst* DC3000 carrying *AvrRpt2*. As control, leaves from the same transgenic lines have been infiltrated with 10 mM $MgCl_2$ buffer as control. Error bars indicate standard deviation.

Altogether these results suggest that during the normal HR development HopAI1 is inactivated by the NO induced during the HR by a mechanism which is dependent on the presence of the cysteine[138]. Even if the *S*-nitrosylation of HopAI1 *in vivo* could

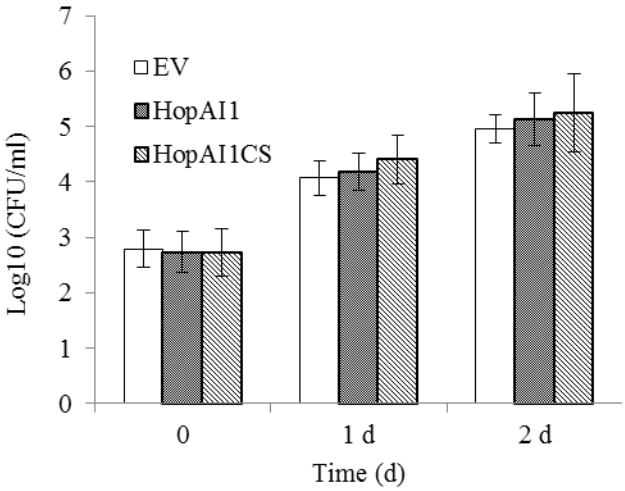

Figure 23 Bacterial growth measurement in transgenic lines expressing *EV orhopAI1* or *HopAI1^{CS}*
Six leaf disks from seven-week-old Empty vector (EV), HopAI1 and HopAI1^{CS} transgenic plants sprayed with 40 μM β-estradiol for 6h prior to pathogen infiltration were taken at the indicated times after infection with *Pst* DC3000 carrying *AvrRpt2*. Error bars indicate standard deviation.

not be reported yet, this support the possibility that HopAI1 is *S*-nitrosylated and then inhibited also *in vivo*, in agreement with our previous *in vitro* data. Finally the kinetics of the bacterial growth in plants was also investigated in the same transgenic lines. Six hours after gene induction plants were infiltrated with the same avirulent bacterial strain ($5x10^7$ cfu/ml inoculum). This experiment anyway did not allow us to correlate the previously reported compromised HR development in lines carrying the mutated form of the *hopAI1* gene with a higher bacterial growth in plant, at least in the conditions that we tested (Figure 23).

5. Discussion

The aim of this thesis was to investigate the possible role of NO produced by plants challenged with an avirulent pathogen as an inhibitor of HR-suppressing effectors, in particular HopAI1 from the model bacterial pathogen *Pst* DC3000.

Using different methodologies, we first demonstrated that the recombinant protein HopAI1 is *S*-nitrosylated *in vitro* by the NO donor GSNO, in a dose-dependent manner. Moreover NO-treatment dramatically decreases HopAI1 activity. The use of other *S*-nitrosylating agents, CysNO and DEA-NONOate confirmed that the inhibition is effectively due to NO. Moreover, the mutation of the unique Cys present in the sequence of HopAI1 at position 138 ($HopAI1^{CS}$) resulted in a protein insensitive to the inhibition by GSNO, confirming that NO blocks HopAI1 activity by *S*-nitrosylation of this residue. As observed for other *S*-nitrosylated proteins the activity of which is affected by such modification on critical Cys residues, it is worth noting that the activity of $HopAI1^{CS}$ is only about 30% of the activity of the native form of the protein. Such reduction of $HopAI1^{CS}$ activity confirms that Cys^{138} is crucial for full HopAI1 activity and is consistent with our findings that *S*-nitrosylation at Cys^{138} negatively regulates the phosphothreonine lyase activity of HopAI1.

In order to understand the mechanism of HopAI1 *S*-nitrosylation and to uncover the effect of such post-translational modification on protein structure to correlate with the inhibition of the activity, we performed a bioinformatics analysis of the sequence of the protein and built a 3D structure model in presence and absence of S-NO at Cys^{138}. We found that the target Cys is surrounded by an acid-base consensus motif that is known to promote *S*-nitrosylation (Perez-Mato et al., 1999), composed of two basic amino acids, $Asp^{135}$and Asp^{142} and two acidic amino acids, Lys^{73} and Lys^{75}, which could thus account for the modification. Moreover, the *S*-nitrosylation of Cys^{138} significantly modifies the electrostatic potential distribution in HopAI1 structure, with the occurrence of negative charges in the microenvironment around SNO-Cys, as observed for instance in the blackfin tuna myoglobin (Marino and Gladyshev, 2010). Such negative charges within HopAI1 structure may lead to the rejection of the substrate, at the level of its Phe residue that is also located close to negatively charged

amino acids (S<u>E</u>S<u>D</u>**F**MTEYVVTR). It could be thus assumed that *S*-nitrosylation may inhibit HopAI1 activity through a reduction of its binding property with the substrate. In this context the study of HopAI1 binding with phosphorylated MAPKs deserves attention in the future to fully understand the mechanism of HopAI1 inhibition by *S*-nitrosylation.

To further analyze the effect of HopAI1 *S*-nitrosylation *in vivo*, we first used a simplified model that consists in the transient expression of an active MKK in tobacco plants. Indeed, it has been previously reported that the transient expression in tobacco of a constitutively active form of AtMKK4/AtMKK5, mutated in the activation loop to mimic its phosphorylation, leads to an HR-like cell death via the activation of the two MAKPs, SIPK and WIPK, homologs of AtMPK3 and AtMPK6 (Ren et al., 2002). We thus assumed that HopAI1 could inhibit cell death when co-expressed with active MKKs. As expected, the transient co-expression of HopAI1 in *Nicotiana tabacum* cv. SR1 inhibits the cell death induced by the active AtMKK4 ($AtMKK4^{DE}$) and AtMKK5 ($AtMKK5^{EE}$), confirming that HopAI1 can target the homologs of AtMPK3/AtMPK6 in tobacco. Meanwhile the mutant $HopAI1^{CS}$ is also able to suppress $AtMKK4^{DE}$ / $AtMKK5^{EE}$-induced cell death, suggesting that in this system the residual activity of 30% is enough to block the activity of endogenous MAPKs. This is likely due to the high level of $HopAI1^{CS}$ expression that can compensate the low activity by increasing the ratio $HopAI1^{CS}$/MAPKs. Moreover, the fumigation of tobacco plants transiently co-expressing both HopAI1 and $AtMKK5^{EE}$ with NO gas at 50 ppm can revert cell death inhibition, suggesting that NO is able to inhibit HopAI1 activity. Supporting a role for *S*-nitrosylation in HopAI1 inhibition under NO fumigation, while $HopAI1^{CS}$ is still able to suppress $AtMKK5^{EE}$-induced cell death in these conditions, confirming the data obtained *in vitro*.

Although this system represented a good tool to start the investigations about HopAI1 inhibition by NO *in vivo*, we proceeded with a more physiological system in order to highlight the biological relevance of such regulation of a pathogen effector via *S*-nitrosylation. We thus decided to use transgenic *Arabidopsis thaliana* plants expressing both proteins under the control of an inducible promoter. Transgenic plants

expressing HopAI1 provided by Dr. Jianmin Zhou (National Institute of Biological Sciences, China) were assessed for their homozygosis and their level of HopAI1 expression, whereas plants expressing HopAI1^{CS} have been produced in our laboratory, using the Gateway technology. Both genes are under the control of an estrogen-inducible promoter. It is worth noting that as reported previously for HopAI1 (Li et al., 2005), HopAI1^{CS} leads to the occurrence of similar chlorosis symptoms after 5 days of induction, reminiscent of disease symptoms. This confirms that also in stable transgenic *Arabidopsis thaliana* plants, the high level of HopAI1^{CS} expression compensates the residual 30% of activity of the mutant protein to exert HopAI1 effect on target MAPK.

The analysis of the phenotype of the different transgenic plants challenged with an avirulent pathogen was further analyzed within the first three days after expression induction with *β*-estradiol in order to avoid any side effect attributable to leaf yellowing. The infection with the avirulent strain of *Pst* DC3000 carrying the avirulence gene *AvrRpt2* (*Pst* DC3000 *avrRpt2*) triggered the same symptoms of hypersensitive cell death at 20 hours post-infection (hpi) in transgenic plants expressing HopAI1 as compared with control plants (transformed with empty vector). In literature, it is reported that MAPK cascades play an important role in mediating cell death during the HR. For instance, the cascade consisting in MAPKKK-MEK1/MEK2-SIPK/NTF6 is required for Pto-mediated HR and resistance against *Pseudomonas syringae* pv. *tomato* in tobacco (Ekengren et al., 2003; del Pozo et al., 2004). Moreover, hypersensitive cell death induced by several avirulence factors, such as Avr9 from *Cladosporium fulvum*, AvrPtoBD6 recognized by the R protein Rsb, or AvrPto from *Pseudomonas syringae*, is suppressed in *N. benthamiana* leaves silenced for *NbMKKKα* (del Pozo et al., 2004). Thus, since a normal hypersensitive cell death is observed in HopAI1-expressing plants, this suggests that MAPKs are active and thus that HopAI1 is inhibited. Since flg22-induced MAPK activity is compromised in these plants (Zhang et al., 2007a), this further indicates that the activity of HopAI1 is compromised specifically during the HR induced by AvrRpt2. Conversely, we observed that the expression of HopAI1^{CS} strongly reduced

cell death symptoms as compared with HopAI1-expressing and control plants. This suggests that MAPK activity required for AvrRpt2-induced cell death is suppressed by HopAI1^{CS} and thus that the activity of the mutant HopAI1^{CS} is not inhibited in these conditions.

Taking together the data obtained *in vitro* and *in vivo*, it is likely to assume that the activity of the native HopAI1 is affected by the NO produced by the plant during the HR, which would be responsible for its *S*-nitrosylation.

Using *Arabidopsis thaliana* plants silenced for *AtMPK6*, it has been previously reported that this MAPK is involved in plant resistance during the infection with the avirulent *Pst* DC3000 *avrRpt2* (Menke et al., 2004). Curiously, while we expected a decrease of the resistance in plants expressing HopAI1^{CS} as compared with wild-type and HopAI1-expressing plants, no difference in bacterial growth was observed between the different plant lines, suggesting that plant resistance is not affected by the presence of a mutated form of HopAI1 insensitive to *S*-nitrosylation. One explanation could be the conditions used to carry out the experiment. Indeed, whereas 24h of induction with β-estradiol prior to infection have been used to study AvrRpt2-induced cell death, only 6h of induction have been used for bacterial count experiment. Meanwhile such lapse of time resulted insufficient to get significant reproducible differences even for cell death analysis. According to such observation, it has been reported that the level of HopAI1 expression is critical to observe its effect on plant defense alteration (Shan et al., 2007). Indeed, contradictory results have been obtained concerning suppressor activity of HopAI1 on MAPK activity that could depend on the ratio of HopAI1 to MAPK protein level (He et al., 2006; Zhang et al., 2007). We can thus assume that since HopAI1^{CS} shows only 30% of residual activity as compared with the native form of the enzyme, the level of expression in plants should be high enough to ensure the complete inhibition of MAPK cascade components.

Taken together, our results demonstrate that NO produced during the HR induced by an avirulent pathogen, not only contributes to defense signal transduction and defense gene expression but also participates in suppressing virulence activity of the effectors released by the pathogen during the infection in order to ensure plant

resistance. A model can be proposed to explain the role of HopAI1 inhibition by NO during the HR (Figure 1).

This model is consistent with the concept of host-mediated effector inhibition to promote resistance against infection. The first effector identified to be modified by plant cells is AvrPtoB, which is phosphorylated by the Pto kinase within the E3 ligase domain, inhibiting its ubiquitination activity (Ntoukakis et al., 2009). HopAI1 *S*-nitrosylation would thus represent a novel mechanism for the suppression of phytopathogen effector activity, as observed in animal pathogens including viruses and bacteria (Saura et al., 1999; Badorff et al., 2000; Cao et al., 2003; Padalko et al., 2004; Kemball et al., 2009; Ntoukakis et al., 2009; Savidge et al., 2011). This highlights the capacity of host cells, from animal or plants, to use the same molecular events to transduce defense signals, which is not only *S*-nitrosylation of host proteins but also *S*-nitrosylation of pathogen virulent protein to suppress their virulence. Such inhibition of virulence activity by plant cells could participate in the selection pressure imposed by plants to pathogens that led during the evolution to the creation of many different effector repertoires among the different strains of bacterial pathogens. A recent work reported the comparison of the effectors present in 18 strains of

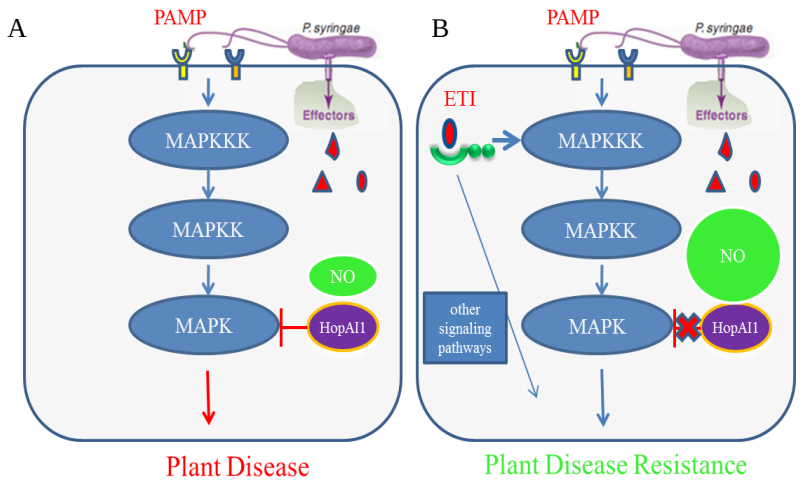

Figure 1 Proposed models for the modulation of HopAI1 activity during PTI (A) and ETI (B).

(A) NO burst triggered by PTI is not sufficient to revert the suppression of MAPK signaling caused by HopAI1.

(B) NO burst triggered by ETI inhibits HopAI1 activity by S-nitrosylation and reverts the suppression of MAPK signaling caused by HopAI1.

Pseudomonas syringae. According to this study, HopAI1 ORF exists in 7 strains of *Pseudomonas syringae*, whereas it is absent in 6 strains and disrupted or truncated in 5 other strains, corresponding to a medium distribution of this effector compared with others within Pseudomonas strains (Baltrus et al., 2011), suggesting a negative selection pressure for this effector. Since Cys mutation renders HopAI1 insensitive to *S*-nitrosylation, the mutated form of the effector could have been selected during the evolution to overcome NO-mediated inhibition. However, we demonstrated in this work that HopAI1^{CS} displays only 30% of native activity. Even if sufficient in a context of a high level of expression mediated by a strong promoter in plants, it could be assumed that such residual activity would not be enough to ensure the complete inhibition of ETI-induced MAPK cascade when introduced at physiological levels by the type III secretion system. Thus, according to the results obtained in the present work, the medium distribution of HopAI1 and its disappearance in some *Pseudomonas* strains is likely due to a selection against its presence that is useless for pathogen virulence and that cannot be modified by mutations, as it is observed usually for effectors that lead to recognition by a plant immune receptor and this is consistent with the concept that loss of effector function may be an important factor in the evolution of *Pseudomonas syringae* virulence(Schechter et al., 2006).

To test this hypothesis we transformed a strain *Pseudomonas* to express HopAI1 and HopAI1^{CS}. It has been reported that in *Pst* DC3000 genome the *hopAG1-hopAH1-hopAI1* operon is interrupted by a transposon insertion in *hopAG1* (Vinatzer et al., 2005), leading to the reduction or the abolishment of the expression of *HopAI1* by this strain of *Pseudomonas syringae*. Thus both HopAI1 and HopAI1^{CS} have been introduced into an avirulent strain of *Pst* DC3000 carrying the avirulent gene *AvrB*. The aim of such approach was to demonstrate i) that the HR induced by AvrB carried by the strain was not affected by HopAI1 expression, due to its possible inhibition by NO produced during this process, and ii) that the residual 30% activity HopAI1^{CS} expressed at physiological levels was not sufficient to suppress defense responses. Unfortunately the strains transformed with pERK415-*HopAI1/HopAI1*^{CS} displayed lower growth efficiency as compared with the control strain carrying the

empty vector. This could be due to a negative impact of the expressed genes on transformed bacteria. It has thus been impossible to use such strains for further studies on plant defense because it would have led to unreliable data attributable to a different behavior of the strains within plant cells.

Because Cys residues are widely distributed in various type III effectors, and some of them a critical for effector activity, the role of NO-mediated *S*-nitrosylation could represent a novel mechanism for suppression virulence effector activity during the HR. In this context, the protein HopAO1 (also known as HopPtoD2) could represent a good target for NO-mediated activity suppression. This protein is another effector from *Pseudomonas syrinage* pv. *tomato*, which possesses a protein tyrosine phosphatase activity that targets MAPK cascade (Bretz et al., 2003; Espinosa et al., 2003). Consistent with such enzymatic activity, the transient overexpression of HopAO1 in tobacco suppresses the cell death induced by an active tobacco MKK, $NtMEK2^{DD}$ and this cell death suppression function of HopAO1 requires the conserved catalytic Cys residue (Espinosa et al., 2003). Contrary to HopAI1, HopAO1 is secreted in bacterial culture by the type III secretion system of *Pst* DC3000 (Petnicki-Ocwieja et al., 2002). Interestingly, despite its release by the pathogen into host cells and although it is able to block successfully PAMP-induced basal defense, it fails to suppress the HR induced by several avirulent genes (Underwood et al., 2007), suggesting like for HopAI1 the existence of an inhibitory mechanism related to HR events. Moreover, HopAO1 displays also a medium distribution among *Pseudomonas* strains, as mentioned for HopAI1 (Baltrus et al., 2011), indicating a negative selection of this effector as well. Thus, according to the presence of a crucial Cys residue required for its activity, it could be assumed that, as demonstrated in this work for HopAI1, the *S*-nitrosylation of HopAO1 by NO could lead to an inhibition of its activity, rendering useless this effector toward resistant plants able to induce ETI. In such a scenario, the effector HopAO1 deserves attention in the future.

Besides S-nitrosylation, also tyrosine nitration mediated by peroxynitrite is thought to play an important role during plant defense responses (Vandelle and

Delledonne, 2011). Moreover, in animals, it has been reported that peroxynitrite can nitrate and cross-link coxsackievirus capsid polypeptides, leading to the inhibition of viral uncoating that is necessary for viral entry into the host cell (Padalko et al., 2004). We could thus assume that such protein modification could also account for effector inhibition by plant host cells to ensure plant resistance.

Additionally, three MAPKs, namely AtMPK3, AtMPK4 and AtMPK6 have been confirmed as substrates of HopAI1 (Zhang et al., 2007a; Zhang et al., 2012), it is likely to assume that other MAPKs can be target of its phosphothreonine lyase activity. Indeed, the sequence of synthetic phosphopeptide (SESDFMTEYVVTR) used for *in vitro* kinase assay and which corresponds to the AtMPK6 T-X-Y motif, is highly conserved among plant MAPK family (Rodriguez et al., 2010), suggesting that many MAPKs out the 20 encoded in the genome of Arabidopsis thaliana (Hamel et al., 2006), could be target of dephosphorylation by HopAI1. Such MAPKs yet unidentified could represent other virulence targets of HopAI1 suppressed by *Pseudomonas* not to inhibit plant defense like AtMPK3/AtMPK6 but to promote disease establishment.

As a conclusion, this work highlights that the study of inactivated or disrupted effector-encoding genes and their effect on plant defense suppression is of high interest for evolutionary studies and demonstrate that also the study of post-translational modifications, in particular the ones mediated by reactive nitrogen species produced by host cells, should be considered in order to fully understand the molecular dialog that exists between plants and their pathogens.

6. References

Abagyan, R., Totrov, M., and Kuznetsov, D. (1994). ICM—A new method for protein modeling and design: Applications to docking and structure prediction from the distorted native conformation. Journal of Computational Chemistry **15,** 488-506.

Abat, J.K., and Deswal, R. (2009). Differential modulation of S-nitrosoproteome of Brassica juncea by low temperature: change in S-nitrosylation of Rubisco is responsible for the inactivation of its carboxylase activity. Proteomics **9,** 4368-4380.

Abat, J.K., Mattoo, A.K., and Deswal, R. (2008). S-nitrosylated proteins of a medicinal CAM plant Kalanchoe pinnata- ribulose-1,5-bisphosphate carboxylase/oxygenase activity targeted for inhibition. FEBS J **275,** 2862-2872.

Abramovitch, R.B., Anderson, J.C., and Martin, G.B. (2006). Bacterial elicitation and evasion of plant innate immunity. Nat Rev Mol Cell Biol **7,** 601-611.

Alamillo, J.M., and Garcia-Olmedo, F. (2001). Effects of urate, a natural inhibitor of peroxynitrite-mediated toxicity, in the response of Arabidopsis thaliana to the bacterial pathogen Pseudomonas syringae. Plant J **25,** 529-540.

Ali, R., Ma, W., Lemtiri-Chlieh, F., Tsaltas, D., Leng, Q., von Bodman, S., and Berkowitz, G.A. (2007). Death don't have no mercy and neither does calcium: Arabidopsis CYCLIC NUCLEOTIDE GATED CHANNEL2 and innate immunity. Plant Cell **19,** 1081-1095.

Almeida, N.F., Yan, S., Lindeberg, M., Studholme, D.J., Schneider, D.J., Condon, B., Liu, H., Viana, C.J., Warren, A., Evans, C., Kemen, E., Maclean, D., Angot, A., Martin, G.B., Jones, J.D., Collmer, A., Setubal, J.C., and Vinatzer, B.A. (2009). A draft genome sequence of Pseudomonas syringae pv. tomato T1 reveals a type III effector repertoire significantly divergent from that of Pseudomonas syringae pv. tomato DC3000. Mol Plant Microbe Interact **22,** 52-62.

Andersson, M.X., Kourtchenko, O., Dangl, J.L., Mackey, D., and Ellerstrom, M. (2006). Phospholipase-dependent signalling during the AvrRpm1- and AvrRpt2-induced disease resistance responses in Arabidopsis thaliana. Plant J **47,** 947-959.

Andreasson, E., Jenkins, T., Brodersen, P., Thorgrimsen, S., Petersen, N.H., Zhu, S., Qiu, J.L., Micheelsen, P., Rocher, A., Petersen, M., Newman, M.A., Bjorn Nielsen, H., Hirt, H., Somssich, I., Mattsson, O., and Mundy, J. (2005). The MAP kinase substrate MKS1 is a regulator of plant defense responses. EMBO J **24,** 2579-2589.

Apel, K., and Hirt, H. (2004). Reactive oxygen species: metabolism, oxidative stress, and signal

transduction. Annu Rev Plant Biol **55,** 373-399.

Asai, S., and Yoshioka, H. (2009). Nitric oxide as a partner of reactive oxygen species participates in disease resistance to nectrotophic pathogen Botryis cinerea in Nicotiana benthamiana. Mol Plant Microbe Interact **22,** 619-629.

Asai, T., Tena, G., Plotnikova, J., Willmann, M.R., Chiu, W.L., Gomez-Gomez, L., Boller, T., Ausubel, F.M., and Sheen, J. (2002). MAP kinase signalling cascade in Arabidopsis innate immunity. Nature **415,** 977-983.

Ashtamker, C., Kiss, V., Sagi, M., Davydov, O., and Fluhr, R. (2007). Diverse subcellular locations of cryptogein-induced reactive oxygen species production in tobacco Bright Yellow-2 cells. Plant Physiol **143,** 1817-1826.

Astier, J., Rasul, S., Koen, E., Manzoor, H., Besson-Bard, A., Lamotte, O., Jeandroz, S., Durner, J., Lindermayr, C., and Wendehenne, D. (2011). S-nitrosylation: An emerging post-translational protein modification in plants. Plant Sci **181,** 527-533.

Badorff, C., Fichtlscherer, B., Rhoads, R.E., Zeiher, A.M., Muelsch, A., Dimmeler, S., and Knowlton, K.U. (2000). Nitric oxide inhibits dystrophin proteolysis by coxsackieviral protease 2A through S-nitrosylation: A protective mechanism against enteroviral cardiomyopathy. Circulation **102,** 2276-2281.

Baltrus, D.A., Nishimura, M.T., Romanchuk, A., Chang, J.H., Mukhtar, M.S., Cherkis, K., Roach, J., Grant, S.R., Jones, C.D., and Dangl, J.L. (2011). Dynamic evolution of pathogenicity revealed by sequencing and comparative genomics of 19 Pseudomonas syringae isolates. PLoS Pathog **7,** e1002132.

Bari, R., and Jones, J.D. (2009). Role of plant hormones in plant defence responses. Plant Mol Biol **69,** 473-488.

Beckers, G.J., Jaskiewicz, M., Liu, Y., Underwood, W.R., He, S.Y., Zhang, S., and Conrath, U. (2009). Mitogen-activated protein kinases 3 and 6 are required for full priming of stress responses in Arabidopsis thaliana. Plant Cell **21,** 944-953.

Besson-Bard, A., Pugin, A., and Wendehenne, D. (2008a). New insights into nitric oxide signaling in plants. Annu Rev Plant Biol **59,** 21-39.

Besson-Bard, A., Griveau, S., Bedioui, F., and Wendehenne, D. (2008b). Real-time electrochemical detection of extracellular nitric oxide in tobacco cells exposed to cryptogein, an elicitor of defence

responses. J Exp Bot **59,** 3407-3414.

Bethke, G., Unthan, T., Uhrig, J.F., Poschl, Y., Gust, A.A., Scheel, D., and Lee, J. (2009). Flg22 regulates the release of an ethylene response factor substrate from MAP kinase 6 in Arabidopsis thaliana via ethylene signaling. Proc Natl Acad Sci U S A **106,** 8067-8072.

Block, A., and Alfano, J.R. (2011). Plant targets for Pseudomonas syringae type III effectors: virulence targets or guarded decoys? Curr Opin Microbiol **14,** 39-46.

Block, A., Li, G., Fu, Z.Q., and Alfano, J.R. (2008). Phytopathogen type III effector weaponry and their plant targets. Curr Opin Plant Biol **11,** 396-403.

Boller, T., and Felix, G. (2009). A renaissance of elicitors: perception of microbe-associated molecular patterns and danger signals by pattern-recognition receptors. Annu Rev Plant Biol **60,** 379-406.

Bradford, M.M. (1976). A rapid and sensitive method for the quantitation of microgram quantities of protein utilizing the principle of protein-dye binding. Anal Biochem **72,** 248-254.

Brennan, D.F., and Barford, D. (2009). Eliminylation: a post-translational modification catalyzed by phosphothreonine lyases. Trends Biochem Sci **34,** 108-114.

Bretz, J.R., Mock, N.M., Charity, J.C., Zeyad, S., Baker, C.J., and Hutcheson, S.W. (2003). A translocated protein tyrosine phosphatase of Pseudomonas syringae pv. tomato DC3000 modulates plant defence response to infection. Mol Microbiol **49,** 389-400.

Brodersen, P., Petersen, M., Bjorn Nielsen, H., Zhu, S., Newman, M.A., Shokat, K.M., Rietz, S., Parker, J., and Mundy, J. (2006). Arabidopsis MAP kinase 4 regulates salicylic acid- and jasmonic acid/ethylene-dependent responses via EDS1 and PAD4. Plant J **47,** 532-546.

Cao, W., Baniecki, M.L., McGrath, W.J., Bao, C., Deming, C.B., Rade, J.J., Lowenstein, C.J., and Mangel, W.F. (2003). Nitric oxide inhibits the adenovirus proteinase *in vitro* and viral infectivity *in vivo*. FASEB J **17,** 2345-2346.

Cecconi, D., Orzetti, S., Vandelle, E., Rinalducci, S., Zolla, L., and Delledonne, M. (2009). Protein nitration during defense response in Arabidopsis thaliana. Electrophoresis **30,** 2460-2468.

Chen, L., Wang, H., Zhang, J., Gu, L., Huang, N., Zhou, J.M., and Chai, J. (2008). Structural basis for the catalytic mechanism of phosphothreonine lyase. Nat Struct Mol Biol **15,** 101-102.

Chisholm, S.T., Coaker, G., Day, B., and Staskawicz, B.J. (2006). Host-microbe interactions: shaping the evolution of the plant immune response. Cell **124,** 803-814.

Choi, H.W., Kim, Y.J., Lee, S.C., Hong, J.K., and Hwang, B.K. (2007). Hydrogen peroxide

generation by the pepper extracellular peroxidase CaPO2 activates local and systemic cell death and defense response to bacterial pathogens. Plant Physiol **145,** 890-904.

Clark, D., Durner, J., Navarre, D.A., and Klessig, D.F. (2000). Nitric oxide inhibition of tobacco catalase and ascorbate peroxidase. Mol Plant Microbe Interact **13,** 1380-1384.

Clough, S.J., and Bent, A.F. (1998). Floral dip: a simplified method for Agrobacterium-mediated transformation of Arabidopsis thaliana. Plant J **16,** 735-743.

Coll, N.S., Epple, P., and Dangl, J.L. (2011). Programmed cell death in the plant immune system. Cell Death Differ **18,** 1247-1256.

Collins, N.C., Thordal-Christensen, H., Lipka, V., Bau, S., Kombrink, E., Qiu, J.L., Huckelhoven, R., Stein, M., Freialdenhoven, A., Somerville, S.C., and Schulze-Lefert, P. (2003). SNARE-protein-mediated disease resistance at the plant cell wall. Nature **425,** 973-977.

Cunnac, S., Lindeberg, M., and Collmer, A. (2009). Pseudomonas syringae type III secretion system effectors: repertoires in search of functions. Curr Opin Microbiol **12,** 53-60.

Curtis, M.D., and Grossniklaus, U. (2003). A gateway cloning vector set for high-throughput functional analysis of genes in planta. Plant Physiol **133,** 462-469.

Daudi, A., Cheng, Z., O'Brien, J.A., Mammarella, N., Khan, S., Ausubel, F.M., and Bolwell, G.P. (2012). The apoplastic oxidative burst peroxidase in Arabidopsis is a major component of pattern-triggered immunity. Plant Cell **24,** 275-287.

de Montaigu, A., Sanz-Luque, E., Galvan, A., and Fernandez, E. (2010). A soluble guanylate cyclase mediates negative signaling by ammonium on expression of nitrate reductase in Chlamydomonas. Plant Cell **22,** 1532-1548.

del Pozo, O., Pedley, K.F., and Martin, G.B. (2004). MAPKKKalpha is a positive regulator of cell death associated with both plant immunity and disease. EMBO J **23,** 3072-3082.

Delledonne, M. (2005). NO news is good news for plants. Curr Opin Plant Biol **8,** 390-396.

Delledonne, M., Xia, Y., Dixon, R.A., and Lamb, C. (1998). Nitric oxide functions as a signal in plant disease resistance. Nature **394,** 585-588.

Delledonne, M., Zeier, J., Marocco, A., and Lamb, C. (2001). Signal interactions between nitric oxide and reactive oxygen intermediates in the plant hypersensitive disease resistance response. Proc Natl Acad Sci U S A **98,** 13454-13459.

Deslandes, L., Olivier, J., Peeters, N., Feng, D.X., Khounlotham, M., Boucher, C., Somssich, I.,

Genin, S., and Marco, Y. (2003). Physical interaction between RRS1-R, a protein conferring resistance to bacterial wilt, and PopP2, a type III effector targeted to the plant nucleus. Proc Natl Acad Sci U S A **100,** 8024-8029.

Doares, S.H., Syrovets, T., Weiler, E.W., and Ryan, C.A. (1995). Oligogalacturonides and chitosan activate plant defensive genes through the octadecanoid pathway. Proc Natl Acad Sci U S A **92,** 4095-4098.

Dodds, P.N., and Rathjen, J.P. (2010). Plant immunity: towards an integrated view of plant-pathogen interactions. Nat Rev Genet **11,** 539-548.

Durner, J., Wendehenne, D., and Klessig, D.F. (1998). Defense gene induction in tobacco by nitric oxide, cyclic GMP, and cyclic ADP-ribose. Proc Natl Acad Sci U S A **95,** 10328-10333.

Eitas, T.K., and Dangl, J.L. (2010). NB-LRR proteins: pairs, pieces, perception, partners, and pathways. Curr Opin Plant Biol **13,** 472-477.

Ekengren, S.K., Liu, Y., Schiff, M., Dinesh-Kumar, S.P., and Martin, G.B. (2003). Two MAPK cascades, NPR1, and TGA transcription factors play a role in Pto-mediated disease resistance in tomato. Plant J **36,** 905-917.

Espinosa, A., Guo, M., Tam, V.C., Fu, Z.Q., and Alfano, J.R. (2003). The Pseudomonas syringae type III-secreted protein HopPtoD2 possesses protein tyrosine phosphatase activity and suppresses programmed cell death in plants. Mol Microbiol **49,** 377-387.

Feelisch, M. (2008). The chemical biology of nitric oxide--an outsider's reflections about its role in osteoarthritis. Osteoarthritis Cartilage **16 Suppl 2,** S3-S13.

Felix, G., Duran, J.D., Volko, S., and Boller, T. (1999). Plants have a sensitive perception system for the most conserved domain of bacterial flagellin. Plant J **18,** 265-276.

Fritz-Laylin, L.K., Krishnamurthy, N., Tor, M., Sjolander, K.V., and Jones, J.D. (2005). Phylogenomic analysis of the receptor-like proteins of rice and Arabidopsis. Plant Physiol **138,** 611-623.

Frohlich, A., and Durner, J. (2011). The hunt for plant nitric oxide synthase (NOS): is one really needed? Plant Sci **181,** 401-404.

Fu, Z.Q., Guo, M., Jeong, B.R., Tian, F., Elthon, T.E., Cerny, R.L., Staiger, D., and Alfano, J.R. (2007). A type III effector ADP-ribosylates RNA-binding proteins and quells plant immunity. Nature **447,** 284-288.

Gao, M., Liu, J., Bi, D., Zhang, Z., Cheng, F., Chen, S., and Zhang, Y. (2008). MEKK1, MKK1/MKK2 and MPK4 function together in a mitogen-activated protein kinase cascade to regulate innate immunity in plants. Cell Res **18,** 1190-1198.

Gaupels, F., Spiazzi-Vandelle, E., Yang, D., and Delledonne, M. (2011). Detection of peroxynitrite accumulation in Arabidopsis thaliana during the hypersensitive defense response. Nitric Oxide **25,** 222-228.

Gimenez-Ibanez, S., and Rathjen, J.P. (2010). The case for the defense: plants versus Pseudomonas syringae. Microbes Infect **12,** 428-437.

Glazebrook, J. (2005). Contrasting mechanisms of defense against biotrophic and necrotrophic pathogens. Annu Rev Phytopathol **43,** 205-227.

Gohre, V., and Robatzek, S. (2008). Breaking the barriers: microbial effector molecules subvert plant immunity. Annu Rev Phytopathol **46,** 189-215.

Gohre, V., Spallek, T., Haweker, H., Mersmann, S., Mentzel, T., Boller, T., de Torres, M., Mansfield, J.W., and Robatzek, S. (2008). Plant pattern-recognition receptor FLS2 is directed for degradation by the bacterial ubiquitin ligase AvrPtoB. Curr Biol **18,** 1824-1832.

Greenberg, J.T., and Vinatzer, B.A. (2003). Identifying type III effectors of plant pathogens and analyzing their interaction with plant cells. Curr Opin Microbiol **6,** 20-28.

Guo, M., Tian, F., Wamboldt, Y., and Alfano, J.R. (2009). The majority of the type III effector inventory of Pseudomonas syringae pv. tomato DC3000 can suppress plant immunity. Mol Plant Microbe Interact **22,** 1069-1080.

Gupta, K.J., Igamberdiev, A.U., Manjunatha, G., Segu, S., Moran, J.F., Neelawarne, B., Bauwe, H., and Kaiser, W.M. (2011). The emerging roles of nitric oxide (NO) in plant mitochondria. Plant Sci **181,** 520-526.

Hamel, L.P., Nicole, M.C., Sritubtim, S., Morency, M.J., Ellis, M., Ehlting, J., Beaudoin, N., Barbazuk, B., Klessig, D., Lee, J., Martin, G., Mundy, J., Ohashi, Y., Scheel, D., Sheen, J., Xing, T., Zhang, S., Seguin, A., and Ellis, B.E. (2006). Ancient signals: comparative genomics of plant MAPK and MAPKK gene families. Trends Plant Sci **11,** 192-198.

Hann, D.R., and Rathjen, J.P. (2007). Early events in the pathogenicity of Pseudomonas syringae on Nicotiana benthamiana. Plant J **49,** 607-618.

He, P., Shan, L., Lin, N.C., Martin, G.B., Kemmerling, B., Nurnberger, T., and Sheen, J. (2006).

Specific bacterial suppressors of MAMP signaling upstream of MAPKKK in Arabidopsis innate immunity. Cell **125,** 563-575.

Herold, S., and Puppo, A. (2005). Kinetics and mechanistic studies of the reactions of metleghemoglobin, ferrylleghemoglobin, and nitrosylleghemoglobin with reactive nitrogen species. J Biol Inorg Chem **10,** 946-957.

Hess, D.T., Matsumoto, A., Kim, S.O., Marshall, H.E., and Stamler, J.S. (2005). Protein S-nitrosylation: purview and parameters. Nat Rev Mol Cell Biol **6,** 150-166.

Higuchi, R., Krummel, B., and Saiki, R.K. (1988). A general method of *in vitro* preparation and specific mutagenesis of DNA fragments: study of protein and DNA interactions. Nucleic Acids Res **16,** 7351-7367.

Hong, J.K., Yun, B.W., Kang, J.G., Raja, M.U., Kwon, E., Sorhagen, K., Chu, C., Wang, Y., and Loake, G.J. (2008). Nitric oxide function and signalling in plant disease resistance. J Exp Bot **59,** 147-154.

Huffaker, A., Pearce, G., and Ryan, C.A. (2006). An endogenous peptide signal in Arabidopsis activates components of the innate immune response. Proc Natl Acad Sci U S A **103,** 10098-10103.

Ichimura, K., Casais, C., Peck, S.C., Shinozaki, K., and Shirasu, K. (2006). MEKK1 is required for MPK4 activation and regulates tissue-specific and temperature-dependent cell death in Arabidopsis. J Biol Chem **281,** 36969-36976.

Jones, J.D., and Dangl, J.L. (2006). The plant immune system. Nature **444,** 323-329.

Katagiri, F., Thilmony, R., and He, S.Y. (2002). The Arabidopsis thaliana-pseudomonas syringae interaction. Arabidopsis Book **1,** e0039.

Keen, N.T., Tamaki, S., Kobayashi, D., and Trollinger, D. (1988). Improved broad-host-range plasmids for DNA cloning in gram-negative bacteria. Gene **70,** 191-197.

Kemball, C.C., Harkins, S., Whitmire, J.K., Flynn, C.T., Feuer, R., and Whitton, J.L. (2009). Coxsackievirus B3 inhibits antigen presentation *in vivo,* exerting a profound and selective effect on the MHC class I pathway. PLoS Pathog **5,** e1000618.

Kwezi, L., Meier, S., Mungur, L., Ruzvidzo, O., Irving, H., and Gehring, C. (2007). The Arabidopsis thaliana brassinosteroid receptor (AtBRI1) contains a domain that functions as a guanylyl cyclase *in vitro*. PLoS One **2,** e449.

Kwezi, L., Ruzvidzo, O., Wheeler, J.I., Govender, K., Iacuone, S., Thompson, P.E., Gehring, C.,

and Irving, H.R. (2011). The phytosulfokine (PSK) receptor is capable of guanylate cyclase activity and enabling cyclic GMP-dependent signaling in plants. J Biol Chem **286,** 22580-22588.

Kwon, C., Bednarek, P., and Schulze-Lefert, P. (2008). Secretory pathways in plant immune responses. Plant Physiol **147,** 1575-1583.

Lamb, C., and Dixon, R.A. (1997). The Oxidative Burst in Plant Disease Resistance. Annu Rev Plant Physiol Plant Mol Biol **48,** 251-275.

Lange, C., Hemmrich, G., Klostermeier, U.C., Lopez-Quintero, J.A., Miller, D.J., Rahn, T., Weiss, Y., Bosch, T.C., and Rosenstiel, P. (2011). Defining the origins of the NOD-like receptor system at the base of animal evolution. Mol Biol Evol **28,** 1687-1702.

Laurie-Berry, N., Joardar, V., Street, I.H., and Kunkel, B.N. (2006). The Arabidopsis thaliana JASMONATE INSENSITIVE 1 gene is required for suppression of salicylic acid-dependent defenses during infection by Pseudomonas syringae. Mol Plant Microbe Interact **19,** 789-800.

Lee, M.W., and Yang, Y. (2006). Transient expression assay by agroinfiltration of leaves. Methods Mol Biol **323,** 225-229.

Leitner, M., Vandelle, E., Gaupels, F., Bellin, D., and Delledonne, M. (2009). NO signals in the haze: nitric oxide signalling in plant defence. Curr Opin Plant Biol **12,** 451-458.

Leon-Reyes, A., Du, Y., Koornneef, A., Proietti, S., Korbes, A.P., Memelink, J., Pieterse, C.M., and Ritsema, T. (2010). Ethylene signaling renders the jasmonate response of Arabidopsis insensitive to future suppression by salicylic Acid. Mol Plant Microbe Interact **23,** 187-197.

Leon-Reyes, A., Spoel, S.H., De Lange, E.S., Abe, H., Kobayashi, M., Tsuda, S., Millenaar, F.F., Welschen, R.A., Ritsema, T., and Pieterse, C.M. (2009). Ethylene modulates the role of NONEXPRESSOR OF PATHOGENESIS-RELATED GENES1 in cross talk between salicylate and jasmonate signaling. Plant Physiol **149,** 1797-1809.

Li, H., Xu, H., Zhou, Y., Zhang, J., Long, C., Li, S., Chen, S., Zhou, J.M., and Shao, F. (2007). The phosphothreonine lyase activity of a bacterial type III effector family. Science **315,** 1000-1003.

Li, J., Ding, J., Zhang, W., Zhang, Y., Tang, P., Chen, J.Q., Tian, D., and Yang, S. (2010). Unique evolutionary pattern of numbers of gramineous NBS-LRR genes. Mol Genet Genomics **283,** 427-438.

Li, X.Y., Lin, H.Q., Zhang, W.G., Zou, Y., Zhang, J., Tang, X.Y., and Zhou, J.M. (2005). Flagellin induces innate immunity in nonhost interactions that is suppressed by Pseudomonas syringae effectors. Proc Natl Acad Sci U S A **102,** 12990-12995.

Lindeberg, M., Cunnac, S., and Collmer, A. (2012). Pseudomonas syringae type III effector repertoires: last words in endless arguments. Trends Microbiol.

Lindeberg, M., Cartinhour, S., Myers, C.R., Schechter, L.M., Schneider, D.J., and Collmer, A. (2006). Closing the circle on the discovery of genes encoding Hrp regulon members and type III secretion system effectors in the genomes of three model Pseudomonas syringae strains. Mol Plant Microbe Interact **19,** 1151-1158.

Lindeberg, M., Stavrinides, J., Chang, J.H., Alfano, J.R., Collmer, A., Dangl, J.L., Greenberg, J.T., Mansfield, J.W., and Guttman, D.S. (2005). Proposed guidelines for a unified nomenclature and phylogenetic analysis of type III Hop effector proteins in the plant pathogen Pseudomonas syringae. Mol Plant Microbe Interact **18,** 275-282.

Lindermayr, C., Saalbach, G., and Durner, J. (2005). Proteomic identification of S-nitrosylated proteins in Arabidopsis. Plant Physiol **137,** 921-930.

Liu, Y., and Zhang, S. (2004). Phosphorylation of 1-aminocyclopropane-1-carboxylic acid synthase by MPK6, a stress-responsive mitogen-activated protein kinase, induces ethylene biosynthesis in Arabidopsis. Plant Cell **16,** 3386-3399.

Livak, K.J., and Schmittgen, T.D. (2001). Analysis of relative gene expression data using real-time quantitative PCR and the 2(-Delta Delta C(T)) Method. Methods **25,** 402-408.

Lotze, M.T., Zeh, H.J., Rubartelli, A., Sparvero, L.J., Amoscato, A.A., Washburn, N.R., Devera, M.E., Liang, X., Tor, M., and Billiar, T. (2007). The grateful dead: damage-associated molecular pattern molecules and reduction/oxidation regulate immunity. Immunol Rev **220,** 60-81.

Ludidi, N., and Gehring, C. (2003). Identification of a novel protein with guanylyl cyclase activity in Arabidopsis thaliana. J Biol Chem **278,** 6490-6494.

Lukasik, E., and Takken, F.L. (2009). STANDing strong, resistance proteins instigators of plant defence. Curr Opin Plant Biol **12,** 427-436.

Ma, W., and Berkowitz, G.A. (2007). The grateful dead: calcium and cell death in plant innate immunity. Cell Microbiol **9,** 2571-2585.

Ma, W., Qi, Z., Smigel, A., Walker, R.K., Verma, R., and Berkowitz, G.A. (2009). Ca2+, cAMP, and transduction of non-self perception during plant immune responses. Proc Natl Acad Sci U S A **106,** 20995-21000.

Mackey, D., Belkhadir, Y., Alonso, J.M., Ecker, J.R., and Dangl, J.L. (2003). Arabidopsis RIN4 is a

target of the type III virulence effector AvrRpt2 and modulates RPS2-mediated resistance. Cell **112,** 379-389.

Maekawa, T., Kufer, T.A., and Schulze-Lefert, P. (2011). NLR functions in plant and animal immune systems: so far and yet so close. Nat Immunol **12,** 817-826.

Mannick, J.B. (2006). Immunoregulatory and antimicrobial effects of nitrogen oxides. Proc Am Thorac Soc **3,** 161-165.

MAPK-Group. (2002). Mitogen-activated protein kinase cascades in plants: a new nomenclature. Trends Plant Sci **7,** 301-308.

Marino, S.M., and Gladyshev, V.N. (2010). Structural analysis of cysteine S-nitrosylation: a modified acid-based motif and the emerging role of trans-nitrosylation. J Mol Biol **395,** 844-859.

Martinez-Atienza, J., Van Ingelgem, C., Roef, L., and Maathuis, F.J. (2007). Plant cyclic nucleotide signalling: facts and fiction. Plant Signal Behav **2,** 540-543.

Meier, S., and Gehring, C. (2006). Emerging roles in plant biotechnology for the second messenger cGMP - guanosine 3',5'-cyclic monophosphate. Afr J Biotechnol**,** 1687-1692.

Meier, S., Madeo, L., Ederli, L., Donaldson, L., Pasqualini, S., and Gehring, C. (2009). Deciphering cGMP signatures and cGMP-dependent pathways in plant defence. Plant Signal Behav **4,** 307-309.

Meier, S., Ruzvidzo, O., Morse, M., Donaldson, L., Kwezi, L., and Gehring, C. (2010). The Arabidopsis wall associated kinase-like 10 gene encodes a functional guanylyl cyclase and is co-expressed with pathogen defense related genes. PLoS One **5,** e8904.

Melotto, M., Underwood, W., Koczan, J., Nomura, K., and He, S.Y. (2006). Plant stomata function in innate immunity against bacterial invasion. Cell **126,** 969-980.

Menke, F.L., van Pelt, J.A., Pieterse, C.M., and Klessig, D.F. (2004). Silencing of the mitogen-activated protein kinase MPK6 compromises disease resistance in Arabidopsis. Plant Cell **16,** 897-907.

Merkouropoulos, G., Andreasson, E., Hess, D., Boller, T., and Peck, S.C. (2008). An Arabidopsis protein phosphorylated in response to microbial elicitation, AtPHOS32, is a substrate of MAP kinases 3 and 6. J Biol Chem **283,** 10493-10499.

Meyer, A., Puhler, A., and Niehaus, K. (2001). The lipopolysaccharides of the phytopathogen Xanthomonas campestris pv. campestris induce an oxidative burst reaction in cell cultures of Nicotiana

tabacum. Planta **213,** 214-222.

Meyers, B.C., Kozik, A., Griego, A., Kuang, H., and Michelmore, R.W. (2003). Genome-wide analysis of NBS-LRR-encoding genes in Arabidopsis. Plant Cell **15,** 809-834.

Mittler, R., Vanderauwera, S., Gollery, M., and Van Breusegem, F. (2004). Reactive oxygen gene network of plants. Trends Plant Sci **9,** 490-498.

Moeder, W., Del Pozo, O., Navarre, D.A., Martin, G.B., and Klessig, D.F. (2007). Aconitase plays a role in regulating resistance to oxidative stress and cell death in Arabidopsis and Nicotiana benthamiana. Plant Mol Biol **63,** 273-287.

Moller, I.M., and Kristensen, B.K. (2004). Protein oxidation in plant mitochondria as a stress indicator. Photochem Photobiol Sci **3,** 730-735.

Moller, I.M., and Kristensen, B.K. (2006). Protein oxidation in plant mitochondria detected as oxidized tryptophan. Free Radic Biol Med **40,** 430-435.

Moller, I.M., Jensen, P.E., and Hansson, A. (2007). Oxidative modifications to cellular components in plants. Annu Rev Plant Biol **58,** 459-481.

Mulaudzi, T., Ludidi, N., Ruzvidzo, O., Morse, M., Hendricks, N., Iwuoha, E., and Gehring, C. (2011). Identification of a novel Arabidopsis thaliana nitric oxide-binding molecule with guanylate cyclase activity *in vitro*. FEBS Lett **585,** 2693-2697.

Navarro, L., Zipfel, C., Rowland, O., Keller, I., Robatzek, S., Boller, T., and Jones, J.D. (2004). The transcriptional innate immune response to flg22. Interplay and overlap with Avr gene-dependent defense responses and bacterial pathogenesis. Plant Physiol **135,** 1113-1128.

Nelson, M.J. (1987). The nitric oxide complex of ferrous soybean lipoxygenase-1. Substrate, pH, and ethanol effects on the active-site iron. J Biol Chem **262,** 12137-12142.

Nino-Liu, D.O., Ronald, P.C., and Bogdanove, A.J. (2006). Xanthomonas oryzae pathovars: model pathogens of a model crop. Mol Plant Pathol **7,** 303-324.

Nomura, K., Debroy, S., Lee, Y.H., Pumplin, N., Jones, J., and He, S.Y. (2006). A bacterial virulence protein suppresses host innate immunity to cause plant disease. Science **313,** 220-223.

Ntoukakis, V., Mucyn, T.S., Gimenez-Ibanez, S., Chapman, H.C., Gutierrez, J.R., Balmuth, A.L., Jones, A.M., and Rathjen, J.P. (2009). Host inhibition of a bacterial virulence effector triggers immunity to infection. Science **324,** 784-787.

O'Brien, J.A., Daudi, A., Finch, P., Butt, V.S., Whitelegge, J.P., Souda, P., Ausubel, F.M., and

Bolwell, G.P. (2012). A Peroxidase-Dependent Apoplastic Oxidative Burst in Cultured Arabidopsis Cells Functions in MAMP-Elicited Defense. Plant Physiol **158,** 2013-2027.

Padalko, E., Ohnishi, T., Matsushita, K., Sun, H., Fox-Talbot, K., Bao, C., Baldwin, W.M., 3rd, and Lowenstein, C.J. (2004). Peroxynitrite inhibition of Coxsackievirus infection by prevention of viral RNA entry. Proc Natl Acad Sci U S A **101,** 11731-11736.

Palmer, R.M., Hickery, M.S., Charles, I.G., Moncada, S., and Bayliss, M.T. (1993). Induction of nitric oxide synthase in human chondrocytes. Biochem Biophys Res Commun **193,** 398-405.

Palmieri, M.C., Lindermayr, C., Bauwe, H., Steinhauser, C., and Durner, J. (2010). Regulation of plant glycine decarboxylase by s-nitrosylation and glutathionylation. Plant Physiol **152,** 1514-1528.

Pearce, G., Moura, D.S., Stratmann, J., and Ryan, C.A. (2001a). Production of multiple plant hormones from a single polyprotein precursor. Nature **411,** 817-820.

Pearce, G., Moura, D.S., Stratmann, J., and Ryan, C.A., Jr. (2001b). RALF, a 5-kDa ubiquitous polypeptide in plants, arrests root growth and development. Proc Natl Acad Sci U S A **98,** 12843-12847.

Perez-Mato, I., Castro, C., Ruiz, F.A., Corrales, F.J., and Mato, J.M. (1999). Methionine adenosyltransferase S-nitrosylation is regulated by the basic and acidic amino acids surrounding the target thiol. J Biol Chem **274,** 17075-17079.

Petersen, M., Brodersen, P., Naested, H., Andreasson, E., Lindhart, U., Johansen, B., Nielsen, H.B., Lacy, M., Austin, M.J., Parker, J.E., Sharma, S.B., Klessig, D.F., Martienssen, R., Mattsson, O., Jensen, A.B., and Mundy, J. (2000). Arabidopsis map kinase 4 negatively regulates systemic acquired resistance. Cell **103,** 1111-1120.

Petnicki-Ocwieja, T., Schneider, D.J., Tam, V.C., Chancey, S.T., Shan, L., Jamir, Y., Schechter, L.M., Janes, M.D., Buell, C.R., Tang, X., Collmer, A., and Alfano, J.R. (2002). Genomewide identification of proteins secreted by the Hrp type III protein secretion system of Pseudomonas syringae pv. tomato DC3000. Proc Natl Acad Sci U S A **99,** 7652-7657.

Pieterse, C.M., Leon-Reyes, A., Van der Ent, S., and Van Wees, S.C. (2009). Networking by small-molecule hormones in plant immunity. Nat Chem Biol **5,** 308-316.

Pitzschke, A., Schikora, A., and Hirt, H. (2009). MAPK cascade signalling networks in plant defence. Curr Opin Plant Biol **12,** 421-426.

Postel, S., and Kemmerling, B. (2009). Plant systems for recognition of pathogen-associated

molecular patterns. Semin Cell Dev Biol **20,** 1025-1031.

Potter, L.R. (2011). Guanylyl cyclase structure, function and regulation. Cell Signal **23,** 1921-1926.

Ranf, S., Eschen-Lippold, L., Pecher, P., Lee, J., and Scheel, D. (2011). Interplay between calcium signalling and early signalling elements during defence responses to microbe- or damage-associated molecular patterns. Plant J **68,** 100-113.

Ren, D., Yang, H., and Zhang, S. (2002). Cell death mediated by MAPK is associated with hydrogen peroxide production in Arabidopsis. J Biol Chem **277,** 559-565.

Rockel, P., Strube, F., Rockel, A., Wildt, J., and Kaiser, W.M. (2002). Regulation of nitric oxide (NO) production by plant nitrate reductase *in vivo* and *in vitro*. J Exp Bot **53,** 103-110.

Rocklin, A.M., Tierney, D.L., Kofman, V., Brunhuber, N.M., Hoffman, B.M., Christoffersen, R.E., Reich, N.O., Lipscomb, J.D., and Que, L., Jr. (1999). Role of the nonheme Fe(II) center in the biosynthesis of the plant hormone ethylene. Proc Natl Acad Sci U S A **96,** 7905-7909.

Rodriguez, M.C., Petersen, M., and Mundy, J. (2010). Mitogen-activated protein kinase signaling in plants. Annu Rev Plant Biol **61,** 621-649.

Romeis, T., Piedras, P., Zhang, S., Klessig, D.F., Hirt, H., and Jones, J.D. (1999). Rapid Avr9- and Cf-9 -dependent activation of MAP kinases in tobacco cell cultures and leaves: convergence of resistance gene, elicitor, wound, and salicylate responses. Plant Cell **11,** 273-287.

Romero-Puertas, M.C., Campostrini, N., Matte, A., Righetti, P.G., Perazzolli, M., Zolla, L., Roepstorff, P., and Delledonne, M. (2008). Proteomic analysis of S-nitrosylated proteins in Arabidopsis thaliana undergoing hypersensitive response. Proteomics **8,** 1459-1469.

Roy, A., Kucukural, A., and Zhang, Y. (2010). I-TASSER: a unified platform for automated protein structure and function prediction. Nat Protoc **5,** 725-738.

Saito, S., Yamamoto-Katou, A., Yoshioka, H., Doke, N., and Kawakita, K. (2006). Peroxynitrite generation and tyrosine nitration in defense responses in tobacco BY-2 cells. Plant Cell Physiol **47,** 689-697.

Sanabria, N.M., Huang, J.C., and Dubery, I.A. (2010). Self/nonself perception in plants in innate immunity and defense. Self Nonself **1,** 40-54.

Saura, M., Zaragoza, C., McMillan, A., Quick, R.A., Hohenadl, C., Lowenstein, J.M., and Lowenstein, C.J. (1999). An antiviral mechanism of nitric oxide: inhibition of a viral protease. Immunity **10,** 21-28.

Savidge, T.C., Urvil, P., Oezguen, N., Ali, K., Choudhury, A., Acharya, V., Pinchuk, I., Torres, A.G., English, R.D., Wiktorowicz, J.E., Loeffelholz, M., Kumar, R., Shi, L., Nie, W., Braun, W., Herman, B., Hausladen, A., Feng, H., Stamler, J.S., and Pothoulakis, C. (2011). Host S-nitrosylation inhibits clostridial small molecule-activated glucosylating toxins. Nat Med **17,** 1136-1141.

Schechter, L.M., Roberts, K.A., Jamir, Y., Alfano, J.R., and Collmer, A. (2004). Pseudomonas syringae type III secretion system targeting signals and novel effectors studied with a Cya translocation reporter. J Bacteriol **186,** 543-555.

Schechter, L.M., Vencato, M., Jordan, K.L., Schneider, S.E., Schneider, D.J., and Collmer, A. (2006). Multiple approaches to a complete inventory of Pseudomonas syringae pv. tomato DC3000 type III secretion system effector proteins. Mol Plant Microbe Interact **19,** 1180-1192.

Seeliger, D., and de Groot, B.L. (2010). Ligand docking and binding site analysis with PyMOL and Autodock/Vina. J Comput Aided Mol Des **24,** 417-422.

Shan, L., He, P., and Sheen, J. (2007). Intercepting host MAPK signaling cascades by bacterial type III effectors. Cell Host Microbe **1,** 167-174.

Shapiro, A.D., and Zhang, C. (2001). The role of NDR1 in avirulence gene-directed signaling and control of programmed cell death in Arabidopsis. Plant Physiol **127,** 1089-1101.

Shindo, T., and Van der Hoorn, R.A. (2008). Papain-like cysteine proteases: key players at molecular battlefields employed by both plants and their invaders. Mol Plant Pathol **9,** 119-125.

Shiu, S.H., and Bleecker, A.B. (2001). Receptor-like kinases from Arabidopsis form a monophyletic gene family related to animal receptor kinases. Proc Natl Acad Sci U S A **98,** 10763-10768.

Stamler, J.S., Toone, E.J., Lipton, S.A., and Sucher, N.J. (1997). (S)NO signals: translocation, regulation, and a consensus motif. Neuron **18,** 691-696.

Suarez-Rodriguez, M.C., Adams-Phillips, L., Liu, Y., Wang, H., Su, S.H., Jester, P.J., Zhang, S., Bent, A.F., and Krysan, P.J. (2007). MEKK1 is required for flg22-induced MPK4 activation in Arabidopsis plants. Plant Physiol **143,** 661-669.

Suzuki, N., Miller, G., Morales, J., Shulaev, V., Torres, M.A., and Mittler, R. (2011). Respiratory burst oxidases: the engines of ROS signaling. Curr Opin Plant Biol **14,** 691-699.

Takahashi, Y., Nasir, K.H., Ito, A., Kanzaki, H., Matsumura, H., Saitoh, H., Fujisawa, S., Kamoun, S., and Terauchi, R. (2007). A high-throughput screen of cell-death-inducing factors in

Nicotiana benthamiana identifies a novel MAPKK that mediates INF1-induced cell death signaling and non-host resistance to Pseudomonas cichorii. Plant J **49,** 1030-1040.

Tanou, G., Job, C., Rajjou, L., Arc, E., Belghazi, M., Diamantidis, G., Molassiotis, A., and Job, D. (2009). Proteomics reveals the overlapping roles of hydrogen peroxide and nitric oxide in the acclimation of citrus plants to salinity. Plant J **60,** 795-804.

Tao, Y., Xie, Z., Chen, W., Glazebrook, J., Chang, H.S., Han, B., Zhu, T., Zou, G., and Katagiri, F. (2003). Quantitative nature of Arabidopsis responses during compatible and incompatible interactions with the bacterial pathogen Pseudomonas syringae. Plant Cell **15,** 317-330.

Tena, G., Boudsocq, M., and Sheen, J. (2011). Protein kinase signaling networks in plant innate immunity. Curr Opin Plant Biol **14,** 519-529.

Thomma, B.P., Nurnberger, T., and Joosten, M.H. (2011). Of PAMPs and effectors: the blurred PTI-ETI dichotomy. Plant Cell **23,** 4-15.

Torres, M.A. (2010). ROS in biotic interactions. Physiol Plant **138,** 414-429.

Torres, M.A., Jones, J.D., and Dangl, J.L. (2006). Reactive oxygen species signaling in response to pathogens. Plant Physiol **141,** 373-378.

Toth, I.K., Bell, K.S., Holeva, M.C., and Birch, P.R. (2003). Soft rot erwiniae: from genes to genomes. Mol Plant Pathol **4,** 17-30.

Tsuda, K., and Katagiri, F. (2010). Comparing signaling mechanisms engaged in pattern-triggered and effector-triggered immunity. Curr Opin Plant Biol **13,** 459-465.

Underwood, W., Zhang, S., and He, S.Y. (2007). The Pseudomonas syringae type III effector tyrosine phosphatase HopAO1 suppresses innate immunity in Arabidopsis thaliana. Plant J **52,** 658-672.

Vandelle, E., and Delledonne, M. (2011). Peroxynitrite formation and function in plants. Plant Sci **181,** 534-539.

Vellosillo, T., Vicente, J., Kulasekaran, S., Hamberg, M., and Castresana, C. (2010). Emerging complexity in reactive oxygen species production and signaling during the response of plants to pathogens. Plant Physiol **154,** 444-448.

Verhage, A., van Wees, S.C., and Pieterse, C.M. (2010). Plant immunity: it's the hormones talking, but what do they say? Plant Physiol **154,** 536-540.

Vinatzer, B.A., Jelenska, J., and Greenberg, J.T. (2005). Bioinformatics correctly identifies many type III secretion substrates in the plant pathogen Pseudomonas syringae and the biocontrol isolate P.

fluorescens SBW25. Mol Plant Microbe Interact **18,** 877-888.

Wan, J., Zhang, X.C., Neece, D., Ramonell, K.M., Clough, S., Kim, S.Y., Stacey, M.G., and Stacey, G. (2008). A LysM receptor-like kinase plays a critical role in chitin signaling and fungal resistance in Arabidopsis. Plant Cell **20,** 471-481.

Wang, Y., Li, J., Hou, S., Wang, X., Li, Y., Ren, D., Chen, S., Tang, X., and Zhou, J.M. (2010). A Pseudomonas syringae ADP-ribosyltransferase inhibits Arabidopsis mitogen-activated protein kinase kinases. Plant Cell **22,** 2033-2044.

Xiang, T., Zong, N., Zou, Y., Wu, Y., Zhang, J., Xing, W., Li, Y., Tang, X., Zhu, L., Chai, J., and Zhou, J.M. (2008). Pseudomonas syringae effector AvrPto blocks innate immunity by targeting receptor kinases. Curr Biol **18,** 74-80.

Yamaguchi, Y., Pearce, G., and Ryan, C.A. (2006). The cell surface leucine-rich repeat receptor for AtPep1, an endogenous peptide elicitor in Arabidopsis, is functional in transgenic tobacco cells. Proc Natl Acad Sci U S A **103,** 10104-10109.

Zeidler, D., Zahringer, U., Gerber, I., Dubery, I., Hartung, T., Bors, W., Hutzler, P., and Durner, J. (2004). Innate immunity in Arabidopsis thaliana: lipopolysaccharides activate nitric oxide synthase (NOS) and induce defense genes. Proc Natl Acad Sci U S A **101,** 15811-15816.

Zhang, C., Czymmek, K.J., and Shapiro, A.D. (2003). Nitric oxide does not trigger early programmed cell death events but may contribute to cell-to-cell signaling governing progression of the Arabidopsis hypersensitive response. Mol Plant Microbe Interact **16,** 962-972.

Zhang, J., Shao, F., Li, Y., Cui, H., Chen, L., Li, H., Zou, Y., Long, C., Lan, L., Chai, J., Chen, S., Tang, X., and Zhou, J.M. (2007a). A Pseudomonas syringae effector inactivates MAPKs to suppress PAMP-induced immunity in plants. Cell Host Microbe **1,** 175-185.

Zhang, X., Henriques, R., Lin, S.S., Niu, Q.W., and Chua, N.H. (2006). Agrobacterium-mediated transformation of Arabidopsis thaliana using the floral dip method. Nat Protoc **1,** 641-646.

Zhang, X., Dai, Y., Xiong, Y., DeFraia, C., Li, J., Dong, X., and Mou, Z. (2007b). Overexpression of Arabidopsis MAP kinase kinase 7 leads to activation of plant basal and systemic acquired resistance. Plant J **52,** 1066-1079.

Zhang, Z., Wu, Y., Gao, M., Zhang, J., Kong, Q., Liu, Y., Ba, H., Zhou, J., and Zhang, Y. (2012). Disruption of PAMP-Induced MAP Kinase Cascade by a Pseudomonas syringae Effector Activates Plant Immunity Mediated by the NB-LRR Protein SUMM2. Cell Host Microbe **11,** 253-263.

Zipfel, C. (2008). Pattern-recognition receptors in plant innate immunity. Curr Opin Immunol **20,** 10-16.

Zipfel, C., Robatzek, S., Navarro, L., Oakeley, E.J., Jones, J.D., Felix, G., and Boller, T. (2004). Bacterial disease resistance in Arabidopsis through flagellin perception. Nature **428,** 764-767.

7. Appendix

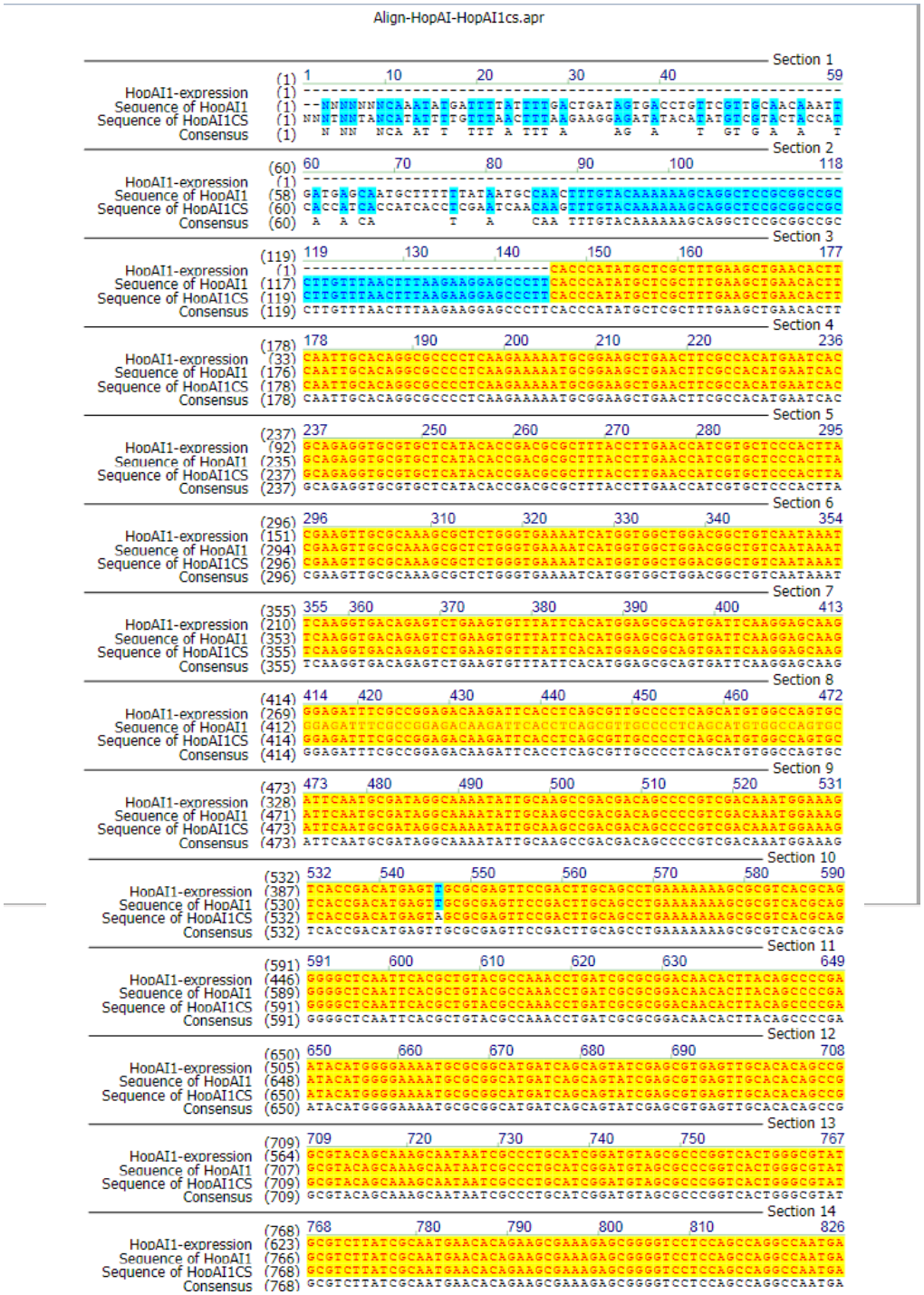
Align-HopAI-HopAI1cs.apr
Section 1
Section 2
Section 3
Section 4
Section 5
Section 6
Section 7
Section 8
Section 9
Section 10
Section 11
Section 12
Section 13
Section 14
HopAI1-expression
Sequence of HopAI1
Sequence of HopAI1CS
Consensus

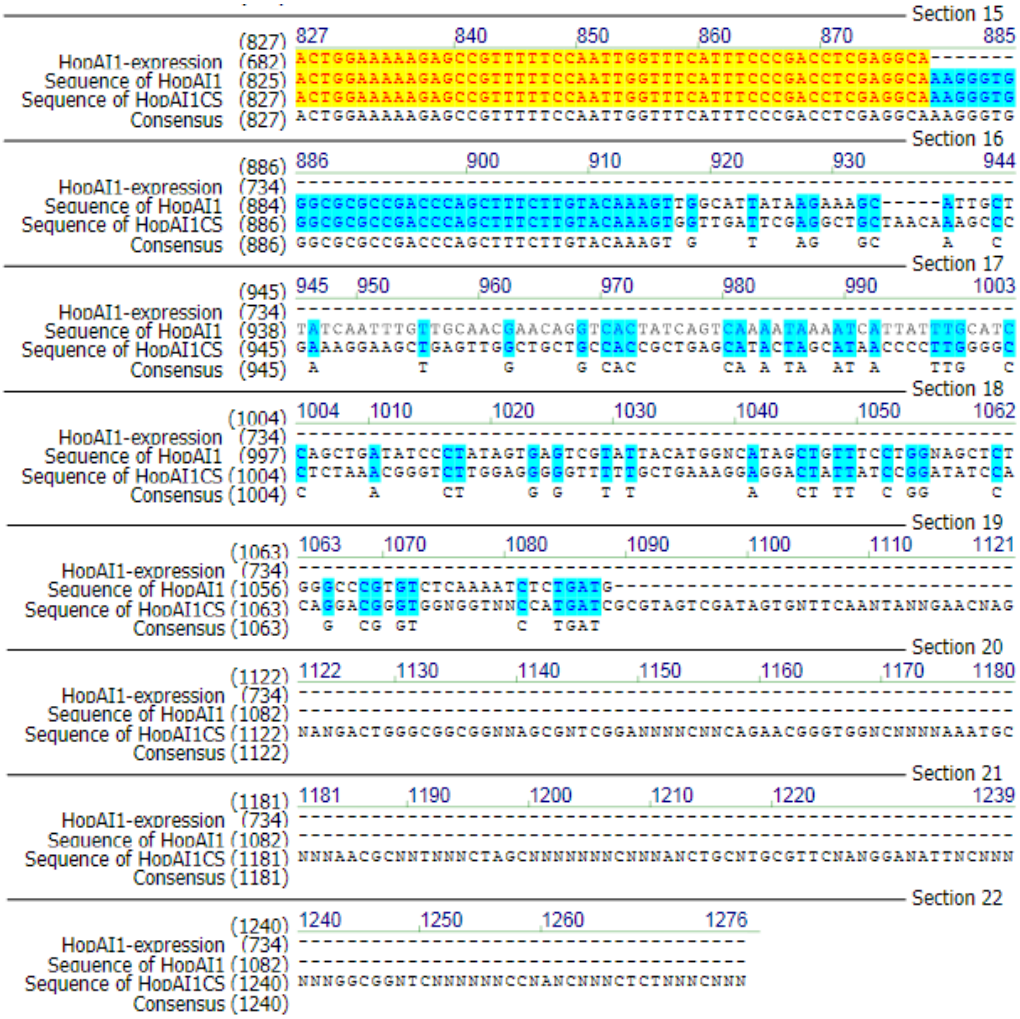

Figure 1. Alignment of sequenced HopAI1 and HopAI1^{CS}

Aliignment was performed by using Align X (Vector NTI9.0, Invitrogen). Black on window default, color non-similar residues blue on cyan consensus residue derived from a block of similar residues at a given position; Black on green, consensus residue derived from the occurrence of greater than 50% of a single residue at a given position; Red on yellow, consensus residue derived from a completely conserved residue at a given position; Green on window default color, residue weakly similar to consensus residue at given position.

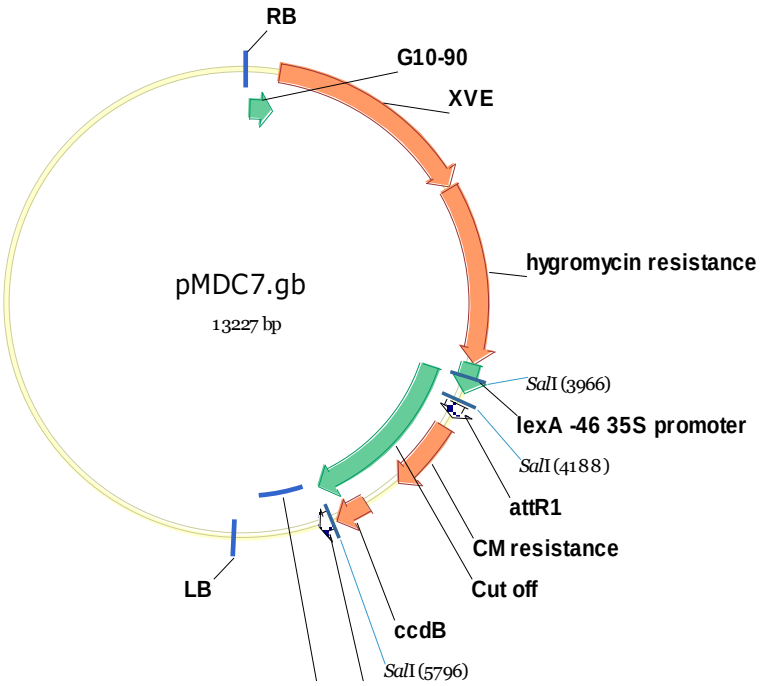

Figure 2 Map of pMDC7

The longest green square with arrow represents the region that is digested by restriction enzyme Sal I.